

**A STUDY ON CODE-MODULATED  
SYNCHRONIZED-OOK TRANSCEIVER FOR  
LOW POWER WIRELESS SENSOR NETWORKS**



**NGUYEN VAN TRUNG**

A DISSERTATION  
PRESENTED TO THE FACULTY  
OF THE UNIVERSITY OF ELECTRO-COMMUNICATIONS  
IN CANDIDACY FOR THE DEGREE  
OF DOCTOR OF PHILOSOPHY

RECOMMENDED FOR ACCEPTANCE  
BY THE DEPARTMENT OF ENGINEERING SCIENCE  
SUPERVISOR: KOICHIRO ISHIBASHI & CONG-KHA PHAM

JANUARY 2019

*This page intentionally left blank*

## Acknowledgements

First of all, I would like to offer my deepest appreciation to my supervisors, Professor Koichiro Ishibashi and Professor Cong-Kha Pham, for their patient guidance, enthusiastic encouragement and useful critiques during the doctoral course at UEC. Throughout the course, I received not only scientific instruction in my research but also useful advice for coping with problems in my life. Thanks to their supporting, originating with lack experience in scientific research, I became more matured. I hope that in the future we still maintain the good relationship and have more chance to cooperate.

Next, I would also like to extend my thanks to Associate Professor Ryo Ishikawa and Doctor Yasuo Sato for their technical support, to our lab secretaries and staffs of Graduate School of Informatics and Engineering, Department of Engineering and Science for their enthusiastic support to complete official procedures.

I wish to thank the University of Electro-Communications (UEC) and Vietnam Ministry of Education and Training, Vietnam International Education and Development (VIED) for giving me a chance to study in Japan. I also would like to thank the International Student Offices (ISO) staffs and lecturers for their supporting during my course.

I would like to acknowledge JST-CREST Grant Number JPMJCR16Q1, Japan and VLSI Design and Education Center (VDEC), the University of Tokyo in collaboration with Synopsys, Inc. and Cadence Design Systems, Inc. for their supporting for this work.

Relating to my health condition, I would like to express my profound gratitude to doctors and nurses in Tokyo Metropolitan Tama Medical Center Hospital for treating my disease and helping me to be able to continue my research and complete the doctoral course.

Last but not least, I would like to express my gratitude to my teachers and my colleagues in the Faculty of Radio-Electronics, Le Quy Don Technical University, Vietnam for provide the best condition for me to pursue the doctoral course; to all members of ISHIBASHI Lab and PHAM Lab for their kindness and their support; to my friends and seniors who always encouraged me to keep going on the research way. Finally, I would like

to thank and give my love to my parents, my relatives for their encouragement, to my wife and my son who sacrificed too much for me and always with me to complete the doctoral course.

Copyright © 2019 Nguyen Van Trung  
All right reserved.

*This page intentionally left blank*

## Abstract

### **A Study on Code-Modulated Synchronized-OOK Transceiver for Low Power Wireless Sensor Networks**

NGUYEN VAN TRUNG

Doctoral Program in Electronics Engineering

The University of Electro-Communications

Wireless Sensor Networks (WSNs) currently has attracted significant attention because of its unlimited potential. Normally, a WSN composes of few or hundreds or even thousands spatially distributed sensor nodes which are able to sense, self-process and communicate through wireless channel. To satisfy these function, a sensor node often consists of sensor, microprocessor, memory, power supply and RF communication device. In which, transmission and reception using RF transceiver consumes most power of a sensor node. In condition that sensor node is supplied by limited power source, reducing power consumption of RF transceivers is critical to prolong lifetime of sensor node. Besides, along to technology advancement, wireless devices have been used popularly, which leads to a scenario that sensor node operates simultaneously with other nodes and other wireless devices in the vicinity. These easily become interference sources which can have negative effects on WSN. Such fact demands enhancing immunity of RF transceiver in WSNs. This thesis studies to design a low power TRX system high immunity to interference using for low power WSNs.

In order to achieve the target, this thesis considers several issues of modulation scheme, operation mode and hardware design. In terms of modulation scheme, the study exploits low power advantage of OOK and S-OOK system in combination with ability of withstanding to interference of spread spectrum technique to propose Code-Modulated Synchronized-OOK (CMS-OOK) scheme. CMS-OOK system not only reduce significantly power consumption but also enhance system immunity to interference by assigning different codes to different nodes. According to this scheme, *DATA* which needs to be sent, firstly, is

transformed to synchronized data (*SDATA*) including synchronized pulses and data pulses. By this way, data '1' is represented by a synchronized pulse and a data pulse while only a synchronized pulse is used to display data '0'. Then, a code, which is generated in those pulses interval, is multiplied with *SDATA* to create Code-Modulated Synchronized Data (*CMSDATA*). Finally, this signal is modulated by 2.4GHz carrier and radiated to free space through antenna. In order to demodulate CMS-OOK signal is sent from the TX, CMS-OOK RX utilizes envelop detector and comparator structure in cooperation with digital correlator. Issue of synchronizing received signal and the pre-agreed code is addressed by using 2x- or 4x-oversampling digital correlator.

Regarding to operation mode, the system deploys intermittent communication or normally-off operation to decrease power consumption. Intermittent and normally-off operation mode are originated as a way of computing which is used for energy saving purpose. Authors who develop Beat sensor networks applied normally-off operation mode to their system and manifested its energy efficiency. Other group implemented their receiver with intermittent operation can reduce a half of power consumption. The challenge of these operation modes is the settling time of carrier oscillator. Whenever sensor node wants to send a data, it takes time to settle the carrier oscillator from sleep (intermittent operation) or power-off (normally-off operation) state. This time is call settling time. During this time, RF TX consumes amount of energy. The longer settling time of TX is, the more power is dissipated. The proposed CMS-OOK TX utilizes low power ring oscillator (RO) as carrier generator, which usually has short settling time. Whereby, TX can be almost completely turned-off (normally-off operation) or consume a small sleeping power (intermittent operation) when no data is sent and wake-up fast from the power-down state or sleep state to start transmitting data. This short wake-up time helps CMS-OOK TX save more power than that of other TXs which use crystal oscillator or PLL oscillator with high stable frequency but long setting time.

Relating to hardware design, the thesis considers about architecture, circuit design and fabrication technology. Firstly, 65nm SOTB CMOS technology is chosen for implementation of CMS-OOK TRX system. With valuable features such as low operation voltage, small leakage current, ability of body bias control, SOTB CMOS commensurate

with low power applications. Besides, the thesis also investigates RF characteristics of SOTB devices. A pair of SOTB NMOS and PMOS with gate length of 60nm, total width of  $8 \times 6 \mu\text{m} = 48 \mu\text{m}$  were designed, fabricated and evaluated. Devices evaluation results show cut-off and maximum frequency of NMOS are, respectively, 40GHz and 28GHz, while those of PMOS are consequently 26GHz and 20GHz. These frequencies are far higher than 2.4GHz frequency, the target frequency of the proposed CMS-OOK TRX, which guarantees that these devices are able to use for RF applications.

Basing on SOTB devices, a pair of 2.4GHz TX and RX using CMS-OOK modulation scheme are designed, simulated and fabricated. On TX side, OOK modulation allows to utilize large jitter carrier oscillator like ring oscillator (RO) as well as high-efficiency and low-linearity E-class power amplifier. This contributes on reducing power for TX. Besides, thanks to code modulation and sweeping body bias voltage of SOTB devices, bandwidth of TX output spectrum is widen and peak power of spectrum is reduced. Evaluated results of 65nm SOTB device-based CMS-OOK TX chip show that the TX consumes average  $83 \mu\text{W}$  at 1kbps data transmission and achieves  $-62 \text{dBm/MHz}$  power spectral density with 15MHz bandwidth (using 31-bit code), which satisfies the FCC radio regulations. On the other side, we also propose a CMS-OOK RX which, then, is simulated and fabricated on 65nm SOTB CMOS. The RX consists of analog RF front-end including a low noise amplifier (LNA) in series with 4-stage RF amplifier, followed by envelope detector and comparator, and a digital part at the end. LNA and RF amplifier contribute on reducing noise figure and increasing gain to improve RX sensitivity. In digital part, a 2x-oversampling digital correlator is used to decode received CMS-OOK signal in order to recover data clock and data sent from the TX. The digital part also generates a window pulse (RFENA) to turn-on and turn-off RF front-end to save power consumption. By simulation using SOTB CMOS models, analog part of the RX consumes average  $38.8 \mu\text{W}$  at 1kbps data rate with  $-76 \text{ dBm}$  sensitivity. Besides, system simulation shows a 10 times lower BER of CMS-OOK system in comparison with that of OOK system in condition that interference is not too strong, which states that immunity of RX is improved. Experiment results of TRX system with discrete TRX RF modules and FPGA board show that CMS-OOK scheme can be implemented successfully.

CMS-OOK TRX brings to us a lot of benefits when applied to low power WSNs. Firstly, in term of power consumption, as the wake-up time is very short, the CMS-OOK TX nearly consumes no power during this time. This helps the TX save much power in comparison with other TXs using crystal oscillator or PLL oscillator. For example, in an experiment in our laboratory with a normally-off WSN using LoRa TRX with crystal oscillator shows that the wake-up time takes 150ms and TX consumes average 25mW, this means TX consumes total 3.75mJ which even is much higher than required power to send necessary data (2.5mJ). On the RX side, applying S-OOK technique in combination with code modulation reduces significant power consumption. Saved power is depends on the ratio between data bit duration and synchronized pulse duration. As a result, maintaining power supply for TRX becomes more relaxed, which is suitable to EHWSN with intermittent or normally-off operation. Secondly, Code-Modulation and sweeping body bias voltage in TX are spreading spectrum technique which produces numerous advantages. With wider bandwidth and lower peak power transmission, CMS-OOK TRX easily satisfies the radio regulations. Moreover, spreading-spectrum technique helps TRX increase not only the sensitivity but also the immunity to interference of RX by 4dB in signal to interference ratio (SIR) in comparison with that of OOK TRX. This means communication range and reliability of TRX are enhanced. With these benefits, CMS-OOK TRX can be applied for low power WSNs.

*This page intentionally left blank*

# Contents

<b>Acknowledgements</b> .....	<b>iii</b>
<b>Abstract</b> .....	<b>vii</b>
<b>List of Tables</b> .....	<b>xv</b>
<b>List of Figures</b> .....	<b>xvi</b>
<b>List of Abbreviations</b> .....	<b>xix</b>
<b>Chapter 1</b> .....	<b>1</b>
<b>Introduction</b> .....	<b>1</b>
1.1    Research background .....	1
1.1.1    Wireless sensor networks .....	1
1.1.2    Energy harvesting WSN with intermittent and normally-off operation .....	4
1.1.3    Interference in wireless communication – Radio regulations .....	6
1.2    Purpose of the study .....	7
1.3    Dissertation layout.....	10
<b>Chapter 2</b> .....	<b>15</b>
<b>Considerations of Wireless Sensor Networks for Low Power, Longer Communication Distance and Immunity to Interference</b> .....	<b>15</b>
2.1 Low power TRX design .....	15
2.1.1 Link budgeting .....	15
2.1.2 Modulation scheme and architecture.....	16
2.1.3 Operation mode .....	18
2.2 Spread-spectrum technique .....	18
2.4 Conclusion.....	22
<b>Chapter 3</b> .....	<b>28</b>
<b>Proposal of Code-Modulated Synchronized – OOK Modulation Scheme</b> .....	<b>28</b>

3.1 Synchronized-OOK modulation.....	29
3.2 Spread-Spectrum communications and Direct-Sequence Spread-Spectrum technique .....	31
3.3 Code-Modulated Synchronized-OOK scheme .....	32
3.4 Chapter conclusion.....	37
<b>Chapter 4.....</b>	<b>39</b>
<b>Wide bandwidth CMS-OOK Transmitter Using 65nm SOTB CMOS Technology with Sweeping Body Bias Technique .....</b>	<b>39</b>
4.1 Block diagram and operation .....	39
4.2 A 65nm SOTB devices-based TX circuit.....	40
4.3 Simulation results.....	41
4.4 Experiment results.....	45
4.5 Chapter conclusion.....	50
<b>Chapter 5.....</b>	<b>52</b>
<b>Low-Power and High Immunity to Interferences CMS-OOK Receiver .....</b>	<b>52</b>
5.1 System architecture of the CMS-OOK RX .....	52
5.2 Circuit level design bases on 65nm SOTB devices.....	53
5.2.1 Analog part.....	53
5.2.2 Digital part.....	59
5.3 Simulation results.....	64
5.5 CMS-OOK TRX system experiment with discrete RF module and FPGA board. ....	69
5.6 Conclusion.....	71
<b>Chapter 6.....</b>	<b>73</b>
<b>Consideration of Applying CMS-OOK Transceiver to Low Power Wireless Sensor Networks .....</b>	<b>73</b>
6.1 Power consumption of the TX .....	73
6.2 Interference resistance of CMS-OOK TRX system .....	78
6.3 Interference experiment of system using discrete RF modules and FPGA.....	82
6.4 Conclusion.....	85

<b>Chapter 7</b> .....	87
<b>CONCLUSION</b> .....	87
<b>APPENDIX A</b> .....	90
<b>APPENDIX B</b> .....	93
<b>AUTHOR BIOGRAPHY</b> .....	95

## List of Tables

1.1	Energy contribution in a sensor node.....	7
2.1	Settling time comparison.....	18
4.1	Comparison with State of Art (TX).....	50
5.1	Comparison with published State of Art (RX).....	68

## List of Figures

1.1	Wireless Sensor Networks	2
1.2	General architecture of a Sensor Node	3
1.3	Power schematic of transmitter in a) Intermittent operation and b) Normally-off operation	4
1.4	Power consumption comparison between conventional operation and normally-off operation [1-14]	5
1.5	Interferences in the vicinity	6
1.6	Power distribution in the low-energy adaptive clustering hierarchy sensor node	8
2.1	A generic low-complexity TRX system architecture	16
2.2	Power versa sensitivity radio survey	17
2.3	Spread Spectrum Communications system	19
2.4	The structure of SOTB CMOS	20
2.5	Chip photo of investigated SOTB	21
2.6	Measured $F_T$ and $F_{max}$ of 65nm SOTB CMOS at $V_d = 1.2V$ , $V_g = 0.65V$ , $V_b = 0$ for NMOS, $V_d = -1.2V$ , $V_g = -0.65V$ , $V_b = 0$ for PMOS	21
3.1	a) Conventional OOK signal    b) S-OOK signal	29
3.2	Current consumption of the S-OOK RF front-end	30
3.3	SS communication system (a) and spectrum transformation (b)	31
3.4	Waveform operation of CMS-OOK TX	32
3.5	Waveform operation of S-OOK RX	33
3.6	Architecture of CMS-OOK TX	35
3.7	Architecture of CMS-OOK RX	35
3.8	Dependence of BW on number of code bit during synchronized pulse duration	36
4.1	Architecture of CMS-OOK Transmitter	39

4.2	Architecture of the digital part	40
4.3	Timing chart of the CMS-OOK TX	40
4.4	Detailed schematic of the analog part of CMS-OOK TX	42
4.5	Waveform of TX produced by HSPICE simulator	43
4.6	Dependence of carrier frequency on body voltage swing (simulated)	43
4.7	Dependence of RO BW AND TX BW on body voltage swing (simulated)	44
4.8	Dependence of TX output spectrum on body voltage swing (simulated)	44
4.9	Layout picture of TX analog part and TX board	46
4.10	Experiment setting up diagram	46
4.11	Measured real-time waveform (31-bit code) (1) Synchronized pulse, (2) Data pulse	47
4.12	Spectrum of CMS-OOK signal with single carrier frequency	47
4.13	Spectrum of S-OOK and CMS-OOK signals	48
5.1	Spectrum of S-OOK and CMS-OOK signals	52
5.2	CMS-OOK RX in combination with Wake-up RX	54
5.3	Operation waveform of CMS-OOK RX	54
5.4	Detailed schematic of RF front-end (Analog part)	55
5.5	LNA schematic	56
5.6	4-stage RF Amplifier	56
5.7	Envelope detector and Comparator	57
5.8	Spiral inductor	58
5.9	An on-chip 14nH spiral inductor in 65nm SOTB process	58
5.10	Block diagram of digital part	59
5.11	Timing chart of digital part	59
5.12	31-bit 2x-sampling digital correlator	60
5.13	Detailed structure of RFENA Generator and S-OOK demodulator	61
5.14	Schematic (a) and symbol (b) of Pulse Forming, Short Pulse and Long Pulse blocks	62
5.15	Timing chart for recovering data	62
5.16	Timing chart for RFENA Generator	63

5.17	Layout picture of CMS-OOK RX	65
5.18	Transient simulation results	66
5.19	Noise figure, S11 and S21 of RF front-end	67
5.20	Simulation results of digital part	67
5.21	Experiment setting up diagram	69
5.22	Experiment setting up	69
5.23	Operation wave form of experiment	70
6.1	Intermittent operation TX	74
6.2	Normally-off operation TX	74
6.3	Normally-off operation of CMS-OOK TX	74
6.4	Waveform of original data, synchronized data and CMS data	76
6.5	Co-located TX inside same WSN as an interference source	78
6.6	Simulation diagram of system with 2 TX and 1 RX	79
6.7	Adjusting threshold of correlator to recover data	80
6.8	BER comparison between OOK and CMS-OOK TRX	81
6.9	BER comparison between OOK and CMS-OOK TRX at low SNR	81
6.10	Interference experiment of CMS-OOK system with 2 TXs and 1 RX configuration	83
6.11	Interference experiment results	84

## List of Abbreviations

ADC	Analog to <b>D</b> igital <b>C</b> onverter
BER	<b>B</b> it <b>E</b> rror <b>R</b> ate
BW	<b>B</b> and <b>W</b> idth
CMOS	Complementary <b>M</b> etal <b>O</b> xide <b>S</b> emiconductor
CMS-OOK	<b>C</b> ode- <b>M</b> odulated <b>S</b> ynchronized- <b>O</b> OK
CS	<b>C</b> ommon <b>S</b> ource
DAC	<b>D</b> igital to <b>A</b> nalog <b>C</b> onverter
DS-SS	<b>D</b> irect <b>S</b> equence <b>S</b> pread <b>S</b> pectrum
EH	<b>E</b> nergy <b>H</b> arvesting
EHWSNs	<b>E</b> nergy <b>H</b> arvesting <b>W</b> ireless <b>S</b> ensor <b>N</b> etworks
FD-SOI	<b>F</b> ully <b>D</b> epleted <b>S</b> ilicon- <b>O</b> n- <b>I</b> nsulator
FOM	<b>F</b> igure <b>O</b> f <b>M</b> erit
FSK	<b>F</b> requency <b>S</b> hift <b>K</b> eying
IoT	<b>I</b> nternet <b>o</b> f <b>T</b> hing
LNA	<b>L</b> ow <b>N</b> oise <b>A</b> mplifier
MCU	<b>M</b> icro <b>C</b> ontroller <b>U</b> nit
OOK	<b>O</b> n- <b>O</b> ff <b>K</b> eying
PLL	<b>P</b> hase <b>L</b> ocked <b>L</b> oop
PSD	<b>P</b> ower <b>S</b> pectral <b>D</b> ensity
PSK	<b>P</b> hase <b>S</b> hift <b>K</b> eying
RF	<b>R</b> adio <b>F</b> requency
RO	<b>R</b> ing <b>O</b> scillator
RX	<b>R</b> eceiver
SN	<b>S</b> ensor <b>N</b> ode
SER	<b>S</b> ymbol <b>E</b> rror <b>R</b> ate
SIR	<b>S</b> ignal to <b>I</b> nterference <b>R</b> atio
SNIR	<b>S</b> inal to <b>N</b> oise and <b>I</b> nterference <b>R</b> atio
SNR	<b>S</b> ignal to <b>N</b> oise <b>R</b> atio

S-OOK	Synchronized- <b>O</b> n- <b>O</b> ff <b>K</b> eying
SOTB	Silicon <b>O</b> n Thin <b>B</b> uried <b>O</b> xide
SS	Spread Spectrum
TRX	Transceiver
TX	Transmitter
ULP	Ultra <b>L</b> ow <b>P</b> ower
UWB	Ultra <b>W</b> ide <b>B</b> and
WSN	Wireless <b>S</b> ensor <b>N</b> etwork

# **Chapter 1**

## **Introduction**

In this chapter, the background of Wireless Sensor Networks, energy harvesting Wireless Sensor Networks with intermittent and normally-off operation modes and interference in wireless communication are presented. Then, the purpose of the study is shown through the challenges to achieve study targets. Finally, that is the dissertation layout for clarifying the structure of this dissertation.

### **1.1 Research background**

#### **1.1.1 Wireless sensor networks**

Recently, Internet-of-Things (IoTs) has been emerged as one of the most important parts of current technology revolution. It helps to realize communication between a lot of objects, machines and devices [1-1, 1-2]. Wireless Sensor Networks (WSNs) are the key elements of the IoTs because they can help users to interact with their environment by sensing or controlling physical parameters. Collaborating of individual nodes is a good way to fulfill tasks that single node is incapable of doing so. Because of downsides of wire communication such as high cost, less flexibility and mobility and so on, wireless communication is commensurate to enabling this collaboration. Applications of WSNs lie on various sections from environment monitoring, smart home to medical applications and so on. Besides, recent advances in technology have made it possible to produce not only tiny size with multiple sensors but also low power consumption, low cost, adaptability, mobility and convenience. These make the usage of WSNs be increasing exponentially and become an attractive object to many researchers. [1-3, 1-4]

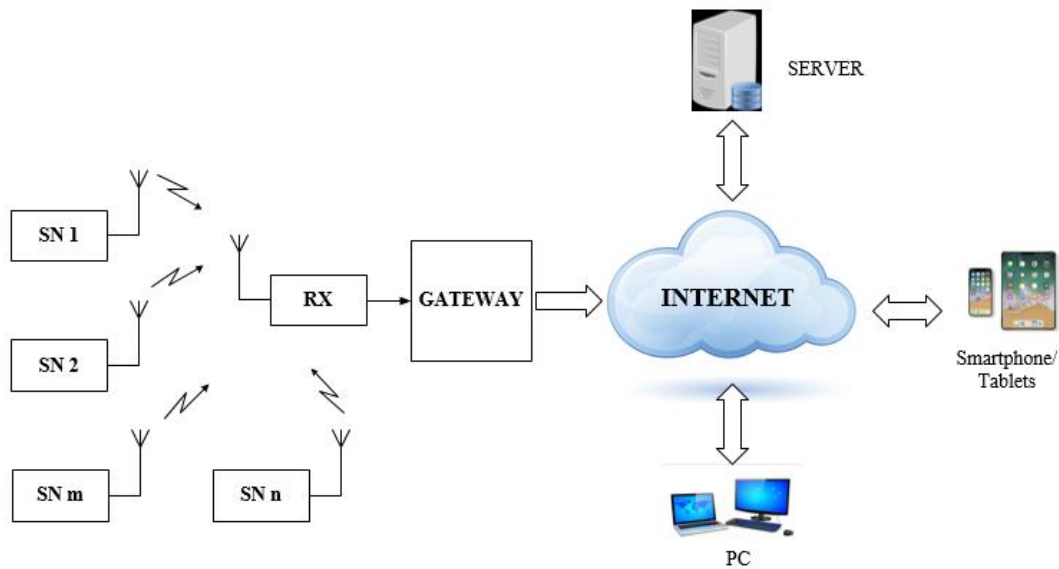


**Fig. 1.1:** Wireless Sensor Networks

A WSN normally composes of few to several hundreds or even thousands spatially sensor nodes which are capable of sensing, data self-processing and communicating to the others through wireless channel [1-5] as shown in Fig. 1.1. In order to fulfill these functions, a sensor node (SN) often consists of five main components: sensors/actuators, microcontroller, memory, power supply and communication device (Fig. 1.2). In which, microcontroller is the heart of a wireless sensor node because it accumulates information from the sensors, self-processes this data, makes decision of when and where to send the data, receives data from other sensor nodes, and decides react of the actuators. The sensors monitor and collect necessary data from its objective in shape of electrical signals which are led to the controller via Analog to Digital Converter (ADC). The actuators are used to execute commands from the controller corresponding to a particular task such as controlling a motor, a light and so on. In many cases, it is necessary to use memory to store intermediated sensors data, packets from other nodes, and so on. Next component of the sensor node is radio communication device which establishes wireless connections to the other sensor nodes. Normally, it is convenient to use a communication device which combines transmitter (TX) and receiver (RX) as a single entity called transceiver (TRX). All sensor node is powered up by power supply which can be batteries or energy harvesting circuits with limited amount of energy, hence limiting the sensor node lifetime. Popularly, battery can

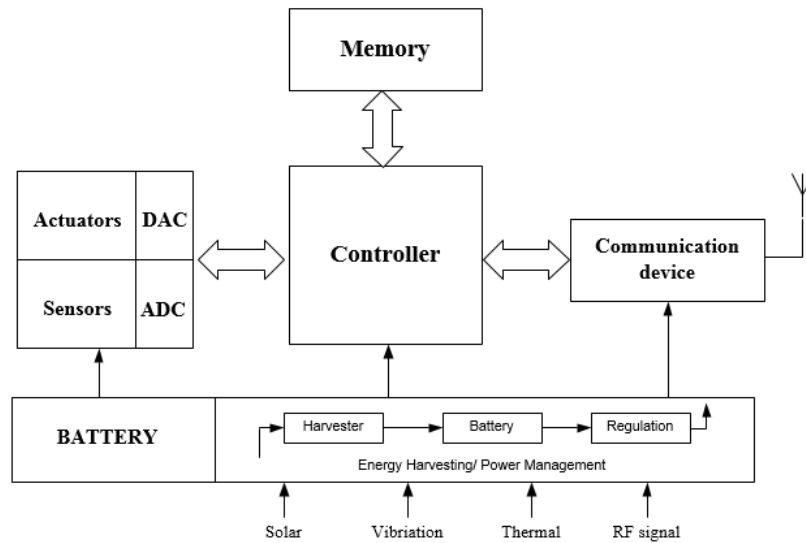


**Fig. 1.2:** General architecture of a Sensor Node

rarely satisfy design goals of long network life time and high reliability while energy harvesting circuits, which convert various kinds of energy to electrical energy, can guarantee for long lifetime but high cost. A hybrid circuit which is a combination of energy harvesting circuit and batteries has desirable potential to deal with the trade-offs of long lifetime and reasonable low cost [1-6].

In order to build a WSN, designers firstly need to understand the requirements and challenges. Depending on applications, the requirements of WSNs are various. However, generally below metrics are considered [1-4, 1-5]:

- Quality of service: Depending on type of specified applications, quality of service can be high reliability or latency or others.
- Lifetime: This is a very important figure of merit (FOM) of a WSN. In many scenarios, sensor node operation has to rely on a limited power supply (batteries or EH circuits or hybrid). It is usually not practicable to replace these energy sources because of huge number of sensor nodes. Thus, WSNs are expected to operate at least for a given mission time or as long as possible. It is noticeable that lifetime has direct trade-offs against quality of services, which need to be considered carefully in designing WSNs.

- Scalability: As the number of sensor nodes can be huge, the employed design must be able to scale to that number.
- Maintainability: The WSNs must be able to change to adapt to change of ambient environment and itself.
- Mobility: It is ability of the WSN to handle mobile nodes and changeable data paths.
- Programmability: WSN with changeable programming can not only self-process information but also react flexibly on changes of it tasks.

### 1.1.2 Energy harvesting WSN with intermittent and normally-off operation

As regarded in previous section, lifetime is one of the most important requirements of a WSN. The sensor nodes lifetime mainly depends on the battery capacity. However, the sensor nodes expenditure is a critical issue in practical WSNs designing. It is usually economically advantageous to discard a sensor nodes rather than sensor nodes recharging

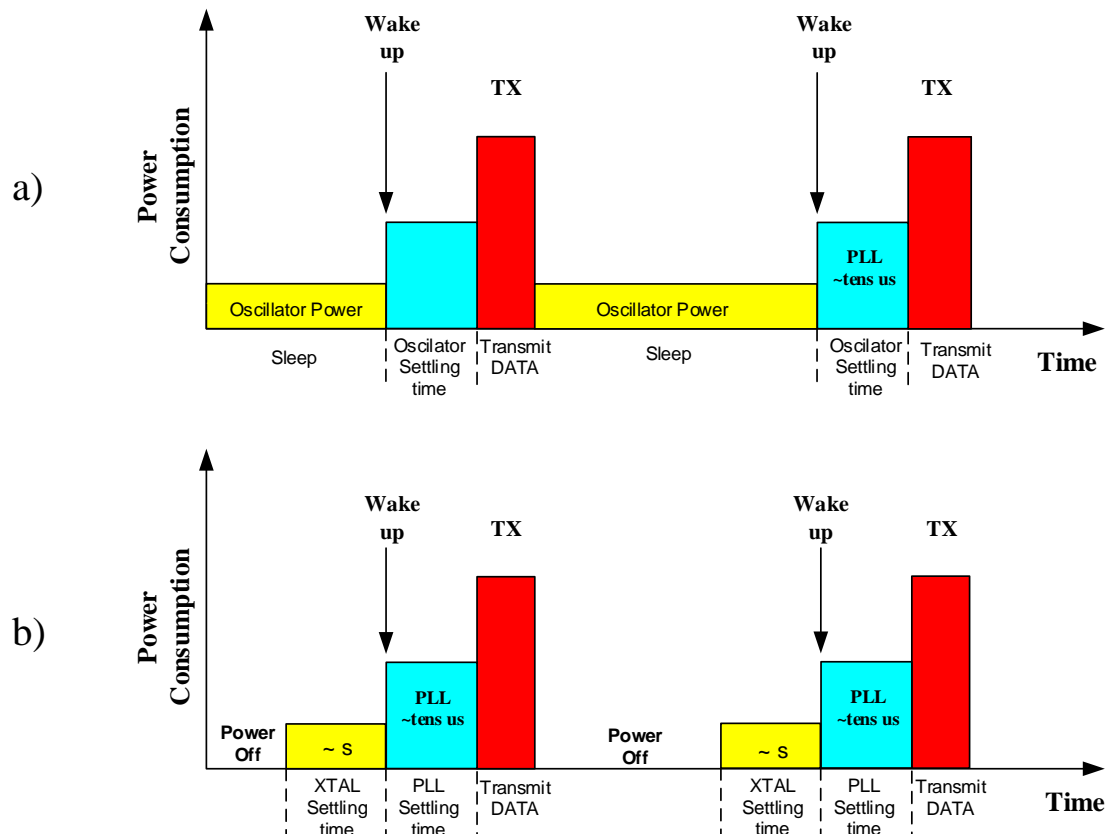
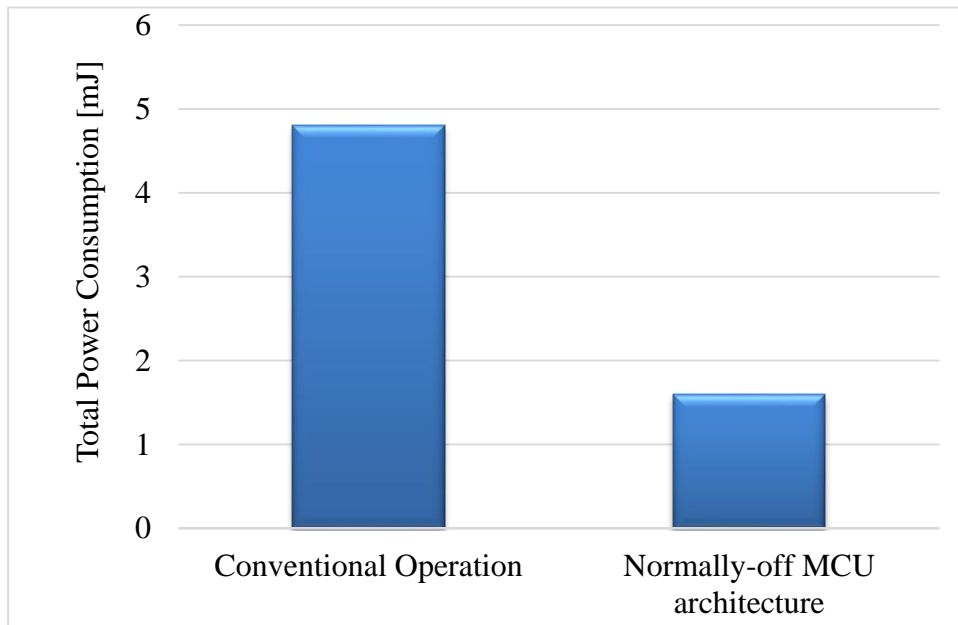


Fig. 1.3: Power schematic of transmitter in  
a) Intermittent operation and b) Normally-off operation



**Fig. 1.4:** Power consumption comparison between conventional operation and normally-off operation [1-14]

[1-7]. There is a range of approaches for resolving this issue is proposed in [1-7 - 1-15] such as collecting energy from ambient environment [1-7 – 1-10, 1-15], routing algorithm [1-11, 1-12], developing power management method [1-13, 1-14, 1-15], etc. One of the most interesting technique to prolong the WSNs lifetime is Energy Harvesting (EH) in which the sensor nodes can recharge their batteries by harvesting renewable energy from ambient environment, such as sunlight, vibration, wind, radio signal and so on, then store it in a battery or super-capacitor [1-16]. This helps WSNs operate quasi-perpetually due to the large number of recharge cycles while the surrounding energy source is nearly unlimited.

Regularly, EH circuits often harvest and buffer energy, then produce for the SN operating as soon as sufficient energy is banked. As energy is not always available or it takes time for harvesting and buffering enough energy to do a useful amount of work, operation in EHSN is usually intermittent [1-15]. Another effective operation mode for EHSN is deploying normally-off radio TRX, which directly cuts down the power consumption of the TRX. Both intermittent and normally-off operation are the ways of computing which switch to sleep mode or aggressively powers off components of computer systems when they need not to operate [1-13, 1-15, 1-16]. The authors in [1-9, 1-10] applied and develop normally-off operation mode to BEAT sensor network which shows a very low power consumption.

Moreover, the low-power sensor node using normally-off MCU architecture in [1-14] can reduce its power consumption by around 70% (Fig. 1.4). In [1-16], thanks to intermittent operation, the RX consumes only a half power in comparison with full-time operation. The power schematic of TX in intermittent and normally-off operation mode are shown in Fig. 1.3. With intermittent operation in Fig. 1.3a), SN often sleeps with small power consumption when no data needs to be sent. As soon as it needs send a data, the oscillator is waken-up firstly then TX will transmit the data. As can be seen from Fig. 1.3b), when there is no data needs to be sent, the TX in the sensor node is in power-off state for saving energy. Whenever the TX needs to send data to other nodes, it will be powered up to transmit data through wireless channel. In both cases, carrier oscillator of the TX require a time duration to start-up before becoming stable to transmit data. This settling time can be short or long, which is depends on what kind of oscillator is deployed. Anyways, it is obvious that the longer start-up time of oscillator is, the more power TX is consumed definitely. Hence, finding out a solution to reduce start-up time of TX carrier oscillator promises much power consumption cut-down.

### 1.1.3 Interference in wireless communication – Radio regulations

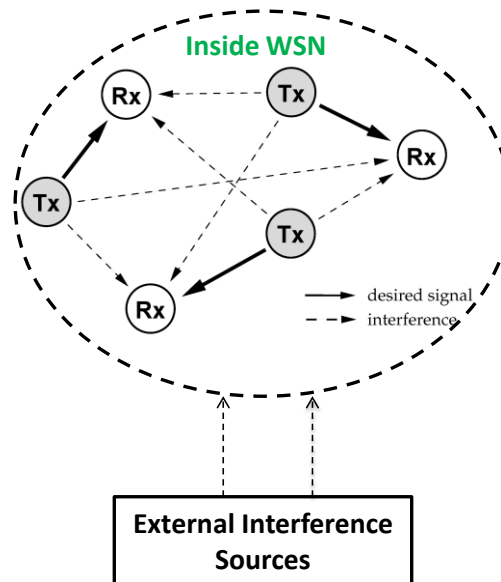


Fig. 1.5: Interferences in the vicinity

**Table 1.1:** Energy contribution in a sensor node

Component	Percentage (%)
Sensor	6.8
CPU	15.7
Transceiver	77.5
Total	100

Wireless system designers always have to cope with interferences from both natural sources and other users of medium [1-18]. Especially, advances of technologies make demand of connections become more and more, which leads to a scenario that any wireless system has to live with interference created by other systems in the vicinity (Fig. 1.5). Besides, as the fact that exploiting very high frequency applications up to hundreds GHz or beyond face to many tough challenges, radio frequency is a valuable and limited resources. For example, 2.4 GHz ISM band is the most widely used frequency by applications of WiFi, ZigBee, short-range communication, and so on. Such a fact makes wireless systems have to share the same frequency band, which is easily to create negative effects on other systems. Bad impacts of interference often make performance of WSNs become worse, from reducing quality of services to congest the communication, even blocking the communication in WSNs. Therefore, all wireless systems must be robust against interference from other systems.

As regarded above, sharing common valuable frequency resource easily creates interferences to other same frequency band. In principle, the stronger desired signal power in comparison with the interferences, the less negative effects on the system are. However, that can result in a race of increasing TX power, which makes the situation become worse and worse. That such fact demands a radio regulations to guarantee that wireless systems can operate functionally with less bad effects from the others. Hence, while developing wireless systems, designers have to consider to not violate the radio regulations.

## **1.2 Purpose of the study**

It is noticeable that most energy of a sensor node is consumed in transmission and reception data by its radio TRX. A study in [1-5] shows that about 77.5% of total sensor node energy

is spent by the radio TRX (Table 1.1). In other work in [1-19] estimated the energy consumption for communication, processing, transient, sensor loggings and sensing of a low-energy adaptive clustering hierarchy sensor node. The pie chart describing of components is shown in Fig. 1.6. It is easy to realize from this pie that more than a half of total sensor node energy is spent on wireless communication.

In major of WSNs study, main energy sources supplying for the sensor node are portable and limited sources such as battery or energy harvesting (EH) circuits. This can lead to a situation that whenever power source becomes exhausted, the sensor node no longer complete its duty unless the power source is replenished. Besides, battery-powered WSNs also reveal other disadvantages such as inconvenience in replacing for numerous number of sensor nodes, capability of posing an environment risk, etc. EH-WSNs accumulating power from renewable source in ambient environment is an excellent solution to address the battery issue. However, even in that such case, power supply still is not unlimited. Thus, it is necessary to use the power effectively to prolong the sensor nodes lifetime.

There are various methods which were proposed to increase lifetime of sensor nodes, in which reducing power consumption of radio TRX, including both TX and RX, is the best

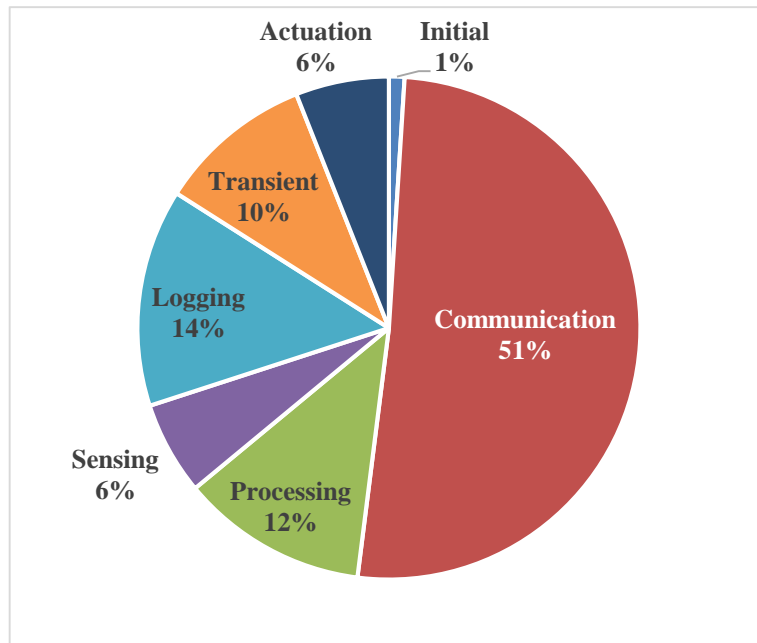


**Fig. 1.6:** Power distribution in the low-energy adaptive clustering hierarchy sensor node

effective and directly way to improve sensor node lifetime. Dealing with this issues demands designers to consider a combination of following issues:

- Modulation scheme

This is one of the most effective factor to reduce power of TRX system. It completely decides the structure of TRX is complex or low-complex, which directly effects on the power consumption of TRX. The simpler modulation scheme, the more power consumption cut-down.

- Operation mode

This controls the way TRX operate. It decides whether TRX works continuously or intermittent or periodically, or in cooperation with wake up receiver and so on.

- Frequency band

This has effects on the selection of device technology and circuit topologies. Also, it constrains the specification of TRX system under the radio regulations at that frequency band.

- Low power architecture and circuit

Basing on the modulation scheme considered above, the architecture of TRX is sketched. To deploy TRX corresponding to the designed structure, low power circuit topologies are considered and exploited carefully.

- Device technology

It is obvious that development of RF TRX is always accompany with the pace of device technologies. Designers need to consider to select the best suitable and feasible technology for their design.

Besides, in circumstance that there are a lot of co-allocated RF devices operate simultaneously, robustness against noise and interference from environment and other RF systems is a crucial metric needs to be considered. These unwanted signals can come from other TXs sending in the same band at the same time (multiple access interference) or from other devices such as microwave ovens, these create co-channel interference. Adjacent-channel interference works in a neighbor band of TRX can inject a part of it power to TRX because of poor-slope filters [1-5]. All of them can make errors for TRX operation, this often is estimated via symbol or bit error rate (SER or BER). SER or BER of TRX system depends

on the actual modulation scheme and on the ratio of the received signal power and the noise and interference power (SNIR). In theory, the lower SNIR is, the smaller SER or BER is. There are some solutions for TRX robustness against interference such as using angle modulation (frequency and phase modulation) or utilizing coherent receiver or applying spread spectrum technique. These solutions produce not only good resistance against interference but also excellent sensitivity. However, they cost complex structure and as a consequence, consume more power.

Thus, addressing this trade-offs between low power operation and robustness against interference is one of the purposes of this study.

In addition, this study also concerns about the communication range of the TRX system according to the range of WSN applications. Theoretically, communication distance can be increased by raising TX output power, RX sensitivity and gain of the antenna. Consider in the case of same antenna, we can lengthen communication range by increasing TX output power or enhancing RX sensitivity or both. Regarding to the former solution, increasing output power of TX can be done easily but the downside of this is that TRX system can suffer violence the radio regulations. On the other hand, improving sensitivity is very popular but it often costs more power consumption. These trade-offs also are the other objective of this study.

In general, in this study, we focus on finding the solutions to design a TRX system with low power consumption, robustness to interference and good communication range which is used for low power WSNs.

### **1.3 Dissertation layout**

The dissertation composes of seven chapters as followed:

- Chapter 1 gives an overview of WSNs in terms of requirements, specifies the purpose of the study and the challenges need to be addressed to fulfill the objective.
- Chapter 2 present the consideration in low power design in terms of modulation scheme, operation mode, architecture and circuit, and device technology to give the solutions to cope with the challenges shown in Chapter 1.

- Chapter 3 presents a new modulation scheme so-called as Code-Modulation Synchronized-OOK (CMS-OOK) with the waveform, architecture and basic benefits of this scheme
- Chapter 4 describes the architecture of CMS-OOK transmitter with low-complexity, suitability to normally-off operation mode. A CMS-OOK TX using sweeping body bias technique based on 65nm SOTB CMOS technology is designed, simulated and evaluated.
- Chapter 5 demonstrates architecture of CMS-OOK receiver which allows to increase sensitivity and enhance resistance to interference. A CMS-OOK RX is designed, simulated and fabricated in 65nm SOTB CMOS technology.
- Chapter 6 analyze the benefits and consider the suitability of CMS-OOK TRX to low power WSNs.
- Finally, Chapter 7 summarizes the research issues and the achieved results; discusses limitations need to continue dealing with in the future.

## References

- [1-1] “Tech Trends 2018: The symphonic enterprise.” [Online]. Available: [https://www2.deloitte.com/content/dam/insights/us/articles/Tech-Trends-2018/4109\\_TechTrends-2018\\_FINAL.pdf](https://www2.deloitte.com/content/dam/insights/us/articles/Tech-Trends-2018/4109_TechTrends-2018_FINAL.pdf). [Accessed: 10<sup>th</sup> Nov. 2018]
- [1-2] I. Khan, F. Belqasmi, R. Glitho, N. Crespi, M. Morrow, and P. Polakos, “Wireless Sensor Network Virtualization: A Survey,” *IEEE Communication Surveys & Tutorials*, Vol. 18, No. 1, First quarter 2016, pp. 553-576.
- [1-3] V. Jindal, “History and Architecture of Wireless Sensor Networks for Ubiquitous Computing,” *International Journal of Advanced Research in Computer Engineering & Technology (IJARCET)*, Vol. 7, Issue 2, Feb. 2018, pp. 214-217.
- [1-4] C. Chong and S. P. Kumar, “Sensor Networks: Evolution, Opportunities, and Challenges,” *Proceedings of the IEEE*, Vol. 91, No. 8, Aug. 2003, pp. 1247-1256.
- [1-5] H. Karl, and A. Willig, “Protocols and architectures for Wireless Sensor Networks,” John Wiley & Sons, West Sussex, England, 2005.
- [1-6] A. E. Zonouz, L. Xingm, V. M. Vokkarane, Y. L. Sun, “Hybrid wireless sensor networks: a reliability, cost and energy-aware approach,” *Journals IET Wireless Sensor Systems*, Vol.6, Iss. 2, Jan. 2016, pp. 42-48.
- [1-7] V. Shakhov, “On efficiency Improvement of Energy Harvesting Wireless Sensor Networks,” *39<sup>th</sup> International Conference on Telecommunications and Signal Processing (TSP)*, 2016, pp. 56-59.
- [1-8] S. Ulukus, A. Yener, E. Erkip, O. Simeone, M. Zorzi, P. Grover, and K. Huang, “Energy Harvesting Wireless Communications: A Review of Recent

Advances”, *IEEE Journal on Selected Areas in Communications*, Vol. 33, No. 3, pp. 360-381, March 2015.

- [1-9] S. Ishigaki and K. Ishibashi, “Power Beat: A Low-cost and Energy Harvesting Wireless Electric Power Sensing Scheme for BEMS,” *IEEE ICBEST 2015*, Aug 2015.
- [1-10] R. Takitoge and K. Ishibashi et. al., “Temperature Beat: Persistent and Energy Harvesting Wireless Temperature Sensing Scheme,” *IEEE SENSORS 2016*, Nov. 2016.
- [1-11] P. Kaushik, J. Singhai, “Energy Efficient Routing Algorithm For Maximizing the Minimum Lifetime of Wireless Sensor Network: A Review,” *Intenational Journal of Ad hoc, Sensor & Ubiquitous Computing (IJSUC)* Vol.2, No.2, pp. 25-36, June 2011.
- [1-12] J. H. Chang, L. Tassiulas, “Maximum Lifetime Routing in Wireless Sensor Networks, *IEEE/ACM Transactions on Networking*,” Vol. 12, No.4, August 2004, pp. 609-619.
- [1-13] H. Nakamura, T. Nakada, and S. Miwa, “Normally-Off Computing Project: Challenges and Opportunities,” 19th Asia and South Pacific Design Automation Conference (ASP-DAC), pp. 1-5, Jan. 2014.
- [1-14] M. Hayashikoshi, H Ueki, H. Kawai, and T. Shimizu, “Normally-Off MCU Architecture and Power Management Method for Low-Power Sensor Network,” *2015 International SoC Design Conference (ISOCC)*, Nov. 2015, pp. 151-152.
- [1-15] B. Lucia, V. Balaji, A. Colin, K. Maeng, abd E. Ruppel, “Intermittent Computing: Challenges and Opportunities,” *2<sup>nd</sup> Summit on Advances in Programming Languages (SNAPL2017)*, 2017.

- [1-16] T. Terada et. al., "A CMOS UWB-IR Receiver Analog Front End with Intermittent Operation," *2007 Symposium on VLSI Circuits Digest of Technical Papers*, 2007, pp. 86-87.
- [1-17] M. A. Khan, Z. A.Khan, S. Ahmed, F. Haldi, and S. H. Ahmed, "Toward Energy Harvesting in Wireless Sensor Networks," *IEEE The 4<sup>th</sup> HCT Information Technology trends (ITT2017)*, Dubai, UAE, Oct. 2017.
- [1-18] C. Rose, S. Uluku, and R. D. Yates, "Wireless Systems and Interference Avoidance," *IEEE Transactions on Wireless Communications*, Vol. 1, No. 3, July 2002, pp. 415-428.
- [1-19] M. N. Halgamuge, M. Zukerman, and K. Ramamohanarao, "An estimation of sensor energy consumption," *Progress In Electromagnetics Research B*, Vol.12, 2009, pp. 259-295.

## **Chapter 2**

### **Considerations of Wireless Sensor Networks for Low Power, Longer Communication Distance and Immunity to Interference**

In this Chapter, some issues of low power consumption, lengthening communication distance and enhancing immunity to interference of TRX are considered. Basing on that, some potential solutions will be proposed and considered to apply.

#### **2.1 Low power TRX design**

Designing radios with ultra-low-power consumption is always an attraction and challenge to RF designers. It can enable a lot of new and exciting applications such as WSNs, IoTs and so on. As RF TRXs often consume most of the power budget in small SNs [2-1], decreasing TRX power consumption is a useful way to reduce device size as well as increase lifetime of SNs. In principle, RF TRX designing often must deal with numerous trade-offs, that is a complex relationship between power, sensitivity, noise, frequency, gain, linearity and supply voltage. Thus, cutting down radio power can be challenging. For purpose of low power, designers must consider to sacrifice one or more other metrics.

##### **2.1.1 Link budgeting**

Consider a representative WSN system operating with 2.4GHz carrier frequency in short range communication. The minimum TX output power can be calculated based on Friis equation for free space as a baseline case [2-2]:

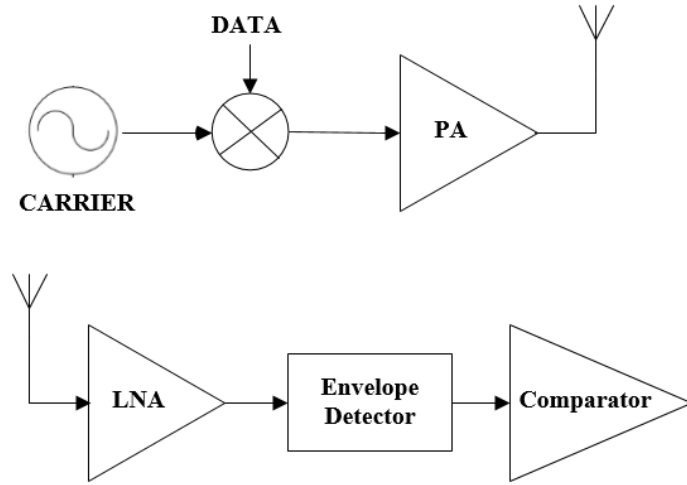


**Fig. 2.1:** A generic low-complexity TRX system architecture

$$P_{receiver} = P_{transmit} + G_{antenna} + 20 \log_{10} \frac{\lambda}{4\pi d} \quad (2 - 1)$$

where  $\lambda$  is the carrier wavelength and  $d$  is the distance between TX and RX. According to equation (2-1), in free space a 10m link suffers from about 60dB of path loss at 2.4GHz band. With a typical surface mount antenna for 2.4GHz has a gain of 0dBi and other reasons can make TX signal experience as much as 30dB loss, TX should have output power of 0 dBm [2-3]. In order to achieve successful operation of TRX, the condition of “ $P_{receiver}$  is higher than RX sensitivity” must be guaranteed. Maximum communication distance is fulfilled under condition of  $P_{sensitivity} = P_{receiver}$  is satisfied. Therefore, communication distance  $d$  can be raised by increasing power of TX or increasing sensitivity of RX. It is notice that increasing power of TX must guarantee to not violate the radio regulations while improving sensitivity of RX often cost more power consumption by using LNA and RF amplifiers.

### 2.1.2 Modulation scheme and architecture

To achieve low power operation, designer has to optimize across all design layers from modulation scheme, architecture to circuits and devices. One of the most effective way to reduce power is decreasing the complexity of modulation scheme which leads to make architecture of TRX become simpler. Conventional super-heterodyne TRX architecture

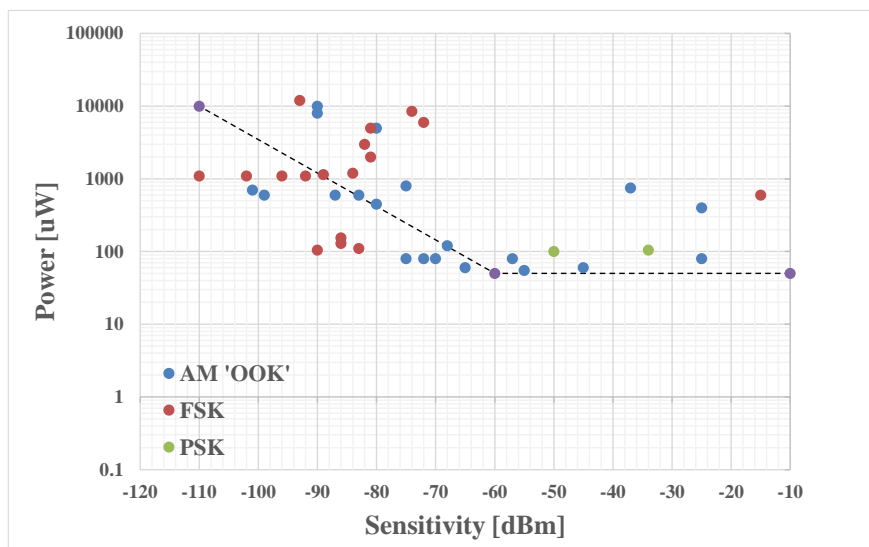


**Fig. 2.2:** Power versa sensitivity radio survey

often adopts quadrature amplitude modulation (QAM) or angle modulation [2-3]. Although, this structure has a lot of advantages, it also brings more additional complexities into TRX system such as phase-locked loop (PLL), high-linear power amplifier (PA). Of course, this means the power of TRX increases.

Employing a non-coherent modulation scheme such as On-Off Keying (OOK) can significantly simplify the architecture of TRX, such as eliminating the PLL, using nonlinear but high efficiency PAs which allows to reduce further power consumption. Hence, low power TRX designers have trend of utilizing OOK modulation scheme with low-complexity architecture as shown in Fig. 2.1. For the same reason, RX structure with envelope detector or super regenerative is prefer. However, adopting this kind of modulation scheme with low-complexity architectures has to face to trade-offs performance in terms of sensitivity, spectral efficiency, resistance to interference etc. Fig. 2.2 shows a low power radio survey in recent time [2-4 – 2-18]. As can be seen, most of OOK RX consumes lower power in comparison with FSK and PSK RX.

This study endeavors to achieve better spectral efficiency, immunity to interference at low power operation.

**Table 2.1:** Settling time comparison

	<b>ISSCC'15 [2-20]</b>	<b>IRFICS'18 [2-21]</b>	<b>LoRa [2-22]</b>	<b>JSSC'16 [2-23]</b>
<b>Type of Oscillator</b>	PLL	PLL	Crystal	Ring Oscillator
<b>Settling time</b>	15 $\mu$ s	0.4 $\mu$ s	250 $\mu$ s	<u><b>0.5ns</b></u>
<b>Frequency Accuracy</b>	High	High	High	Low

### 2.1.3 Operation mode

Normally, the active power of TXs is usually much higher than that of RX [2-19]. Thus, one of the best way to reduce power consumption of TRX is cutting down power consumption of TX. Intermittent and normally-off operations which are discussed in Chapter 1 are the most directly efficient solutions. In order to achieve reducing energy with this operation mode, carrier oscillator of TX must be designed in such a way that TX will completely turn-off or consume a tiny power when no data is sent but wake-up quickly from power-down state to start transmitting data. A comparison between settling time of a ring oscillator, two PLL oscillators and a crystal oscillator is carried on and the comparison results are exhibited in Table 2.1. Obviously, the RO has the shortest-settling time in comparison with other kinds of oscillator, which indicates that RO is completely suitable to intermittent and normally-off operation.

It is popular that OOK TRXs often utilize ring oscillator as carrier source. Besides, as regarded in previous section that OOK modulation scheme is usually preferred for low power purpose. This suggests that OOK TRXs using ring oscillator with low power and short-settling time can reduce huge power when they operate in normally-off or intermittent mode.

## 2.2 Spread-spectrum technique

SS communications with its inherent interference attenuation capability and low peak power spectral density has been very popular. These crucial features of SS technique are noticeable for finding solutions to improve immunity to interference of TRX and increase the power of TX while still ensure to meet radio regulations.

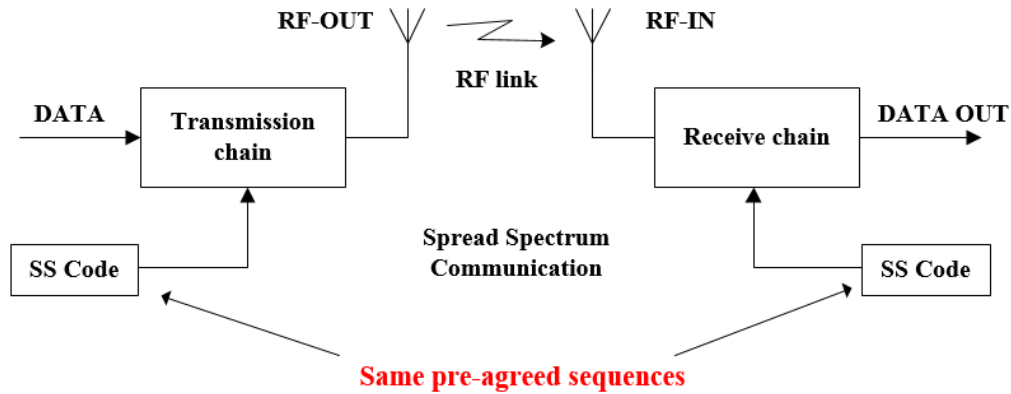


**Fig. 2.3:** Spread Spectrum Communications system

Several of the techniques are “direct-sequence SS” (DS-SS) modulation in which a fast pseudo-randomly generated sequence is multiplied with low rate DATA need to be sent, “frequency hopping SS” (FHSS) in which the carrier is caused to shift frequency in a pseudorandom way and “time hopping SS” wherein burst of signal are initiated at pseudorandom time [2-24, 2-25]. Among them the first is the simplest in implementing the hardware.

A simple SS communication channel is shown in Fig. 2 [2-26]. It is noticeable that the SS RX must pre-understand the code of the TX. So that the RX can demodulate to recover data by using matched filter. RX can utilize analog matched filter or digital matched filter depending on the situation. RX with analog matched filter can receive SS signal from TX with very low SNR and TXs can use the same frequency band to communicate without making interference to the others. However, structure of analog matched filter is complex according to high power consumption. For low power operation, digital matched filter which is deployed in digital circuit is more reasonable, but it cost limitation of interference resistance. This will be discussed more in Chapter 6.

Besides, as soon as SS technique is used for TRX system, it produces wider bandwidth signal and process gain which helps sensitivity of RX increase. Sensitivity of a SS communication system is calculated as below [2-24, 2-25]:

$$P_{sensitivity}[dBm] = NF(dB) + kTB_{RF}[dBm] + \frac{E_b}{N_0}[dB] - PG(dB) \quad (2 - 2)$$

where NF is noise figure of RX,  $k = 1.38 \cdot 10^{-23}$  J/K is Boltzmann constant,  $T = 290\text{K}$  at room temperature,  $B_{RF}$  is RF carrier bandwidth in Hz which is equal to chip rate for the SS system,  $E_b/N_0$  is signal to ratio (SNR) corresponding to a given bit error rate (BER),  $PG$  is process gain which is calculated by the ratio between code rate and data bit rate. Hence, we can rewrite above equation for SS system operates at room temperature as followed:

$$P_{sensitivity}[dBm] = -174 + NF(dB) + 10\log B_{RF}[Hz] + \frac{E_b}{N_0}[dB] - PG(dB) \quad (2-3)$$

Comparing with sensitivity of general RX which is calculated according to equation (2-4) [2-26]:

$$P_{sensitivity}[dBm] = -174 + NF(dB) + 10\log B_{RF}[Hz] + \frac{E_b}{N_0}[dB] \quad (2-4)$$

It is easy to realize that with the same bandwidth of signal, SS RX can improve the sensitivity by process gain  $PG [dB]$ . Thus, this study intends to apply spread spectrum technique to the proposed TRX system in order to exploit its advantage of excellently withstanding to interference.

### 2.3 RF Characteristics of 65nm SOTB CMOS Device

The Silicon-On-Thin Buried Oxide (SOTB) CMOS, which is one of the FD-SOI CMOS processes, has been developed recently with a lot of advantages in comparison to

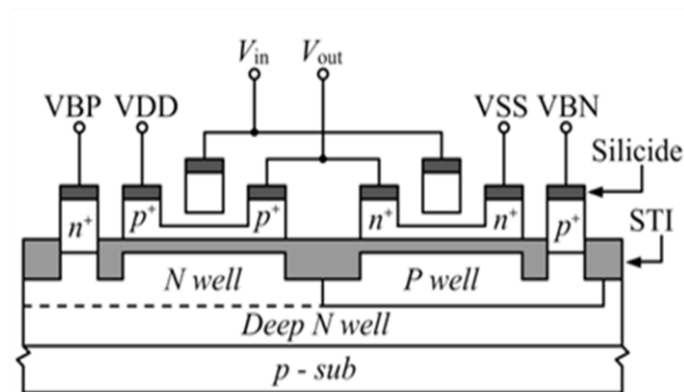


Fig. 2.4: The structure of SOTB CMOS

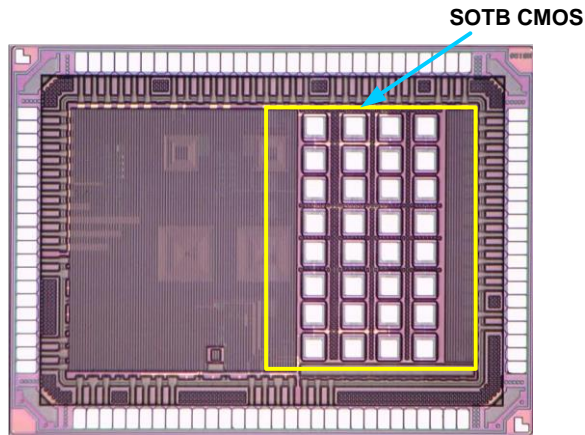


Fig. 2.5: Chip photo of investigated SOTB

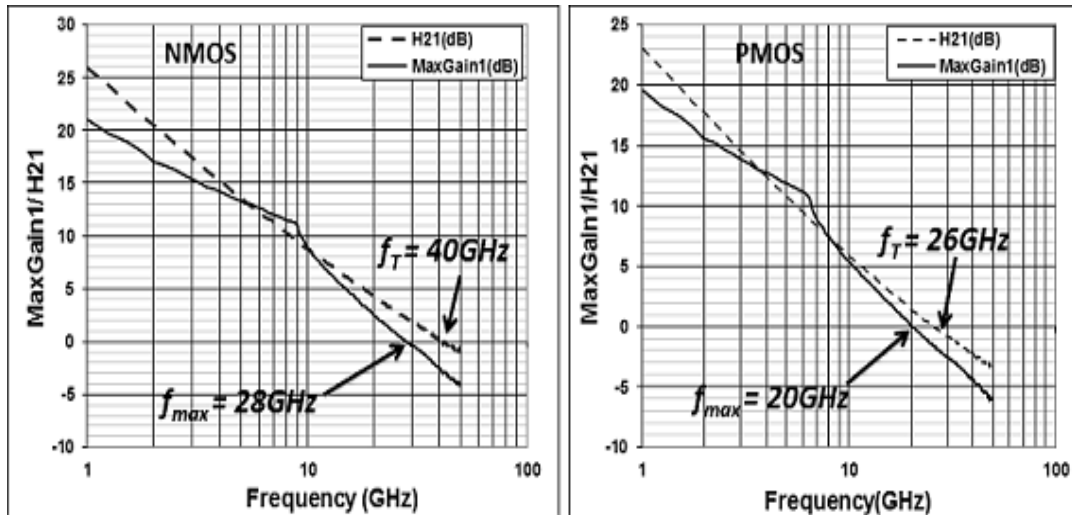


Fig. 2.6: Measured  $F_T$  and  $F_{max}$  of 65nm SOTB CMOS at  
 $V_d = 1.2V$ ,  $V_g = 0.65V$ ,  $V_b = 0$  for NMOS  
 $V_d = -1.2V$ ,  $V_g = -0.65V$ ,  $V_b = 0$  for PMOS

conventional BULK CMOS [2-27 - 2-29]. These merits indicate that the SOTB CMOS is a brilliant candidate for low voltage, low-power applications [2-30, 2-31].

Figure 2.4 shows the cross section of SOTB CMOS devices [2-28, 2-29]. Unlike conventional SOI CMOS with a thick BOX layer, SOTB CMOS has much thinner BOX thickness of about 10nm and has deep Nwell layer, thus the body voltages of PMOS and NMOS can be controlled separately. As a result, designers can control operation of circuits using SOTB devices easily by adjusting body bias voltage. Changing in body bias voltages

is consequence in variation of threshold voltage of SOTB devices, and then of devices operation. This feature is very useful because it helps us change frequency of a based-on SOTB devices oscillator circuit by varying body bias voltage of NMOS and PMOS.

Besides, being a kind of SOI device with small drain conductance SOTB devices help analog circuits using them can operate at low voltages [2-30]. Whereby, SOTB devices are commensurate with low power design.

A question that is SOTB device suitable to RF circuit design or not? To answer this question, we, firstly, investigated RF characteristics of SOTB NMOS and PMOS. A couple of 8-finger SOTB NMOS and PMOS with same size of 6 $\mu$ m width (48 $\mu$ m total width) and 60nm length were laid-out, fabricated and evaluated. Micrograph of the fabricated CMOS chip is exhibited in Fig. 2.5.

Evaluation of SOTB CMOS RF characteristics was carried out under followed conditions:  $V_d = 1.2V$ ,  $V_g = 0.65V$ ,  $V_b = 0$  for NMOS and  $V_d = -1.2V$ ,  $V_g = -0.65V$ ,  $V_b = 0$  for PMOS. Measured results of the cut-off frequency  $F_T$  and the maximum oscillation frequency  $F_{max}$  of the CMOS are shown in Fig. 2.6. It is easy to see that the SOTB NMOS owns quite high  $F_T$  and  $F_{max}$  of 40 GHz and 28 GHz, respectively, while those of PMOS are consequently smaller values of 26 GHz and 20GHz [2-31]. In comparison to operation frequency 2.4GHz of proposed CMS-OOK TRX in this study, these values are much higher. This guarantees that 65nm SOTB CMOS is capable of implementing well for 2.4 GHz band application designs.

## 2.4 Conclusion

In this Chapter, consideration of TRX system in terms of power, communication distance and immunity to interference is present.

In order to reduce power consumption of TRX, intermittent and normally-off operation of TX is selected in combination with utilizing low-complexity architecture of OOK TRX. 65nm SOTB CMOS devices are chosen for implementing physical TRX system because of its excellent advantages. Especially, body bias control of SOTB CMOS can

diffuse spectrum of carrier frequency, which results in spreading spectrum of TX output signal. Whereby, bandwidth efficiency of the TRX is improved.

Regarding to lengthening communication distance, solutions to increase TX output power and RX sensitivity are considered. Among them, spread spectrum technique by code modulation in combination with sweeping carrier frequency by controlling body bias voltage of SOTB devices are applied. Thanks to this combination, not only TX output power can be raised without radio regulations violence but also TRX has more process gain to increase sensitivity. Moreover, this also can help TRX improve immunity to interference by widening BW and assigning different codes to different TXs.

Based on above considerations and selections, a new modulation scheme is proposed in Chapter 3 and implementation of a TRX system based on 65nm SOTB CMOS technology was carried out and evaluated in Chapter 4 and Chapter 5.

## References

- [2-1] J. M. Rabaey, J. Ammer, T. Karalar, S. Li, B. Otis, M. Sheets, T. Tuan, “PicoRadios for wireless sensor networks: The next challenge in ultra-low power design,” *IEEE International Digest of Technical papers, Solid-State Circuits Conference*, 2002, pp. 2001-2002.
- [2-2] H. T. Friis, “A note on a simple transmission formular,” *Proceeding s of the I. R. E. and Waves and Electrons*, May 1946, pp. 254-256.
- [2-3] H. Karl, and A. Willig, “Protocols and architectures for Wireless Sensor Networks,” John Wiley & Sons, West Sussex, England, 2005.
- [2-4] J. Bae et al., “A 490 uW fully MICS compatible FSK transceiver for implantable devices,” *2009 Symposium on VLSI Circuits Digest of Technical Papers*, pp. 36–37
- [2-5] S. Wu, B. Razavi, “A 900-MHz/1.8-GHz CMOS receiver for dual-band applications,” *IEEEJ.Solid-State Circuits* **33**, 2178–2185 (1998)
- [2-6] M. Vidojkovic et al., “A 0.33 nJ/b IEEE802.15.6/proprietary-MICS/ISM band transceiver with scalable data-rate from 11 kb/s to 4.5 Mb/s for medical applications,” *ISSCC*, 2014, pp. 170–172
- [2-7] S. Chakraborty et al., “An ultra-low power reconfigurable multi-standard transceiver using fully digital PLL,” *Proc. Symp. VLSI Circuits*, June 2013, pp. 148–149
- [2-8] R. Kumar et al., “A fully integrated 2x2 b/g and 1x2 a-band MIMO WLAN SoC in 45nmCMOS for multi-radio IC,” *ISSCC*, 2013.
- [2-9] J. Masuch et al., “A 1.1 mW RX 81.4 dBm sensitivity CMOS transceiver for Bluetooth low energy,” *IEEE Trans. Microw. Theory Tech.* **61**, 1660–1673 (2013)

- [2-10] Y.H. Liu et al., “A 2.7 nJ/bit multi-standard 2.3/2.4 GHz polar transmitter for wireless sensor networks,” *ISSCC Dig. Tech. Papers*, February 2012, pp. 448–450
- [2-11] R.E. Crochiere, L.R. Rabiner, “Multirate Digital Signal Processing,” Prentice-Hall Inc., Englewood Cliffs, New Jersey 07632 (Prentice Hall, 1983)
- [2-12] T. Ha, S. Lee, J. Jim, “Low-complexity correlation system for timing synchronization in IEEE802.11a wireless LANs,” in *Proceedings of Radio and Wireless Conference*, 2003
- [2-13] J.C. Roh, A. Batra, S. Hosur, “Packet detection and coarse symbol timing for rotated differential M-ary PSK modulated preamble signal,” US Patent 8,630,374
- [2-14] H.-S. Kim, S.-J. Lee, M. Goel, “Method, device, and digital circuitry for providing a closed-form solution to a scaled error locator polynomial used in BCH decoding,” US Patent 8,392,806
- [2-15] P. Reviriego, C. Argyrides, J.A. Maestro, “Efficient error detection in Double Error Correction BCH codes for memory applications,” *Microelectron. Reliab.* **52**(7), 1528–1530 (2012)
- [2-16] J. Kwong, Y.K. Ramadass, N. Verma, A.P. Chandrakasan, “A 65 nm sub-V<sub>t</sub> microcontroller with integrated SRAM and switched capacitor DC–DC converter,” *IEEE J. Solid-State Circuits* **44**(1), 115–126 (2009)
- [2-17] R. Tabrizian et al., “A 27 MHz temperature compensated MEMS oscillator with sub-ppm instability,” in *IEEE 25th Int’l Conf. on Micro-Electro Mechanical Systems (MEMS)*, 29<sup>th</sup> January - 2nd February 2012, pp. 23–26
- [2-17] N. Fletcher, J.M. Rabaey, “Ultra-Low Power Wakeup Receivers for Wireless Sensor Networks,” (EECS Department, University of California Berkeley, 2008)

- [2-18] X. Huang, S. Rampu, X. Wang, G. Dolmans, H. de Groot, "A 2.4 GHz/915 MHz 51 W wake-up receiver with offset and noise suppression," in *IEEE Solid-State Circuits Conference*, February 2010.
- [2-19] M. T. Hoang, "A study on ultra-low power and high sensitivity OOK CMOS RF Receiver for Wireless Sensor Networks," *Doctoral thesis*, the University of Electro-Communications, 2015.
- [2-20] Y. H. Liu et al., "A 3.7mW-RX 4.4mW-TX fully integrated Bluetooth Low-Energy/IEEE802.15.4/proprietary SoC with an ADPLL-based fast frequency offset compensation on 40nm CMOS," *ISSCC*, Feb. 2015, pp. 236-237.
- [2-21] X. Chen, J. Breiholz, F. Yahya, C. Lukas, H. S. Kim, B. Calhoun, D. Wentzloff, "A 486 $\mu$ W All-Digital Bluetooth Low Energy Transmitter with Ring Oscillator Based ADPLL for IoT Applications," *IEEE Radio Frequency Integrated Circuits Symposium*, 2018, pp.168-171.
- [2-22] SX1276/77/78/79 datasheet, Semtech Cor. [Online]. Available: [https://www.semtech.com/uploads/documents/DS\\_SX1276-7-8-9\\_W\\_APP\\_V5.pdf](https://www.semtech.com/uploads/documents/DS_SX1276-7-8-9_W_APP_V5.pdf). Accessed: 10<sup>th</sup> Nov. 2018
- [2-23] W. Bae, H. ju, K. Park, S. Y. Cho, and D. K. Jeong, "A 7.6mW, 414 fs RMS-jitter 10Ghz Phase Locked Loop for a 40 Gb/s Serial Link Transmitter Based on a Two-Stage Ring Oscillator in 65nm CMOS," *IEEE Journal of Solid-State Circuits*, No. 10, Oct. 2016, pp. 2357-2367
- [2-24] J. S. Lee, and L. E. Miller, "CDMA Systems Engineering Handbook," *Artech House Publishers*, 1998.
- [2-25] S. C. Yang, "CDMA RF System Engineering," *Artech House Publishers*, 1998.
- [2-26] B. Razavi, "RF Microelectronics," *Pearson Education, Inc.*, 2012

- [2-27] R. Tsuchiya et al., "Silicon on thin box: a new paradigm of the CMOSFET for low-power high-performance application featuring wide-range back-bias control," *IEEE International Electron Devices Meeting*, Dec. 2004, pp. 631-634
- [2-28] T. Ishigaki, "A study on Silicon-on thin-Box (SOTB) CMOSFET for low power LSIs," *Doctoral Thesis*, Tokyo Institute of Technology, 2012.
- [2-29] S. Morohashi, N. Sugii, C.K. Pham, K. Ishibashi et. al., "10MHz 44 $\mu$ W Operation Power, 4.2nA Sleep Current 50K Gate Logic Design using Adjustable V<sub>b</sub> for SOTB devices," *IEEE S3S Conference*, 2013.
- [2-30] K. Ishibashi, N. Sugii et al., "A perpetuum mobile 32 bit CPU with 13.4 pJ/cycle, 0.14 1A sleep current using reverse body bias assisted 65 nm SOTB CMOS technology," *Cool chip XVII Conference*, pp. 1–3, 2014.
- [2-31] V. T. Nguyen, R. Ishikawa, and K. Ishibashi, "83nJ/bit Transmitter Using Code-Modulated Synchronized-OOK on 65nm SOTB for Normally-Off Wireless Sensor Networks," *IEICE Trans. On Electronics*, Vo1. E101-C.472 Jul. 2018, pp. 472-472

## **Chapter 3**

### **Proposal of Code-Modulated Synchronized – OOK Modulation Scheme**

In order to achieve ULP operation, it is necessary to optimize across all design layers, ranging from modulation schemes and architectures to circuits and devices. One of the most efficient ways to reduce power is to decline the complexity of the modulation schemes, which normally also decreases the overall architectural complexity [3-1]. According to a survey on energy efficient modulation and coding techniques for WSNs, the modulation and coding process are very important to improve the energy efficiency and BW efficiency of a wireless networks. It is popular that non-coherent modulation scheme such as OOK and FSK are mostly modulation used in sensor node radio TRXs. These schemes not only greatly simplify the architecture of TRX but also are compatible with nonlinear but high efficient PAs [3-2], which enable a further reduction in power consumption. In which, direct-modulation TX architectures utilizing OOK modulation scheme and RX with envelope detector or super-regenerative architectures are prefer. Besides ULP issue, in the fact that there are a lot of radio devices operating simultaneously in the vicinity of the TRX [3-1, 3-2]. In this scenario, improving reliability of TRX means enhancing the resistance to interference. In this section, we propose a Code-Modulated Synchronized-OOK (CMS-OOK) scheme which helps us not only reduce power consumption but also enhance immunity to interference.

### 3.1 Synchronized-OOK modulation

The Synchronized-OOK modulation scheme is firstly witnessed in the Impulse-Radio Ultra Wide band (IR-UWB) TRXs of M. Crepaldi [3-3], and then is used in the TRXs system of M. T. Hoang in [3-4]. Theoretically, in the conventional OOK modulation, RF carrier appears during whole duration of data '1' and absents from time of data '0' (Fig. 3.1a). In difference to this, S-OOK signal is established by two kinds of pulse: synchronized pulse and data pulse. According to this, data '1' is displayed by two pulses including a synchronized pulse and a data pulse, while data '0' is represented by only one synchronized pulse (Fig. 3.1b).

Fig. 3.1a) shows the waveform of a data needs to be sent (*DATA*) and the corresponded conventional OOK RF signal. It is easy to realize that RF carrier signal appears continuously during data '1' pulse width,  $T_b$ . Thus, OOK TX here consumes power during this time. On the other hand, the sent data (*DATA*), S-OOK baseband signal (*SDATA*) and S-OOK RF signal are described in Fig. 3.1b). This figure informs that S-OOK TX only expends power during only duration of synchronized pulse and data pulse  $T_p$ , which is much smaller than  $T_b$ . As a result, to send a data at the same rate with the condition that OOK TX and S-OOK TX have same average power  $P_{avg}$ , the energy is used for transmitting a pair of data '1' and data '0' of S-OOK TX is  $T_b/3T_p$  times lower than that of OOK TX. With  $T_p$  is much shorter than  $T_b$ , S-OOK TX swallows much smaller energy than OOK TX does. Besides,

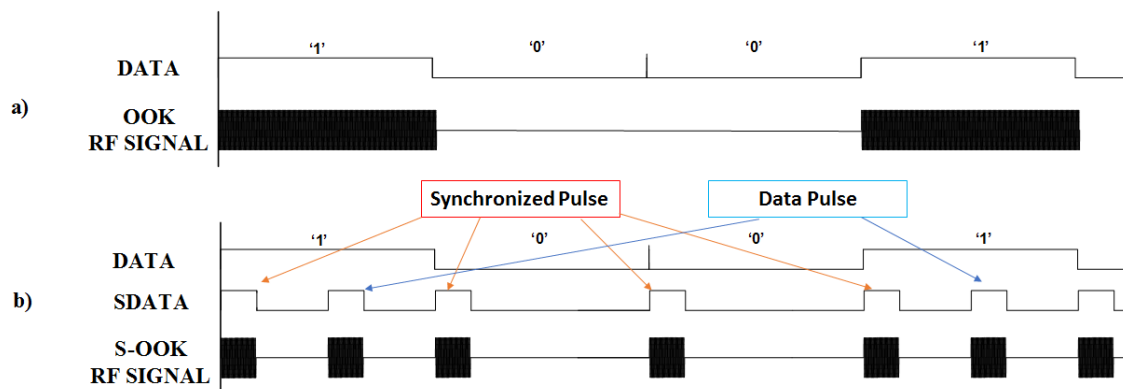


**Fig. 3.1:** a) Conventional OOK signal  
b) S-OOK signal

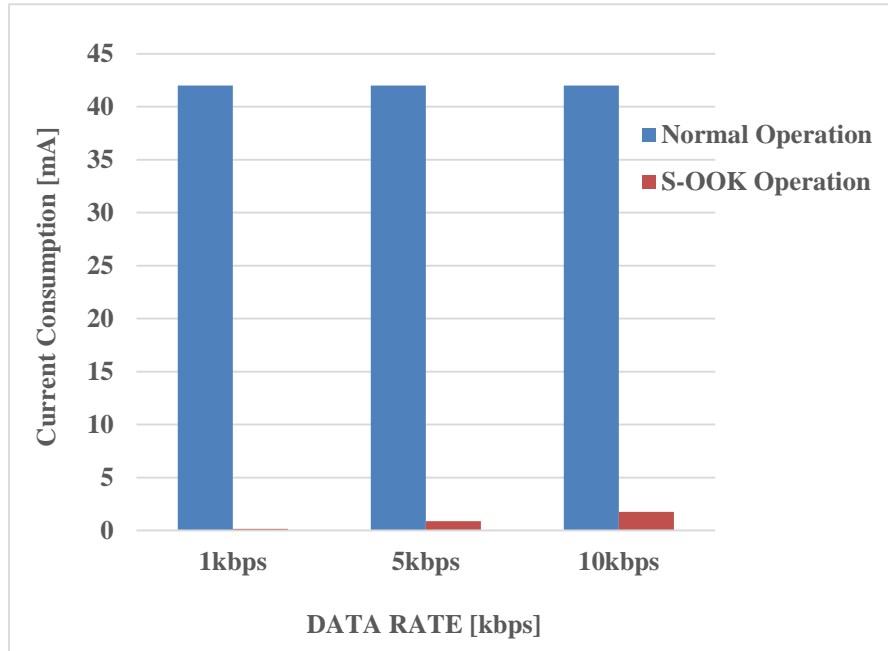


**Fig. 3.2:** Current consumption of the S-OOK RF front-end

this also leads to another effect that BW of S-OOK RF signal is wider than that of OOK RF signal.

In [3-4], authors implemented and evaluated S-OOK RX chip based on 65nm SOTB CMOS technology. It is noticeable that complicated clock and data recovery circuit are vanished from the S-OOK RX. Moreover, the RF circuits in the RX can be heavily duty-cycled using a narrow window, known as *RFENABLE* duration. These help RX nearly consume no power in duration between synchronized pulses and data pulses. Thanks to these techniques, S-OOK RX produced -58dBm sensitivity and 1.36uW power consumption at 10kbps data rate.

The benefit of power efficiency of S-OOK scheme can be seen through the chart in Fig. 3.2. In comparison with normal operation at the same data rate, S-OOK RX consumes nearly 90% lower power.

On the other hand, S-OOK modulation exposes some disadvantages. First, as it is necessary to use 2 RF pulses to represent a bit, data rate is limited and usually pre-determined. Second, less complex architecture of RX provided good power consumption but poor

sensitivity. Finally, it is noticeable that S-OOK essentially is a special case of OOK modulation. Thus, reliability of S-OOK TRX system is reduced in presence of interference. It also demands a method to synchronize data pulse and synchronized pulse.

### 3.2 Spread-Spectrum communications and Direct-Sequence Spread-Spectrum technique

Spread-spectrum (SS) communications technology was first described on paper by an actress and musician in 1941 and was not taken seriously [3-5]. It even was forgotten until the 1980s, when the came alive and has become increasingly popular with initial applications in military anti-jamming tactical communications, anti-multipath systems and so on. Typical applications for the resulting short-range data TRXs include satellite-positioning systems (GPS), 3G mobile telecommunications, W-LAN (IEEE802.11a, IEEE802.11b, IEE802.11g), and Bluetooth. SS technique is a crucial solution for the endless race between communication demands and radio-frequency availability [3-6].

This technique is defined as follows: “Spread spectrum is a means of transmission in which the signal occupies a bandwidth in excess of the minimum necessary to send the information; the band spread is accomplished by means of a code which is independent of the data, and a synchronized reception with the code at the receiver is used for de-spreading and subsequent data recovery” [3-5].

Direct Sequence Spread Spectrum (DS-SS) is one of three main SS techniques. In such this way, data needs to be sent is spread over a wide band by multiplying with a code sequence (Fig. 3.3). On the transmission path, there are narrower interferences which are

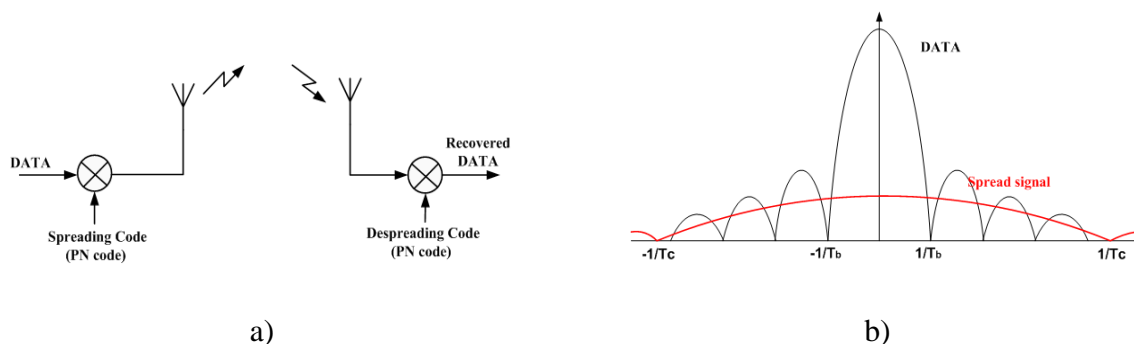


**Fig. 3.3:** SS communication system (a) and spectrum transformation (b)

added to wideband spread signal. A receive using the completely same code sequence to recover correctly the data sent from TX, besides this code also spreads narrow interferences in wideband with much lower magnitude in comparison to that of desired signal. Thus, DS-SS helps communication system to enhance the immunity to interferences. Although DS-SS system has lower immunity to interference than that of frequency hopping and time hopping SS technique, it has advantages of easier code generation, lower demand to carrier oscillator and especially easy implementation by hardware. These features are suitable to low power design.

### 3.3 Code-Modulated Synchronized-OOK scheme

Based on the benefits brought from S-OOK modulation and DS-SS technique, we proposed CMS-OOK scheme. The waveform operation of CMS-OOK TX is described in Fig. 3.4 [3-7].

According to this scheme, firstly, at the TX, a data needs to be sent *DATA* (Fig. 3.4a) is modulated to create synchronized data signal *SDATA* which consists of synchronized pulses and data pulses (Fig. 3.4b). In such this way, data '1' is represented by two pulses: a synchronized pulse and a data pulse, while only a synchronized pulse is used to describe data '0'. In the figure, bit duration of one bit *DATA* is symbolized by  $T_b$  and pulse width of the *SDATA* is notated by  $T_p$ . While *DATA* is transforming to *SDATA*, a code (*CODE*) is generated periodically in a way that code bits are exist during only pulse duration  $T_p$  (Fig. 3.4c). Then,

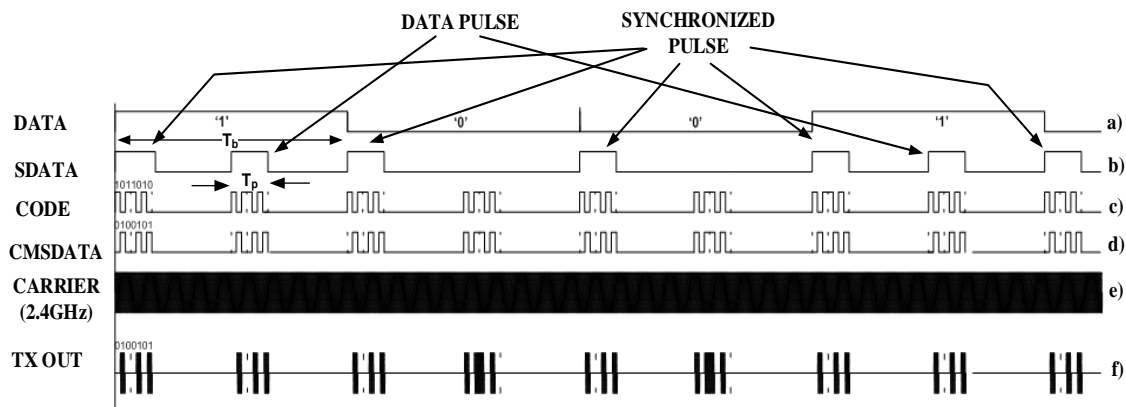
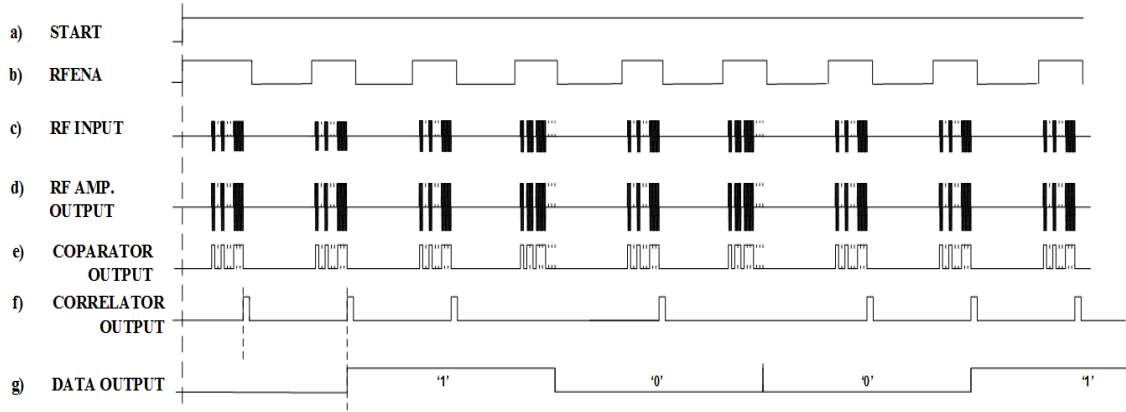


Fig. 3.4: Waveform operation of CMS-OOK TX



**Fig. 3.5:** Waveform operation of S-OOK RX

this code is multiplied with  $SDATA$  signal by exclusive-OR gate to create code-modulated synchronized data, called  $CMSDATA$  (Fig. 3.4d). Finally, this  $CMSDATA$  modulates a 2.4GHz band carrier (Fig. 3.4e) to produce CMS-OOK RF signal ( $TXOUT$ ) to antenna.

As can be seen from Fig. 3.4 that the period of synchronized pulse is exactly equal to data bit duration,  $T_b$ . Data pulses and synchronized pulses have same pulse width of  $T_p$ , which is in relationship with  $T_b$  by a ratio factor  $N$  as the following equation:

$$T_b = N \cdot T_p \quad (3-1)$$

Velocity and the number of bits of the code are chosen so that all code bits completely fit in a  $T_p$ . If the code bit rate is symbolized by  $R_C$ , as a result code bit duration is  $T_C = 1/R_C$ . We notate the number of code bits inside a  $T_p$  is  $M$ , then we have:

$$T_p = M \cdot T_C \quad (3-2)$$

From the equations (3-1) and (3-2), we can infer that with a same data rate, given different values of  $N$  and  $M$ , the duration of the code bit receives different values. As a result, bandwidth (BW) of  $TXOUT$  signal also varies correspondingly. Similar to TRX in [3-7], the gap between synchronized pulse and data pulse is chosen by a half of  $T_b$ . It is familiar to traditional SS technique, carrier frequency should be much higher than the code rate. We chose 31-bit code and  $T_C$  of 322ns,  $M = 31$ , and  $N = 100$ , so that total bit rate becomes 1kbps.

In terms of power, with a same data rate transmission, CMS-OOK TX PA consumes energy only when the  $CMSDATA$  comes. We notate the activity ratio of  $CMSDATA$  as  $A_c$  which is expressed by

$$A_c = \frac{4T_p}{2T_b} = \frac{2}{N} \quad (3-3)$$

where  $N$  is calculated by (3-2). Normally,  $N$  is chosen to be much larger than 1, which means  $A_c$  is much smaller than 1. Hence, the PA can reduce much power to achieve low power operation. For example, if we choose ratio factor  $N = 100$ , the activity ratio  $A_c$  will become 2%. Thus the power can be drastically reduced in this modulation scheme.

It is easy to realize that CMS-OOK modulation is a special form of OOK modulation. Thus, CMS-OOK RX is also insensitive to carrier jitter, which allows us to utilize RO as a carrier oscillator of the TX. In principle, the TXs using angle modulation with precise carrier oscillator such as crystal or PLL oscillator often take a long time for settling the carrier sources. For this reason, the TXs consume more power to wake up from sleep or power off state to start transmitting the data. In contrast, CMS-OOK TX with RO, which can likely

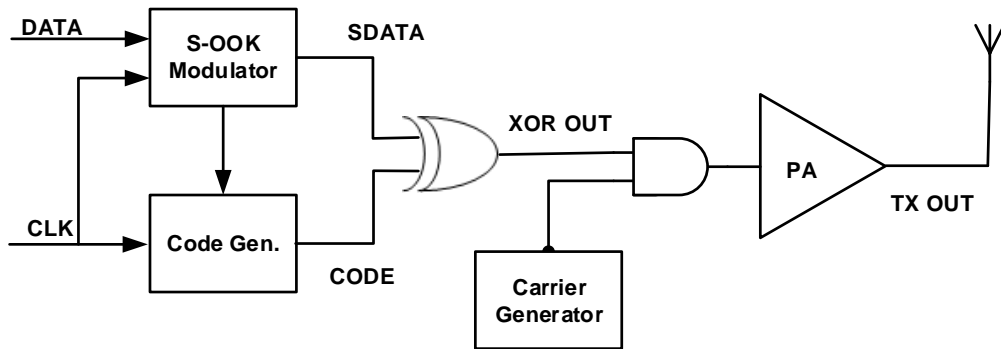


Fig. 3.6: Architecture of CMS-OOK TX

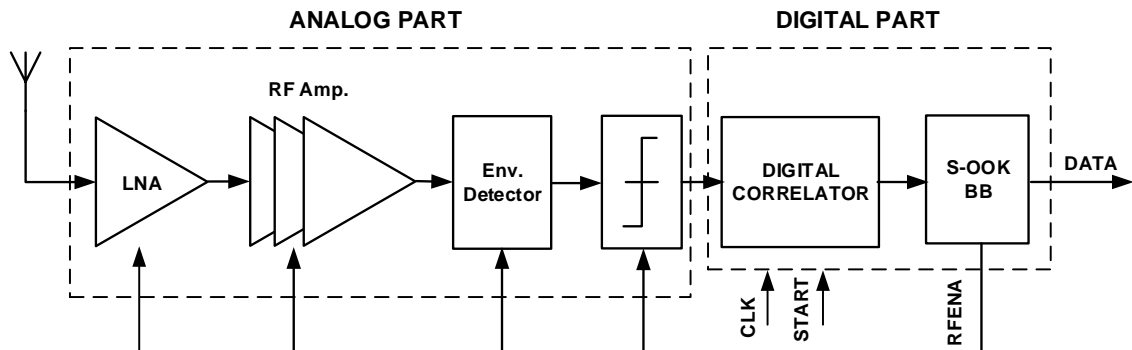


Fig. 3.7: Architecture of CMS-OOK RX

start swiftly as soon as the RX receives a wake up signal from the MCU of the SN, is absolutely commensurate with normally-off as well as intermittent WSNs.

Other benefit of CMS-OOK scheme comes from the broad BW of CMS-OOK RF signal which is spread by using code modulation. Also, the CMS-OOK RX is capable of demodulating received RF signal even with variation of carrier frequency. This allows us to drastically lower the peak power magnitude of the carrier signal by spreading the carrier frequency. Consequently, this supplies not only a lower peak power intensity of the RF signal spectrum, which contributes in meeting fully the radio regulations, but also a broader BW of the RF band-pass signal, which contributes in better withstanding to interference and higher sensitivity of the RX.

In the opposite side, CMS-OOK RX has operation waveform in Fig. 3.5. In order to increase the sensitivity, in comparison with that of RX in [3-7], a low noise amplifier (LNA) with low-Q inductor load and RF amplifier are used. This magnifies the *RFINPUT* (Fig. 3.5c) to larger amplitude signal (*RF AMP. OUTPUT* in Fig. 3.5d). RF front-end consists of a used-on-chip inductor LNA, RF amplifier stages, envelope detector and comparator. The output of comparator is a bit sequence which should be same as transmitted *CMSDATA* from the TX (Fig. 3.5e). This bit stream is input to a digital correlator which plays a role as a matched filter. If the received signal and the code used in RX are matched enough to over a programmable threshold, matched filter will deliver a high pulse at the end of the matched bit sequence (Fig. 3.5f). By using clock frequency much higher than speed of input bit stream, which is known as oversampling technique, synchronization issue in matched filter becomes more relaxed. This is the advantage of digital matched filter in comparison to analog matched filter which originally demands strictly synchronization of code and received data which is often addressed by using complicated acquisition and tracking system [3-5]. Output pulses of the digital correlator are led to S-OOK baseband digital which not only recovers the sent *DATA* (Fig. 3.5g) but also generates *RFENA* pulses (Fig. 3.5b) to turn on and turn off RF front-end. This *RFENA* is created basing on received bit sequence in combination with a *START* signal which is assumed as a wake-up signal from a wake-up RX. Thanks to *RFENA* signal, RF front-end can cut down the power consumption at the most hungry power part of RX as well as whole RX. Besides, low noise figure and high gain RF front-end contributes in raising sensitivity of RX, which helps to lengthen the communication range of the TRX

system. In addition, utilizing code modulation with different codes for different TXs and RXs produces a higher immunity to interference in comparison with TRXs in [3-3] and [3-4].

Originating from waveform operation, we propose the architecture of TX and RX as shown in Fig. 3.6 and Fig.3.7, respectively. Detailed operation and structure of TX and RX will be described clearly in Chapter 4 and Chapter 5.

Fig. 3.8 shows bandwidth efficiency improvement of CMS-OOK system in condition that fixed frequency carrier is used. As can be seen, as the number of bit code per synchronized pulse duration increases, which leads to code rate goes up and then, null-to-null bandwidth CMS-OOK signal is widen.

Detailed architecture and used techniques of the TX and RX will be present in next Chapter 4 and Chapter 5, respectively.

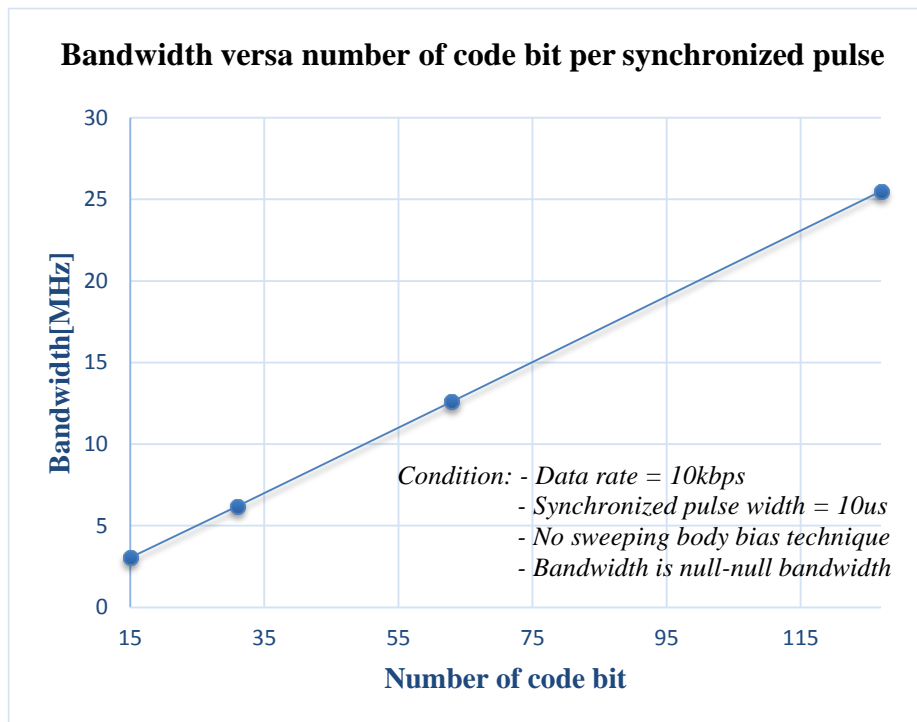


**Fig. 3.8:** Dependence of BW on number of code bit during synchronized pulse duration

### **3.4 Chapter conclusion**

In this Chapter, based on investigating advantages and disadvantages of S-OOK TRX system and spread-spectrum technique, the CMS-OOK modulation is proposed. A first sight of CMS-OOK TRX is presented in term of operation waveform and block architecture. In next Chapter 4 and Chapter 5 will help us have insight of CMS-OOK TX and RX.

## References

- [3-1] M. S. Dawood, R. Aiswaryalakshmi, R. A. Sikkandhar, G. Athisha, "A Review on Energy Efficient Modulation and Coding Techniques for Clustered Wireless Sensor Networks," *International Journal of Advanced Research in Computer Engineering & Technology (IJARCET)*, Volume 2, Issue 2, February 2013, pp. 319-322
- [3-2] P. P. Mercier, and A. P. Chandrakasan, "Ultra-Low-Power Short-range radios," Springer International Publishing Switzerland 2015.
- [3-3] M. Crepaldi, C. Li, "An Ultra-Wideband Impulse-Radio Transceiver Chipset Using Synchronized-OOK Modulation," *IEEE Journal Of Solid-State Circuits*, Vol. 46, No. 10, October 2011
- [3-4] M. T. Hoang, "A Study on Ultra-Low Power and High Sensitivity OOK CMOS RF Receiver for Wireless Sensor Networks," *Doctoral Thesis*, The University of Electro-Communications, Tokyo, 2015
- [3-5] R. L. Pickholtz, D. L. Schilling, and L. B. Milstein, "Theory of Spread-Spectrum Communications-A Tutorial," *IEEE Trans. on Communications*, Vol. Com-30, No. 5, May 1982, pp. 855-884.
- [3-6] "An Introduction to Spread-Spectrum Communications," *Tutorial 1890*, Maxim Integrated. [Online]. Available: <https://www.maximintegrated.com/en/app-notes/index.mvp/id/1890>. Accessed: 10<sup>th</sup> Nov. 2018.
- [3-7] V. T. Nguyen, R. Ishikawa, and K. Ishibashi, "83nJ/bit Transmitter Using Code-Modulated Synchronized-OOK on 65nm SOTB for Normally-Off Wireless Sensor Networks," *IEICE Trans. On Electronics*, Vol. E101-C.472 Jul. 2018, pp. 472-472.
- [3-8] S. Oh, N. E. Roberts, and D. D. Wentzloff, "A 116nW Multi-band Wake-up Receiver with 31-bit Correlator and Interference Rejection," *Proceedings of the IEEE 2013 Custom Integrated Circuits Conference (CICC)*, Sep. 2013.

## Chapter 4

### Wide bandwidth CMS-OOK Transmitter Using 65nm SOTB CMOS Technology with Sweeping Body Bias Technique

In previous chapter, the CMS-OOK scheme was presented in terms of waveform operation as well as the basic benefits of CMS-OOK TRX system. In this section, we will describe a proposed CMS-OOK TX based on 65nm SOTB CMOS technology in detail.

#### 4.1 Block diagram and operation

Block diagram of CMS-OOK TX is exhibited in Fig. 4.1. As can be seen, *DATA* needs to be sent firstly is transformed into synchronized data *SDATA* by the S-OOK modulator. At the same time, a Code Generator produces a pseudo-noise-random code sequence. It is noticeable that the code is generated to completely fit to duration of synchronized pulses and data pulses. This code and *SDATA* then are multiplied by Exclusive-OR gate in order to form Code-Modulated Synchronized Data (*CMSDATA*). To be continue, this *CMSDATA* modulated 2.4GHz-range carrier generated from a Ring Oscillator. Finally, this RF signal is magnified by an E-class power amplifier (PA) and led to antenna to radiate through free

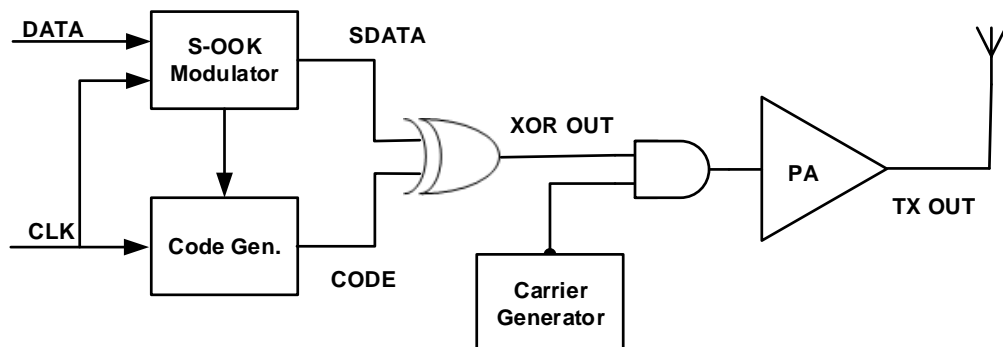


**Fig. 4.1:** Architecture of CMS-OOK Transmitter

space path [4-1]. The digital part operates under an external clock signal (*CLK*) which can come from an external crystal oscillator or from internal oscillator of a MCU of the SN.

Basing on signal type, the TX is divided into two parts: digital part and analog part. The digital circuit includes a S-OOK modulator, a code generator and an exclusive-OR gate. The rest is analog part with a RO plays as the carrier source, an AND gate and E-class power amplifiers was implemented.

#### 4.2 A 65nm SOTB devices-based TX circuit

As considering in Chapter 2, CMS-OOK TX circuit is implemented on 65nm SOTB devices because of their excellent DC and RF characteristics.

To begin with, block diagram and timing chart of digital part is displayed in Fig. 4.2 and Fig. 4.3, respectively.

At first, with the input of sent data *DATA* and clock (*CLK*) signal, SYNCH. PULSE

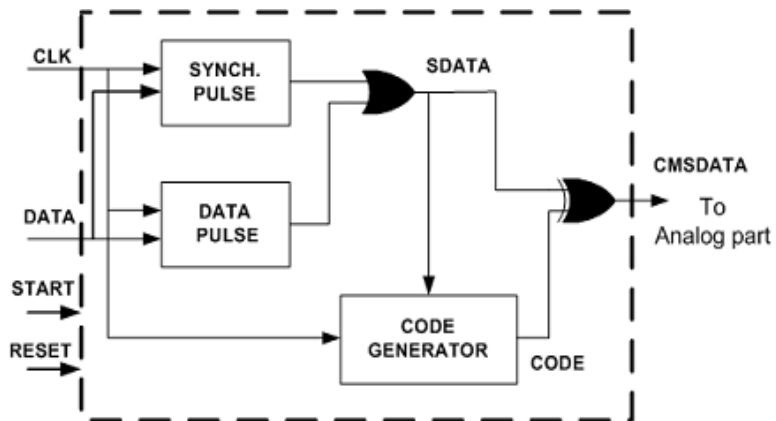


Fig. 4.2: Architecture of the digital part

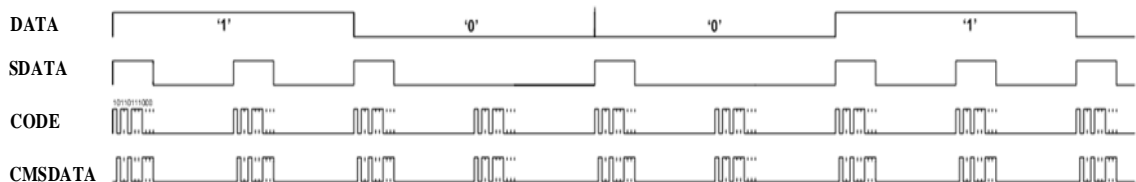


Fig. 4.3: Timing chart of the CMS-OOK TX

and DATA PULSE blocks deliver synchronized pulses and data pulses, respectively. Then, a synchronized data signal  $SDATA$  is generated by combination of these pulses by using an OR gate. At the same time, a code signal ( $CODE$ ) is delivered by a CODE GENERATOR so that this code exists inside the synchronized pulses and the data pulses. Continuously, an exclusive-OR gate multiplies the  $SDATA$  and the  $CODE$ , to provide code-modulated synchronized data  $CMSDATA$  to input of analog part. As regarded in section 3,  $CLK$  signal come from external source such as external crystal oscillator or from MCU of the sensor node. Digital section operates at 0.75V supply voltage.

Detailed schematic of the analog part is showed in Fig. 4.4. As can be seen, carrier generator utilizes free-running RO whom frequency is controlled by body bias voltage. According to this, body bias voltage swept in triangle rule, which can be created and varied simply by RC circuits. By adjusting magnitude of triangle body bias voltage, we can drive center frequency as well as BW of the carrier signal easily. All analog circuits before buffer driver stages are supplied by  $V_{DD} = 0.75V$  DC source.

Theoretically, as conventional OOK schemes nearly do not concern about carrier jitter, PA of the CMS-OOK TX deploys non-linear, high efficiency E-class amplifier [2]. In order to ensure that input signal of the PA is large enough, we design a 3-stage driver as a pre-amplifier. In this design, we utilize on-chip inductors  $L_1$  and  $L_2$  which are used for the PA. Aiming to gain maximum output power of the TX, a matching network is designed. This matching network accounts parasitic parameters of PADs and bonding wire, off-chip inductor  $L_s$  and capacitor  $C_p$ . In order to protect the analog part from electro static discharge (ESD), ESD protect circuit including diodes  $D1, D2, Rs, C_{d1}, C_{d2}$  and grounded-gate NMOS was designed. Both the driver stage and the PA stage operate under 1V DC supply voltage.

### 4.3 Simulation results

The simulation of this design was executed by running netlist file of the TX in HSPICE and NanoSim environment. All circuits before the PA are post-layout simulated in order to fulfill more accuracy results. Since re-extracted software is able to calculated only parasitic resistances and capacitances, is impossible to extract parasitic inductance parameters, we ran pre-layout simulation for PA with equivalent circuit of on-chip inductor including an ideal

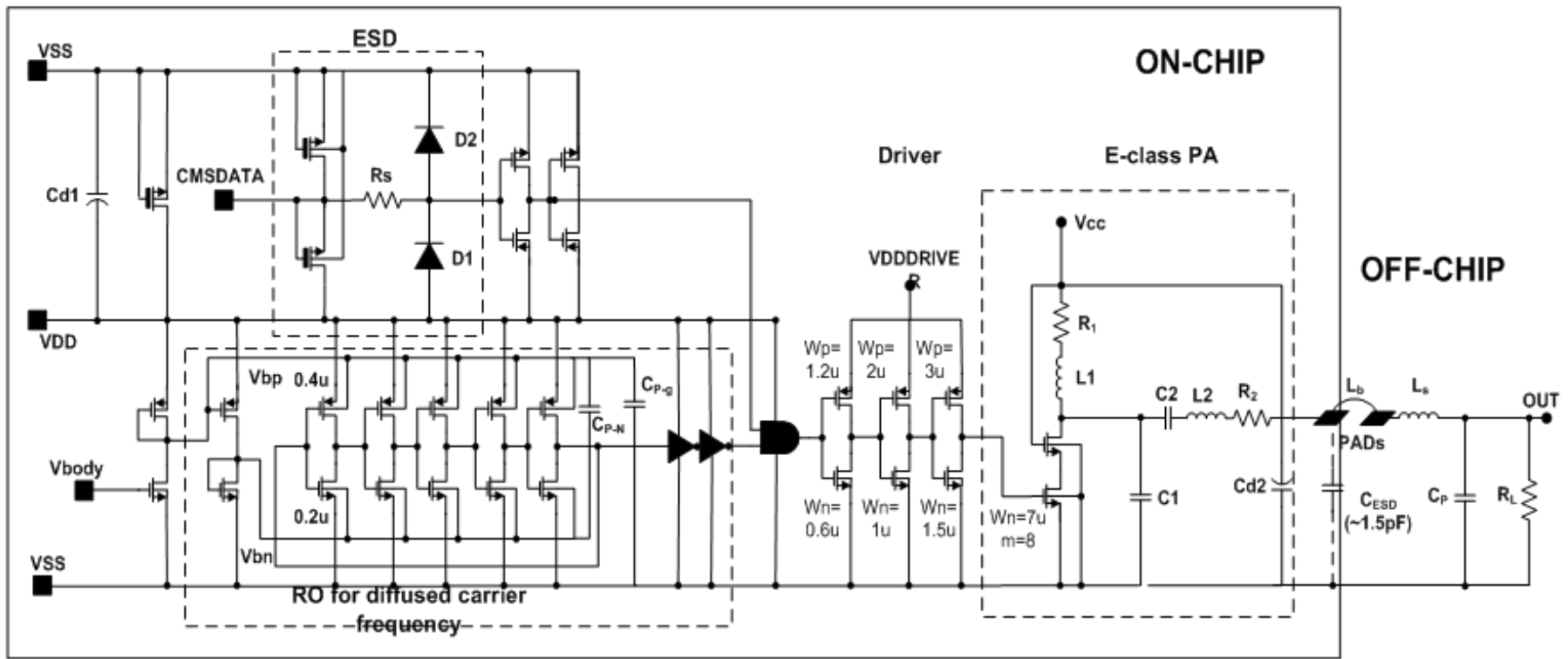


Fig. 4.4: Detailed schematic of the analog part of CMS-OOK TX

inductor and a calculated parasitic series resistor, parasitic parameters of PADs and bonding-wires. At first, Nanosim simulator with high speed was used in order to monitor operation of the designed TX. In this simulation, a linear-feedback shift register (LFSR) was used to generate a code sequence of  $(2^5-1)=31$  bits which plays as the code generator. Then, we used HSPICE simulator to observe accuracy operation of the system, as shown in Fig. 4.5. In this figure, *DATA* at rate of 1kbps is modulated to *SDATA*, including data pulses and synchronized pulses. Then, this *SDATA* signal is multiplied with a 31-bit *CODE* '010 1011

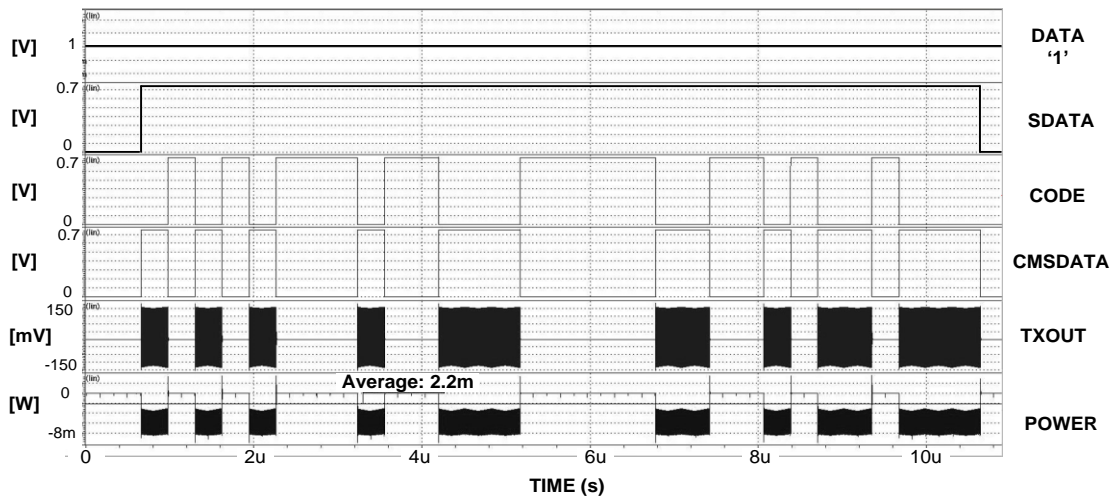


Fig. 4.5: Waveform of TX produced by HSPICE simulator

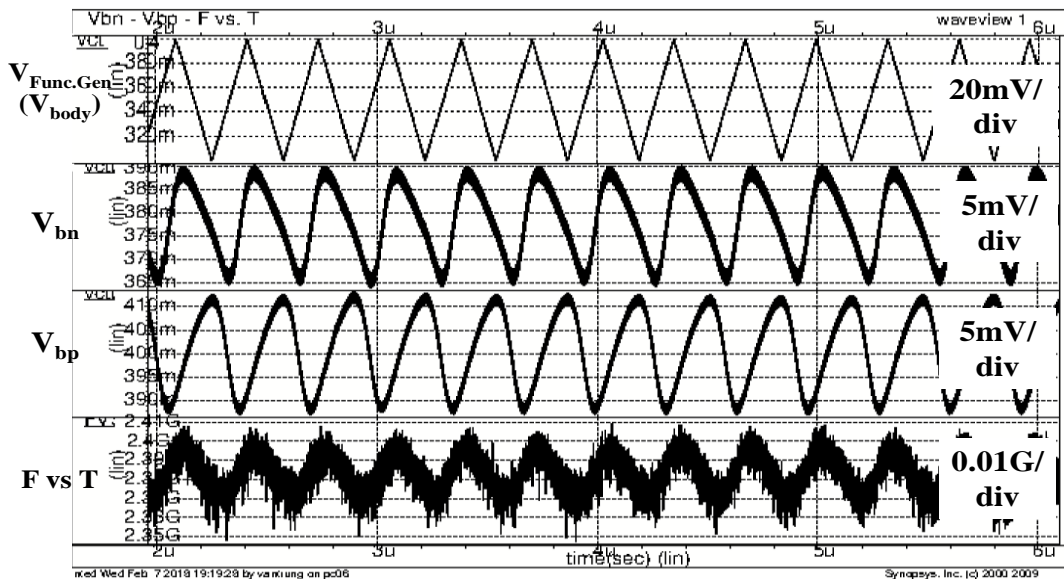


Fig. 4.6: Dependence of carrier frequency on body voltage swing (simulated)

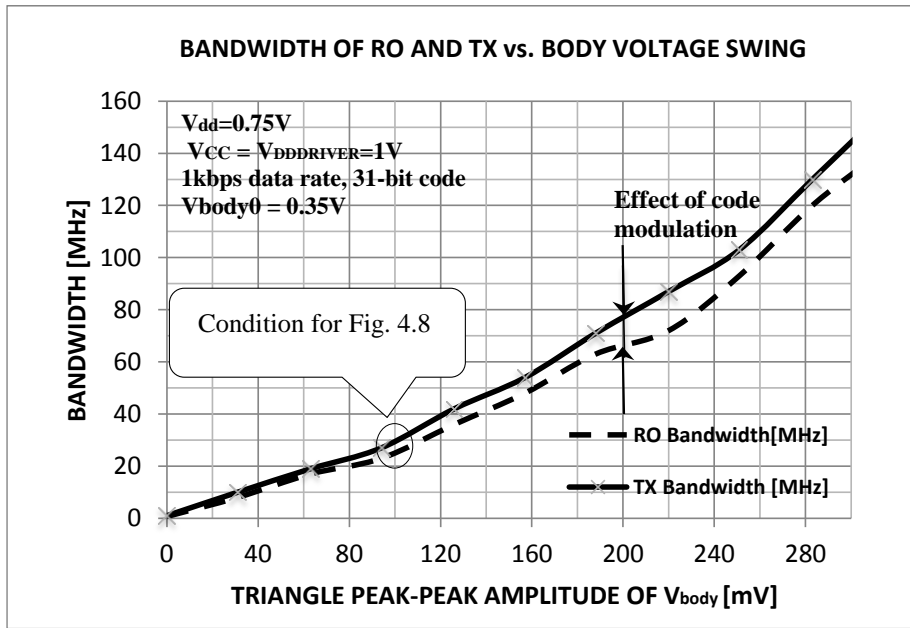


Fig. 4.7: Dependence of TX output spectrum on body voltage swing (simulated)

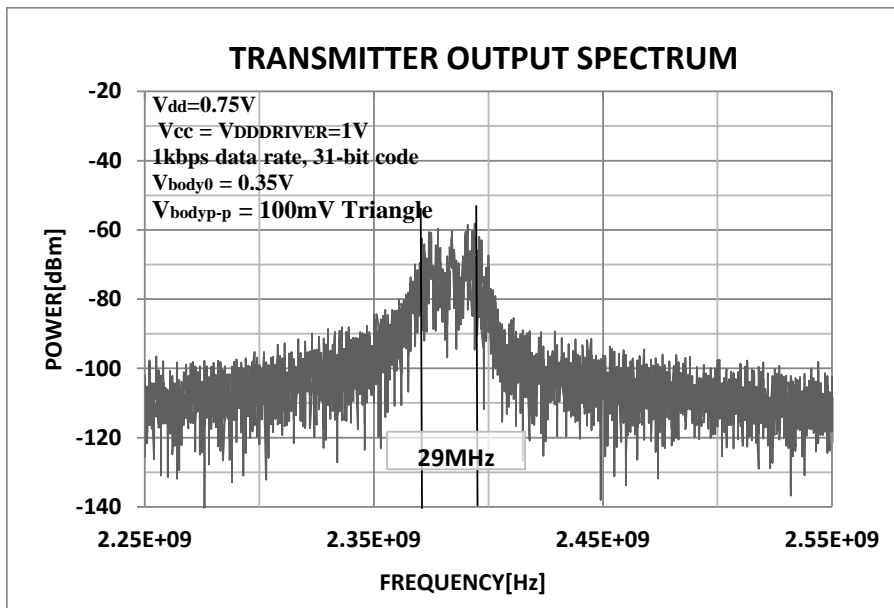


Fig. 4.8: Dependence of TX output spectrum on body voltage swing (simulated)

1101 1000 1111 1001 1010 0100' to produce code-modulated synchronized data *CMSDATA*. Next, this *CMSDATA* signal modulated a 2.4GHz-band carrier, which is delivered from a RO, to generate band-pass signal. To be continued, the PA enlarges this RF signal to output *TXOUT* signal which is then led to a radiated antenna. Carrier frequency of the RO is capable of controlling by sweeping body bias voltage  $V_{body}$ , as illustrated in Fig. 4.6. In this

simulation, a triangle shape of body voltage  $V_{body}$  is used, which generated  $V_{bn}$  and  $V_{bp}$ . Because of effects of parasitic capacitor and resistor,  $V_{bn}$  and  $V_{bp}$  are in likely *SINE* wave although a triangle voltage is applied to body gate  $V_{body}$ . Besides, in condition that a DC bias  $V_{body0} = 0.35V$  is put into  $V_{body}$ , when a 100mV peak-to-peak triangle voltage is led to  $V_{body}$ ,  $V_{bn}$  and  $V_{bp}$  is generated with the same rule but smaller swing of only about 25mV. As a result, the BW of carrier frequency in this case is narrower than the BW in the case that triangle voltage is directly applied to  $V_{bp}$  or  $V_{bn}$ . From Fig. 4.6, we can see that the carrier frequency is changed in the same rule with triangle body voltage  $V_{body}$ . The dependence of BW of the RO and the TX output signal on body voltage swing is shown in Fig. 4.7. As can be seen, the BW of both the RO and the TX rises when  $V_{body}$  swing increases. With the same simulation condition, the BW of the TX output signal is nearly 1.15x wider than that of the carrier signal, which indicates the impact of code modulation. Under simulation condition of 1kbps data rate, used 31-bit code, 100mV  $V_{body}$  swing at  $V_{body0} = 0.35V$ , TX output signal spectrum is demonstrated in Fig. 4.8. It is easy to realize that BW of CMS-OOK signal with sweeping body bias technique is spread over a wideband with much lower peak level in comparison with that of CMS-OOK signal with single carrier frequency.

In terms of power, the results of HSPICE simulation indicates that average power consumption during a synchronized pulse or a data pulse duration of  $T_p$  is 2.2mW. During the time outside of these pulse duration, the TX does not consume power. This simulation is executed under the following conditions: 1kbps data rate (corresponding to  $T_b = 1ms$ ), ratio factor  $N = 100$ , 31-bit code. With given data, we can calculate required energy used transmitting a pair of data ‘0’ and data ‘1’ as follow:

$$E_{1\&0} = 2.2mW * 2T_p = 44nJ \quad (4-4)$$

In the other words, in order to transmit one data bit, the CMS-OOK TX consumes average 22nJ in simulation.

The matching network are design at the output of PA so that self-resonant frequency is 2.4GHz to obtain nearly *SINE* wave output.

#### 4.4 Experiment results

The analog part of the CMS-OOK TX was laid-out and fabricated based on 65nm SOTB CMOS technology. The layout and chip photography are shown in Fig. 4.9. Because at that time, our lab used 12-pin Cascade Unity probe for RF evaluation, the layout was designed

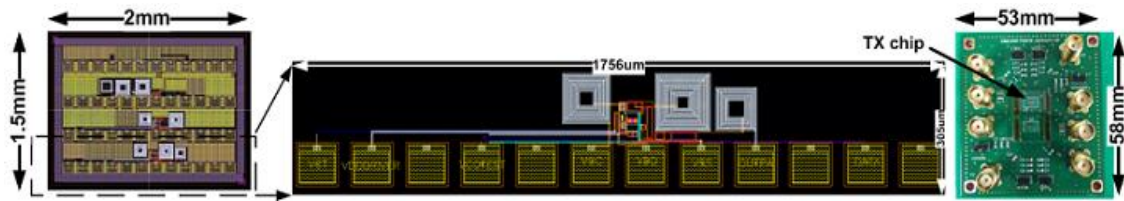


**Fig. 4.9:** Layout picture of TX analog part and TX board

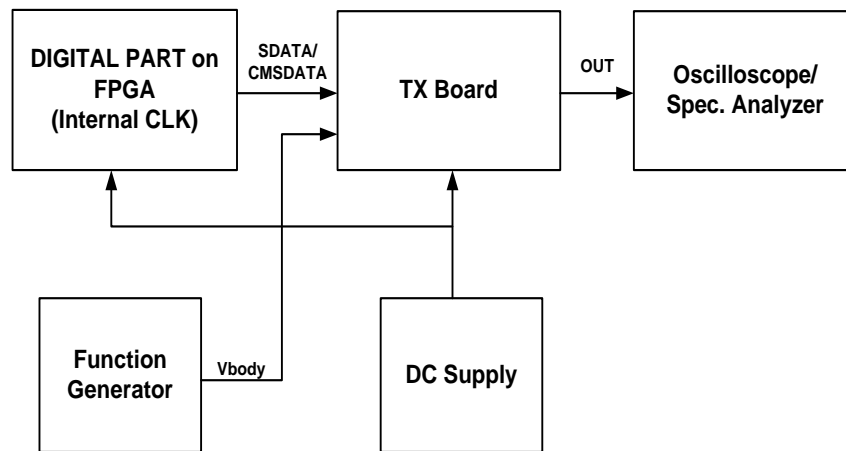


**Fig. 4.10:** Experiment setting up diagram

with on-chip inductors so that it suit to measurement using the probe. The layout occupied an area of  $0.54 \text{ mm}^2$  including PADs.

In Fig. 4.10, the configuration of experiment for evaluating the TX chip is demonstrated. The digital part of the TX was implemented on Altera DE2-115 Development FPGA Kit to deliver synchronized data *SDATA* and code-modulated synchronized data *CMSDATA*. These signals are led to analog TX board as data of analog part. By this way, we can compare the RF S-OOK signal and the RF CMS-OOK signal at the output of TX board in terms of waveform and spectrum. These signals are displayed by using oscilloscopes: ROHDE&SCHWARZ RBT2004 Digital Oscilloscope and RTO 1024 Oscilloscope, and spectrum analyzer CXA Signal Analyzer N9000A.

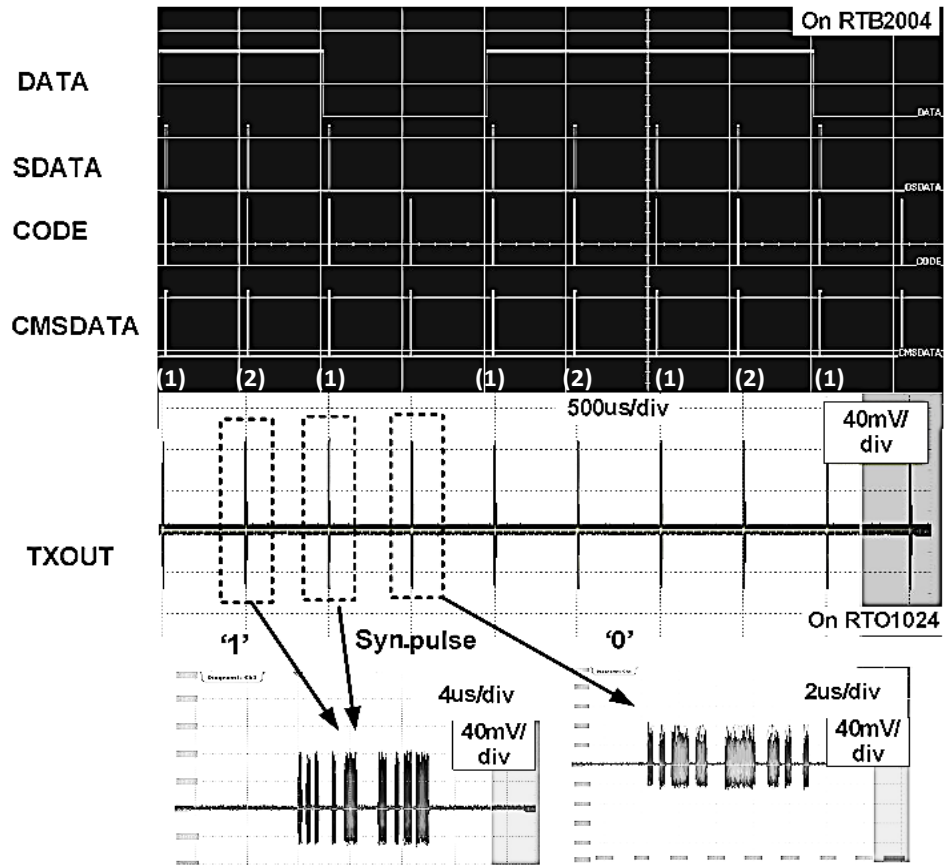


Fig. 4.11: Measured real-time waveform (31-bit code)  
 (1) Synchronized pulse, (2) Data pulse

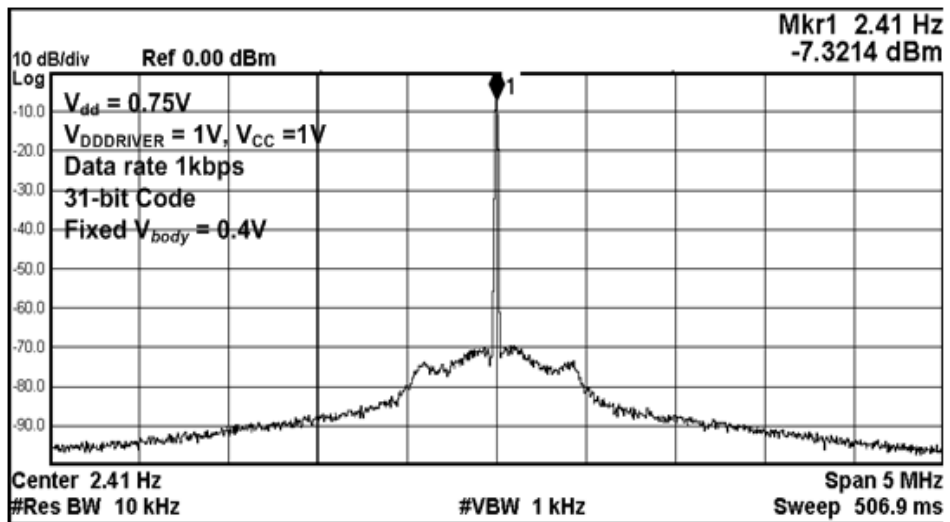


Fig. 4.12: Spectrum of CMS-OOK signal  
 with single carrier frequency

Some parameters of TX were chosen in similar to those in simulation. In detail,  $V_{DD} = 0.75V$ ,  $V_{DDDRIVER} = 1$ ,  $V_{CC} = 1V$ ,  $V_{body}$  sweeps in triangle rule with  $V_{body0} = 0.35$ , 100mV of peak-to-peak amplitude and 322ns of cycle, ratio factor  $N = 100$ , 31-bit code '010 1011 1101 1000 1111 1001 1010 0100' were applied. Data needs to be sent at 1kbps speed.

At first, real-time output waveform is measured and displayed in Fig. 4.11, where the data bit sequence is '10110'. While output digital signal of FPGA board is observed on digital oscilloscope RTB2004, RF signal at output of TX board is shown on oscilloscope.

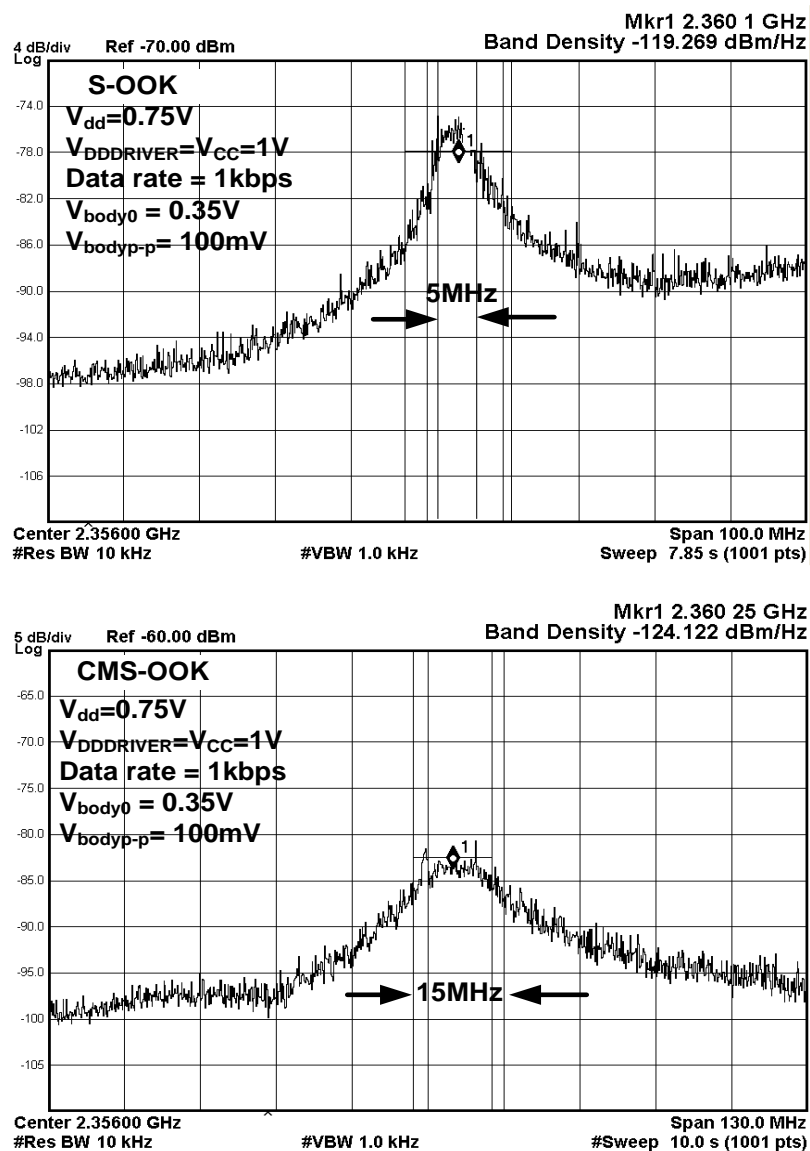


Fig. 4.13: Spectrum of S-OOK and CMS-OOK signals

The measurement results so that the TX output is surely modulated in the manner of CMS-OOK modulation with the carrier signal generated by the RO in the analog board. At first, the spectrum of the CMS-OOK analog part output signal is analyzed with fixed single carrier frequency, as shown in Fig. 4.12. We can see that the spectrum of CMS-OOK RF signal spreads over a wide BW, except a high peak carrier signal of 2.41GHz.

Fig. 4.13 displays the spectrum of S-OOK signal and CMS-OOK signal (with 31-bit code) where the carrier frequency is controlled by sweeping body bias technique. Obviously, the strong carrier signal disappears by carrier frequency diffusing. In comparison with S-OOK modulation, CMS-OOK modulation can spread signal over a wider BW. It is easy to see that BW can be widened from 5MHz of S-OOK RF signal to 15MHz of CMS-OOK RF signal. Besides, the peak power intensity of CMS-OOK RF signal is 6dB below that of S-OOK RF signal. Measurement results indicates that the analog part board consumes 50 $\mu$ A at 1V supply voltage for driver and PA and 60 $\mu$ A at 0.75V for the rest. Totally, the analog part of the TX consumes average power consumption of 83 $\mu$ W corresponding to 83nJ/bit.

Making a comparison between evaluated BW and signal intensity and that of simulated results, we can see that there is a discrepancy. This difference can be explained by followed possible reasons: (1) inaccuracy parasitic extraction tool, (2) small body bias voltage swing of NMOS and PMOS was applied and drop voltage because of parasitic resistor of wire connecting between DC supplier and the TX board, and (3) low-Q and different value of real on-chip inductors and the inductors used in the simulation, which results in different resonant frequency of matching network at the output of the TX. This mis-resonance makes lower power and different center frequency of output signal.

From the measurement results, we can calculate the band density of CMS-OOK signal at the output of TX board is -62dBm/MHz, which completely meets the radio regulations. In a similar condition, with single carrier frequency, CMS-OOK signal with spectrum as in Fig. 17 (no diffused spectrum carrier) has too high peak power density which is tough to be accepted by the regulations. Thus, this fact proves that CMS-OOK modulation scheme with diffused carrier is a good choice for UWB, low-power wireless applications without a license.

A comparison of CMS-OOK TX (analog part) and the others is displayed through Table 4.1. From the table we can realize that CMS-OOK TX consumes much lower power than the others. Thanks to the code modulation and sweeping body voltage technique, CMS-OOK RF signal shows a diffused wide BW with lower peak PSD of -62dBm/MHz. Moreover,

Table 4.1 Comparison with State of Art (TX)					
Parameter	Ref[4-3,4-4]	Ref[4-5]	Ref[4-6]	Ref[4-7]	This work
Technology	65nm	90nm	180nm	LoRa	65nm
Core Area(mm <sup>2</sup> )	0.5(PAD included)	0.6 (PAD included)	0.36	—	0.54 (PAD included)
Modulation	S-OOK	OOK, S-OOK	BPSK	FSK, OOK, GMSK	S-OOK, CMS-OOK
Carrier Generator	RO	LC oscillator	Injection locked RO	Crystall	Sweeping body bias Free-running RO
Frequency range	312-315MHz	2.9-3.8 GHz	400MHz	860-1020 MHz	2.3-2.5GHz
Coding	(no)	(no)	(no)	Manchester	<b>PN code</b>
Supply voltage (V)	0.6/1.0	0.9-1.1	0.8/0.2	1.8/3.7	0.75/1.0
Power consumption	—	0.258mW @1Mpps OOK	0.33mW	125mA	<b>83uW (avg)</b>
Data rate	100/50/10kbps	1Mpulse/s	20Mbps	300kbps	<b>1kbps</b>
FOM*	—	65pJ/pulse +184uW/PRF	16.5pJ/bit	—	<b>83nJ/bit</b> <b>2.59nJ/pulse</b>
Peak PSD (dBm/MHz)	-17@10kbps	-51.95@1Mpulse/s	-42@900MHz	—	<b>-62 @31-bit code</b>
* FOM = Power Consumption/Data rate					

the TX also consumes lower DC power, only  $83\mu\text{W}$ . However, since CMS-OOK modulation is suitable to low data rate, energy efficiency for bit transmission is not high,  $83\text{nJ/bit}$ .

#### 4.5 Chapter conclusion

In this chapter, a Code-Modulated Synchronized-OOK modulation scheme used for low power WSNs was proposed. A CMS-OOK TX was designed, simulated, fabricated using 65nm SOTB technology, and then evaluated. TX RF output signal spectrum is spread by not only code modulation but also carrier frequency diffusion by sweeping body bias voltage applied on carrier RO. Whereby, center frequency and BW of the carrier can be controlled easily by varying the triangle voltage applied to  $V_{body}$  in terms of bias value and peak-peak amplitude. The measurement results show a 15MHz BW with  $-62\text{dBm/MHz}$  PSD peak of CMS-OOK signal, within the radio regulations in Japan. The CMS-OOK TX with an  $83\text{nJ/bit}$  energy at 1kbps data transmission can be achieved.

## References

- [4-1] V. T. Nguyen, R. Ishikawa, and K. Ishibashi, "83nJ/bit Transmitter Using Code-Modulated Synchronized-OOK on 65nm SOTB for Normally-Off Wireless Sensor Networks," *IEICE Trans. On Electronics*, Vol. E101-C.472 Jul. 2018, pp. 472-472.
- [4-2] B. Razavi, "RF Microelectronics," *Pearson Education, Inc.*, 2012
- [4-3] M. T. Hoang, N. Suggi, and K. Ishibashi, "A 1.36 $\mu$ W 312-315MHz Synchronized-OOK Receiver for Wireless sensor Networks Using 65nm SOTB CMOS Technology," *Elsevier Solid-State Electronic* 117, 2016, pp. 161-169.
- [4-4] M. T. Hoang, "A Study on Ultra-Low Power and High Sensitivity OOK CMOS RF Receiver for Wireless Sensor Networks," *Doctoral Thesis*, The University of Electro-Communications, Tokyo, 2015.
- [4-5] M. Crepaldi, C. Li, "An Ultra-Wideband Impulse-Radio Transceiver Chipset Using Synchronized-OOK Modulation," *IEEE Journal Of Solid-State Circuits*, Vol. 46, No. 10, October 2011.
- [4-6] Y. Tsai, C. Y. Lin, B. C. Wang and T. H. Lin, "A 330- $\mu$ W 400MHz BPSK Transmitter in 0.18- $\mu$ m CMOS for Biomedical Applications," *IEEE Transactions on Circuits and Systems - II: Express Brief*, Vol. 63, No. 5, May 2016
- [4-7] SX1276/77/78/79 datasheet, Semtech Cor. [Online]. Available: [https://www.semtech.com/uploads/documents/DS\\_SX1276-7-8-9\\_W\\_APP\\_V5.pdf](https://www.semtech.com/uploads/documents/DS_SX1276-7-8-9_W_APP_V5.pdf). Accessed: 10<sup>th</sup> Nov. 2018

## Chapter 5

### Low-Power and High Immunity to Interferences CMS-OOK Receiver

It is easy to realize that CMS-OOK signal is essentially similar to OOK signal. Thus, at the view point of low power consumption, simple structure with rectifier or envelope detector is prefer. However, this kind of RX has a very limited sensitivity. In order to increase the sensitivity, RX in [1] implement LNA and RF amplifier. Thus, the sensitivity is improved but not too much because of resistive input impedance matching which is resulted in high NF of RF frontend (NF = 28dB). This limitation can be coped with LC impedance matching circuit. It is noticeable that high-Q LC circuit will restrict the bandwidth of RX, which is not suitable to CMS-OOK signal with wide bandwidth. The CMS-OOK RX is designed here using LNA and RF amplifier to increase the sensitivity, using low-Q on-chip inductor in LC matching circuit to reduce NF and widen bandwidth. Besides, code demodulate in digital part helps improve performance in presence of interference [3].

#### 5.1 System architecture of the CMS-OOK RX

The CMS-OOK RX has block diagram circuit and operation waveform are shown in Fig.5.1 and Fig. 5.2, respectively.

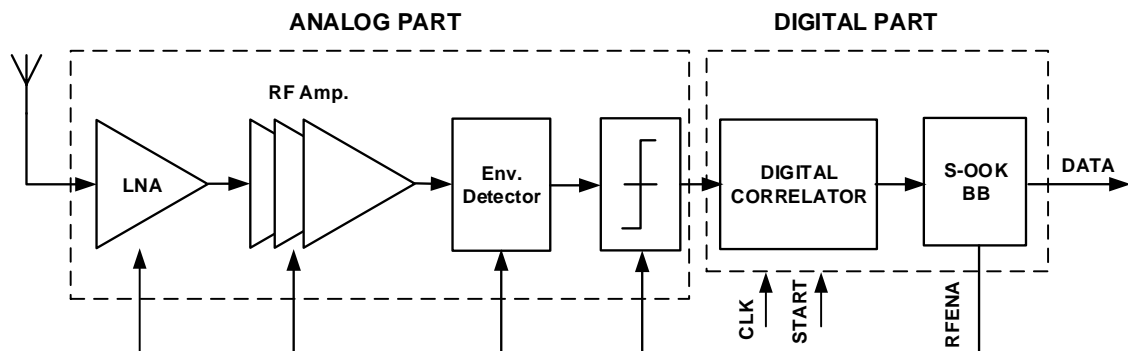


Fig. 5.1: Block diagram of CMS-OOK Receiver

In order to increase the sensitivity of CMS-OOK RX, in comparison with that of RX in [5-1, 5-2], a low noise amplifier (LNA) with low-Q inductor load is used. RF front-end consists of a used on-chip inductor LNA, RF amplifier (RF Amp.) stages, envelope detector (ENV. detector) and a comparator. This is turned-on or turned-off by *RFENA* pulse (Fig. 5.3b) which helps RX save power consumption. CMS-OOK RF signal (*RF INPUT*) with very small amplitude comes to RX in shape as Fig. 5.3c. Before this, a wake-up signal *START* is sent from an assumed wake-up RX to initiate the main CMS-OOK RX. The RF signal is magnified by RF amplifier consisting an LNA and 4-stage RF Amp. to produce output signal *RF AMP. OUTPUT* (Fig. 5.3d) with magnitude high enough. Then, it is led to an envelope detector (ENV. detector) in series with a comparator. The output of comparator is a bit sequence which should be same as transmitted *CMSDATA* from TX (Fig. 5.3e). This bit stream is input to a digital correlator which operates as a matched filter. If the received signal and the code used in RX are matched enough to over a programmable threshold, digital correlator will deliver a pulse at the end of matched bit sequence (Fig. 5.3f). By using clock with much higher frequency than speed of input bit stream, which known as oversampling technique, synchronization issue in digital correlator becomes more relaxed. Output pulses of digital correlator are led to S-OOK baseband digital which not only recovers the sent data (*DATA OUTPUT* in Fig. 5.3g) but also generates *RFENA* pulses (Fig. 5.3b) to turn on and turn off RF front-end. Thanks to *RFENA* signal, RF front-end can cut down the power consumption at the most power hungry part of RX during the time outside of data pulses duration and synchronized pulses duration. Besides, low noise figure (NF) and high gain RF front-end contribute in raising sensitivity of RX, which contributes to lengthening the operation range of TRX system. In addition, utilizing code modulation with different codes for different TX and RX produces a higher immunity to interference in comparison with TRXs in [5-1] and [5-4].

## 5.2 Circuit level design bases on 65nm SOTB devices

CMS-OOK RX consists of two parts: analog part (RF frontend) and digital part in consequence as shown in Fig. 5.4 and Fig. 5.9, respectively.

### 5.2.1 Analog part

The analog path composes of a LNA, a 4-stage RF amplifier, an envelope detector and a comparator in series.

**Fig. 5.2:** CMS-OOK RX in combination with Wake-up RX

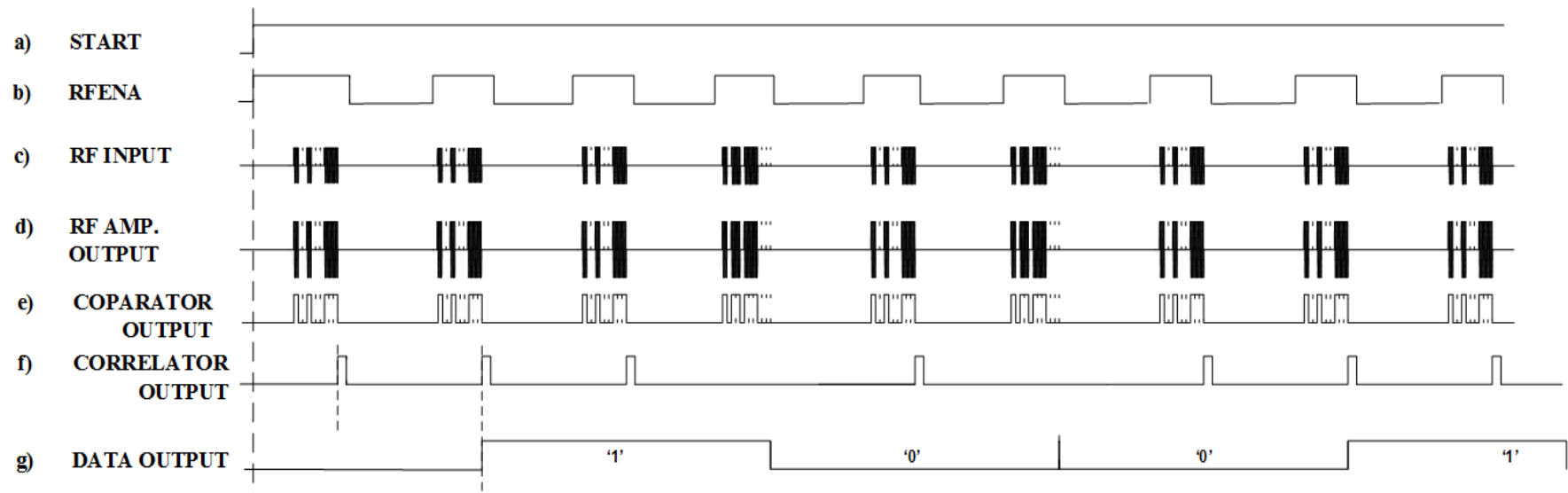
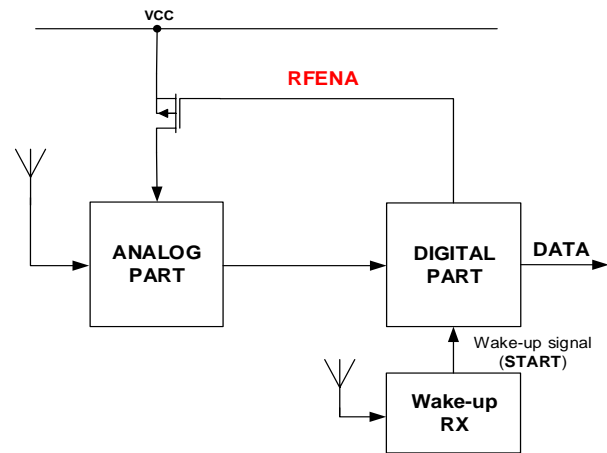


**Fig. 5.3:** Operation waveform of CMS-OOK RX

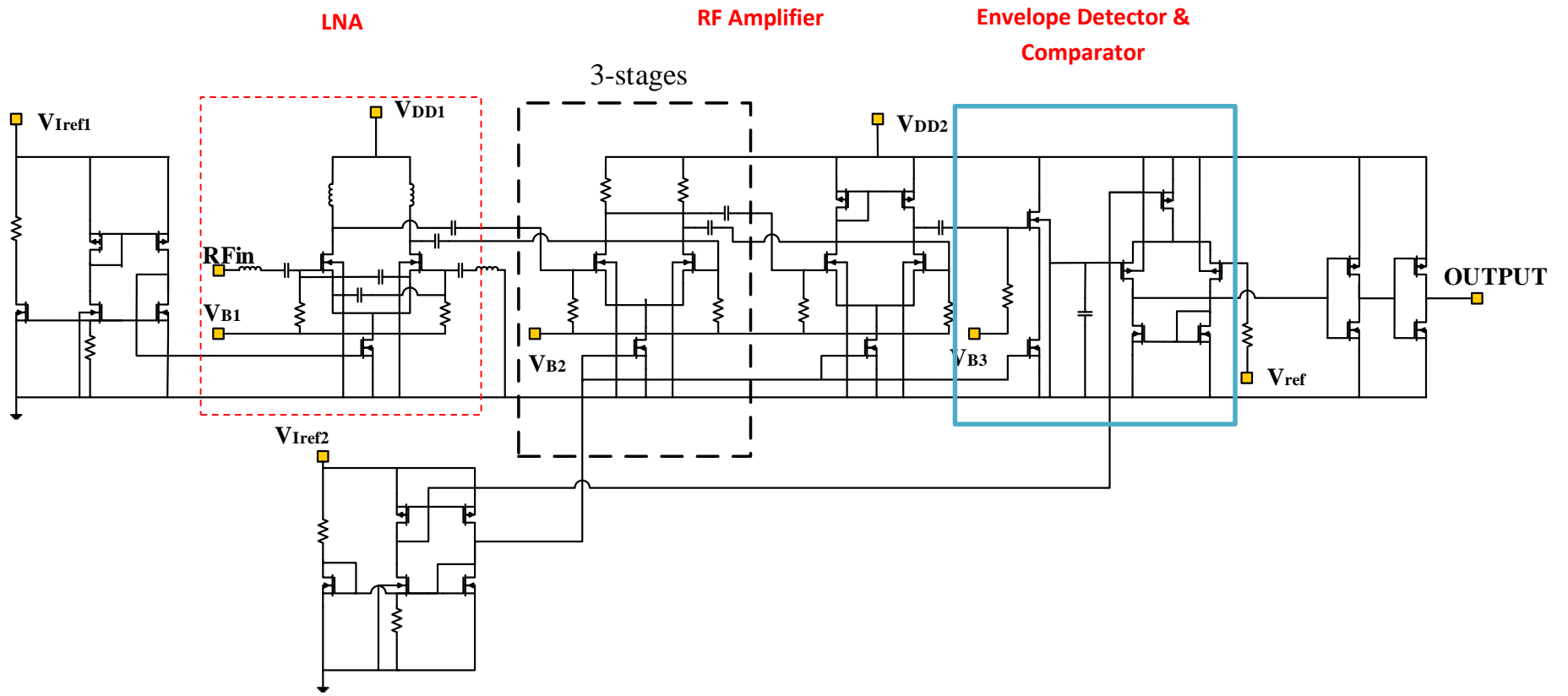


Fig. 5.4: Detailed schematic of RF front-end (Analog part)

To begin with, the RX uses an unbalance input inductive load common source (CS) differential LNA (Fig. 5.5). The main purpose of LNA here is to magnify input signal and decrease general noise figure (NF) in order to raise sensitivity of RX. RF signal from antenna outside of chip goes to one input of the LNA via bonding wire  $L_b$  while the other input is

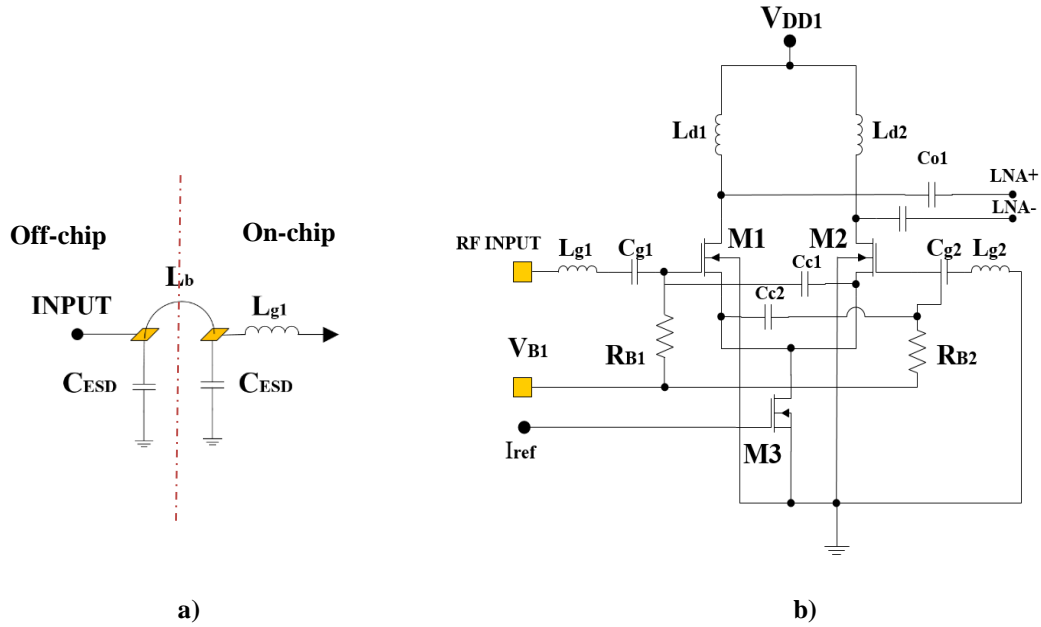


Fig. 5.5: LNA schematic

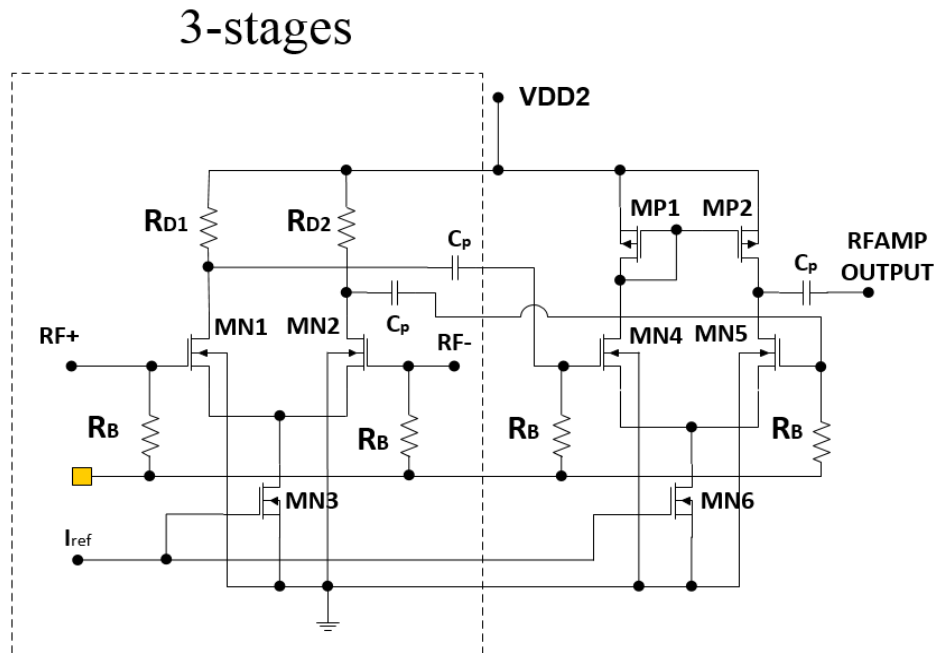
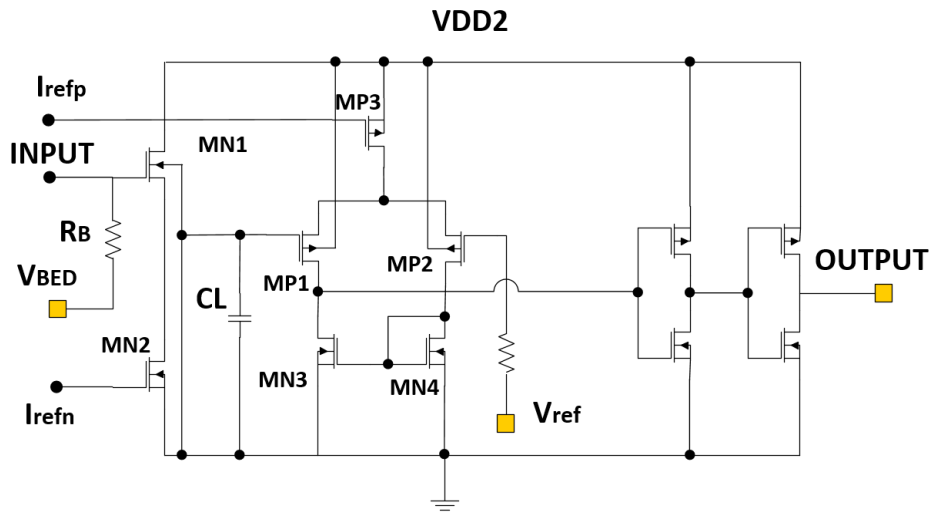


Fig. 5.6: 4-stage RF Amplifier



**Fig. 5.7:** Envelope detector and Comparator

connected to ground. Because of effects of pads on PCB board as well as pads and ESD circuit on the chip,  $L_{g1}$ ,  $C_{g1}$  and  $C_{c1}$  are added for input impedance matching. In this design,  $L_{g1}$ ,  $L_{g2}$ ,  $L_{d1}$  and  $L_{d2}$  are on-chip inductors with low-Q value which help to widen the bandwidth of LNA and integrate matching circuit on chip.

*An on-chip inductor on SOTB process:*

Application circuits at high frequency often require a small inductance. It is impossible to access small value inductance externally because the inductance associated with chip pads and bond wire can exceed that small value. Thus, it is popular to use on-chip inductor in RF applications [5-5]. In this design of CMS-OOK TX and RX, we utilized on-chip planar spiral inductor on 65nm SOTB process.

Normally, on-chip inductors are typically realized as metal spirals (Fig. 5.8). Since the mutual coupling between every two turns, spirals exhibit a higher inductance than a straight line with the same length [5-6]. In principle, to minimize the series inductance and parasitic capacitance of spiral inductor, it is often implemented in the top metal layer - the thickest metal layer. On 65nm SOTB, that is metal 8 (M8) layer. However, although M8 is the thickest metal layer of 65nm SOTB process, it is still thin in comparison with top metal layer of other processes. Thus, series resistance of 65nm SOTB on-chip inductor is significant, which can help us to design low-Q on-chip inductor for CMS-OOK TRX.

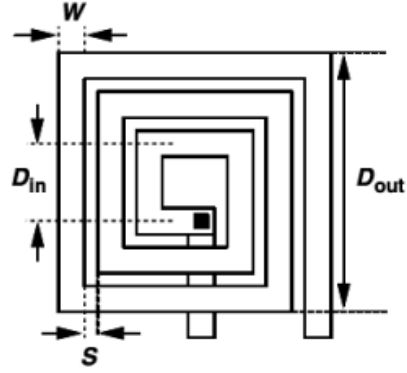


Fig. 5.8: Spiral inductor

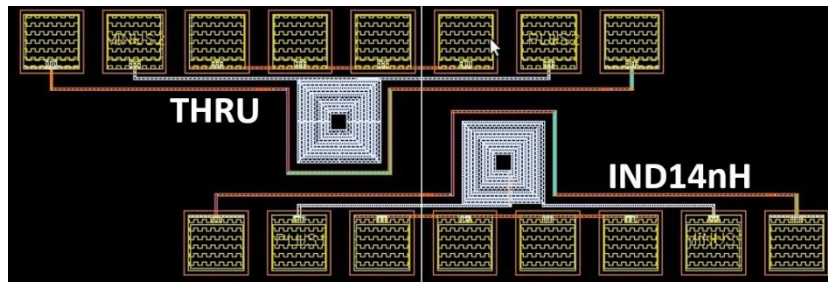


Fig. 5.9: An on-chip 14nH spiral inductor in 65nm SOTB process

The two-dimension square spiral in Fig. 5.8 is fully specified by four quantities: outer dimension,  $D_{out}$ , the line width,  $W$ , the line spacing,  $S$ , and the number of turns,  $N$  (or inner dimension  $D_{in}$ ). Inductance value primarily depends on the diameter of each turn and the number of turns, the width and spacing also have effects on this value indirectly.

For planar square spiral inductor, inductance value can be calculated basing on a formula that has less than 10% error as below [5-6]:

$$L \approx 1.3 \cdot 10^{-7} \frac{l_{total}^{\frac{5}{3}}}{\left[ \frac{l_{total}}{4N} + W + (N-1)(W+S) \right]^{\frac{1}{3}} W^{0.083} (W+S)^{0.25}} \quad (5-1)$$

where  $l_{total}$  is total length of the spiral inductor. In this study, we calculated and designed the on-chip spiral inductors basing on the formula (5-1). In the LNA, the inductor of  $L_g = 4.1\text{nH}$  and  $L_d = 20\text{nH}$  are calculated and designed, then used in design of the LNA.

Back to the design of LNA, the low-Q inductors with internal resistors also contribute on limiting gain and increasing NF of the LNA, especially the internal resistors connect to

the gates of M1 and M2. The LNA is designed in constrain of specify power consumption, thus the NF is not the smallest but acceptable value.

Following the LNA, a 4-stage RF amplifier is used to enlarge RF signal from output of the LNA (Fig. 5.6). The first 3-stage is deployed resistive load differential common source (CS) amplifier while the last is a single-ended differential CS topology to transform differential signal to single signal. CS topology is used in order to achieve a large enough power gain, which contributes in reducing NF and magnifies RF signal to satisfy input requirement of envelop detector and an adjustable reference voltage comparator (as shown in Fig. 5.7). This guarantees that the RX can detect the received signal with a specified reliability.

### 5.2.2 Digital part

Fig. 5.10 and Fig. 5.11 display block diagram and timing chart of RX's digital part,

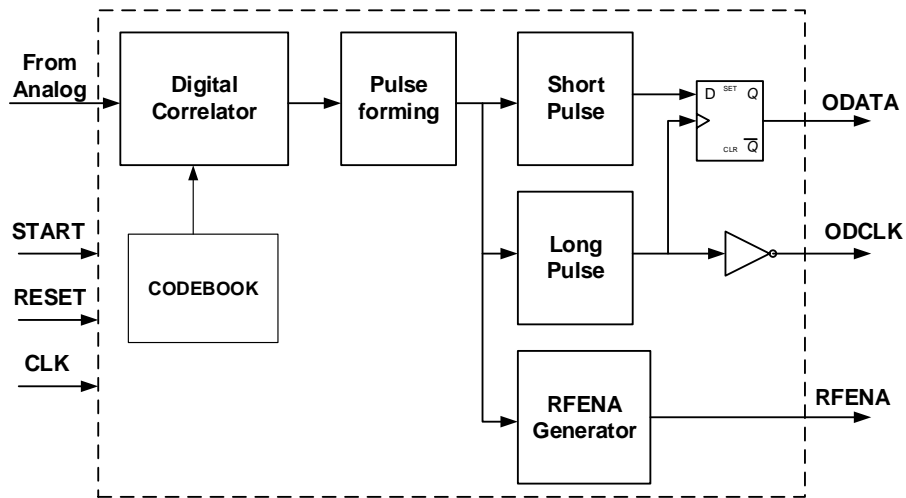


Fig. 5.10: Block diagram of digital part

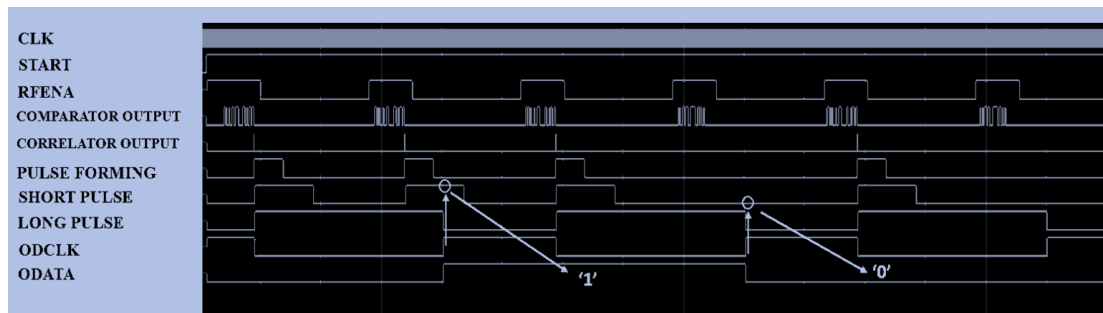
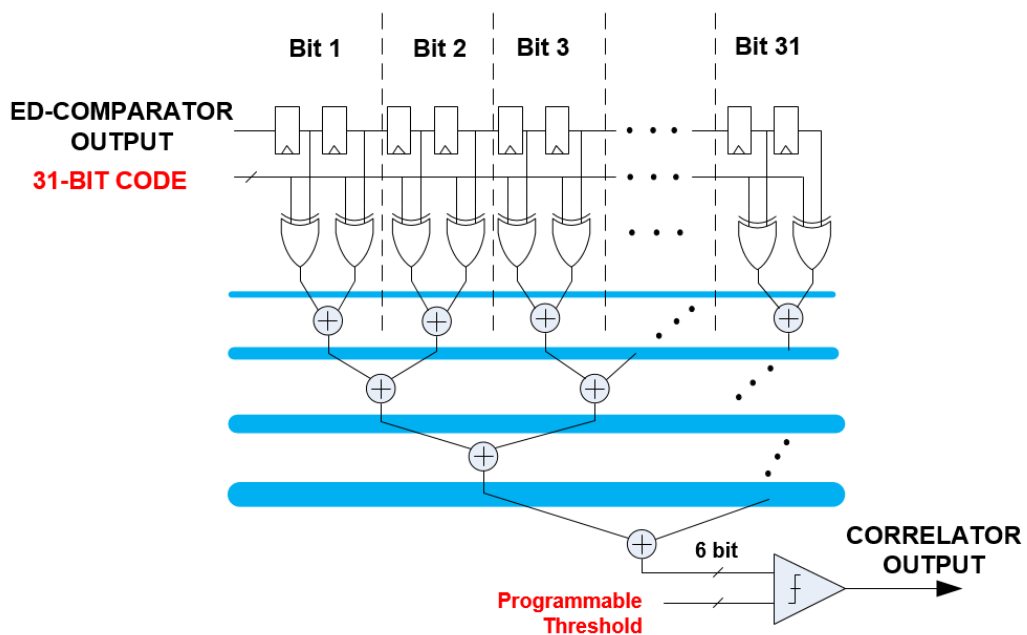


Fig. 5.11: Timing chart of digital part

respectively. The signal from analog part (*COMPARATOR OUTPUT*) is led to a digital correlator while the other input of the digital correlator is codebook. If the received signal is matched with a programmable code, the digital correlator will generate a high pulse (*CORRELATOR OUTPUT*) with the same pulse width of clock signal. Conversely, if the received signal is not matched to the code or signal part corresponding to data pulse '0', no pulse is output from the digital correlator. Digital correlator output signal will go to Pulse forming block to rebuild a new pulse (*PULSE FORMING*) with a longer interval. Next, *PULSE FORMING* signal goes to three blocks: Short Pulse, Long Pulse and RFENA Generator simultaneously. Among them, RFENA Generator block delivers window pulse *RFENA* to control turning on or off RF front-end while Long Pulse block in combination with Short Pulse block generates data clock (*ODCLK*) to recover data (*ODATA*) sent from the TX.

To address asynchronous issue between code and received signal, the digital correlator continuously correlates 2x or 4x-oversampled comparator bit-stream with a programmable 31-bit code. Structure of a 2x-oversampled 31-bit code digital correlator is exhibited in Fig. 5.12. By this way, each bit of *COMPARATOR OUTPUT* signal is sampled



**Fig. 5.12:** 31-bit 2x-sampling digital correlator

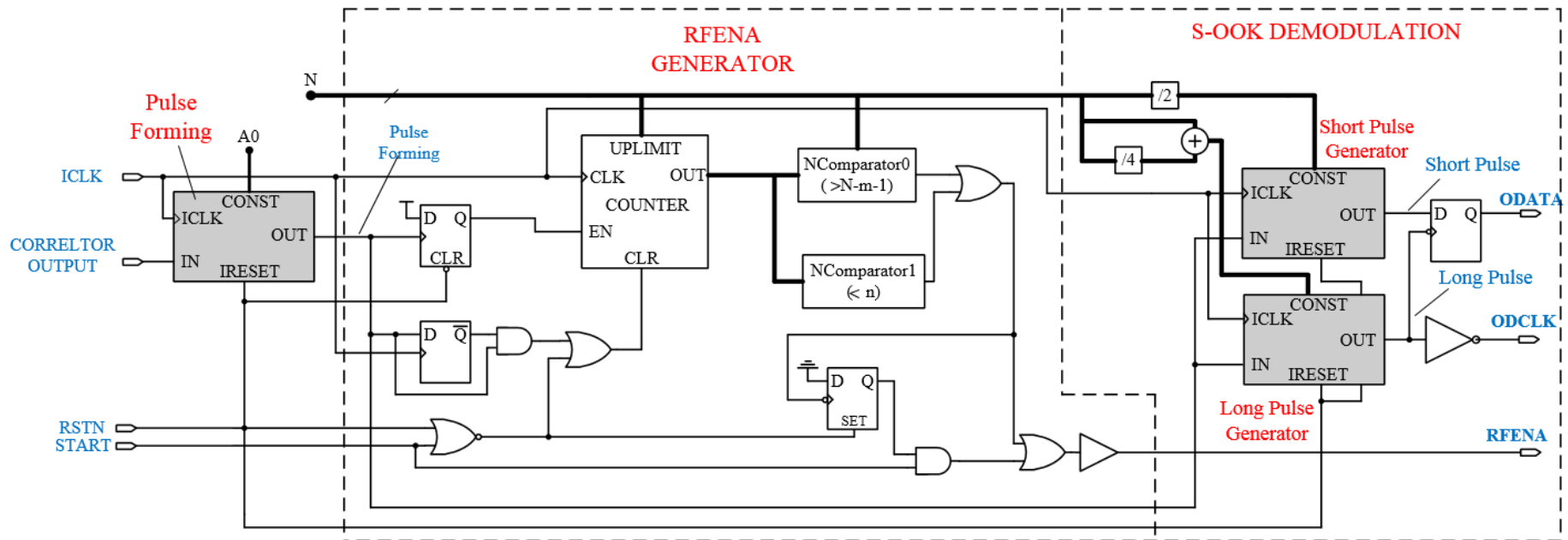
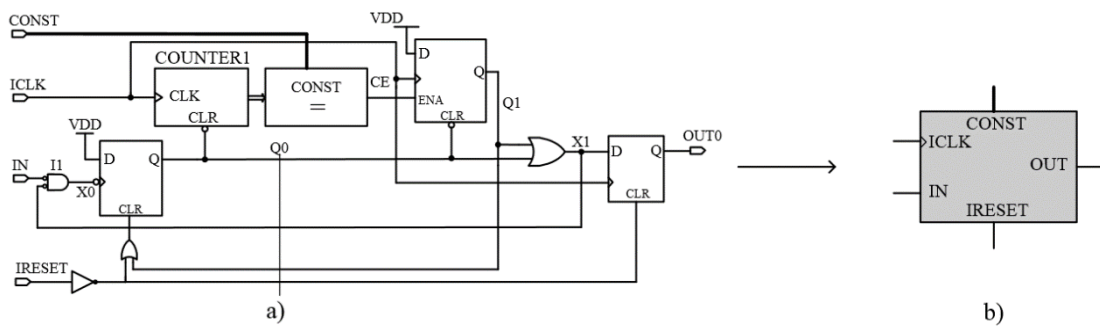
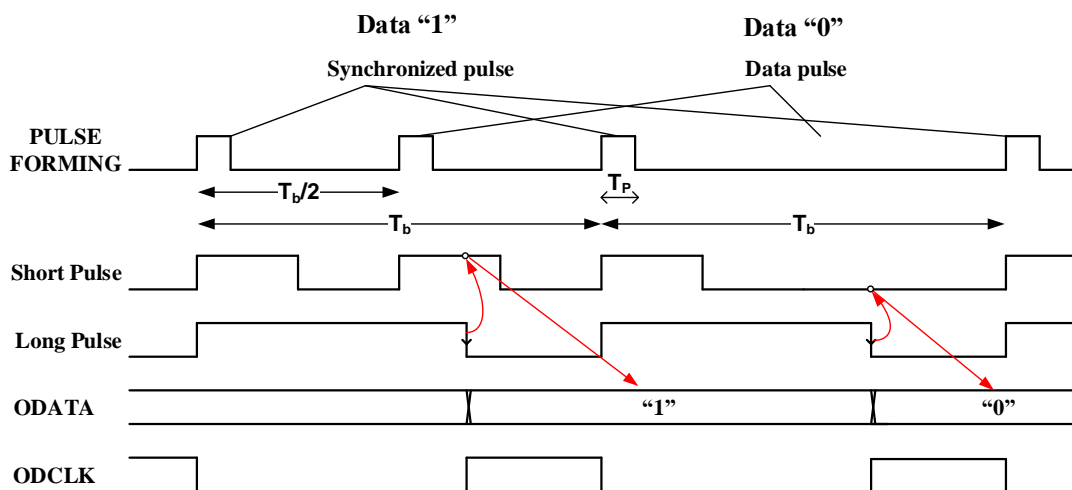


Fig. 5.13: Detailed structure of RFENA Generator and S-OOK demodulator

and multiplied with corresponded code bit by exclusive-OR gates twice a clock cycle of TX. Then, a sum of all exclusive-OR gate output is executed. In this case of 2x-oversampling, there are totally 62 exclusive-OR gates to correlate between code and received signal. In ideal, maximum sum is 62 (6'h3E) when the received signal is completely matched to the code. This sum is compared with a programmable threshold to decide that the received signal is matched to the code or not. In the case that RX receives a sent signal from TX without interference and power large enough, analog part can operate well and produce no error bit-sequence, hence the sum can achieve maximum value. Thus, programmable can be set at highest value of 62. However, normally noise and interference are often available in communication channel, which can make some errors when RX detects received signal. Depending on the intensity of noise and interferences, threshold value is adjusted in order to recover the data with minimum bit error rate. Normally, the lower threshold will be



**Fig. 5.14:** Schematic (a) and symbol (b) of Pulse Forming, Short Pulse and Long Pulse blocks



**Fig. 5.15:** Timing chart for recovering data

programmed when strong interference appears and vice versa. Thank to this technique, interference immunity of CMS-OOK RX is enhanced.

To continue, detailed structure of Pulse Forming, RFENA, Short Pulse and Long Pulse Generator blocks is shown in Fig. 5.13.

Pulse forming, Short Pulse and Long Pulse Generator blocks essentially have the same structure but different input values of counting number  $CONST$  (Fig. 5.14). In fact, this circuit operates as a pulse generator which creates new pulses with the same position to input but different pulse width. The pulse width is defined by programmable  $CONST$  value. This value controls a numerical comparator which yields an output pulse with duration equal to  $CONST$  clock cycle.  $CONST$  values of Short Pulse Generator and Long Pulse Generator are calculated so that  $ShortPulse$  is shorter than  $T_b/2$  while  $LongPulse$  is longer than  $T_b/2$ . Clock used to read data output ( $ODCLK$ ) is generated by inverting  $LongPulse$ . Output data is recovered by reading value of Short Pulse at the rising edge of  $ODCLK$  (Fig. 5.15). As a result, output data  $ODATA$  is delayed by nearly a data bit interval.

The timing chart of RFENA Generator is described in below Fig. 5.16. Generating  $RFENA$  is based on a wake-up signal from the assumed wake-up RX in combination with received signal  $PULSE FORMING$ . Whenever the RX receives wake-up signal  $START$ , whole digital part of the RX will operate to listen the input signal. As soon as  $PULSE FORMING$  comes, the COUNTER0 will begin counting from 0 to  $UPLIMIT$  value  $N-1$

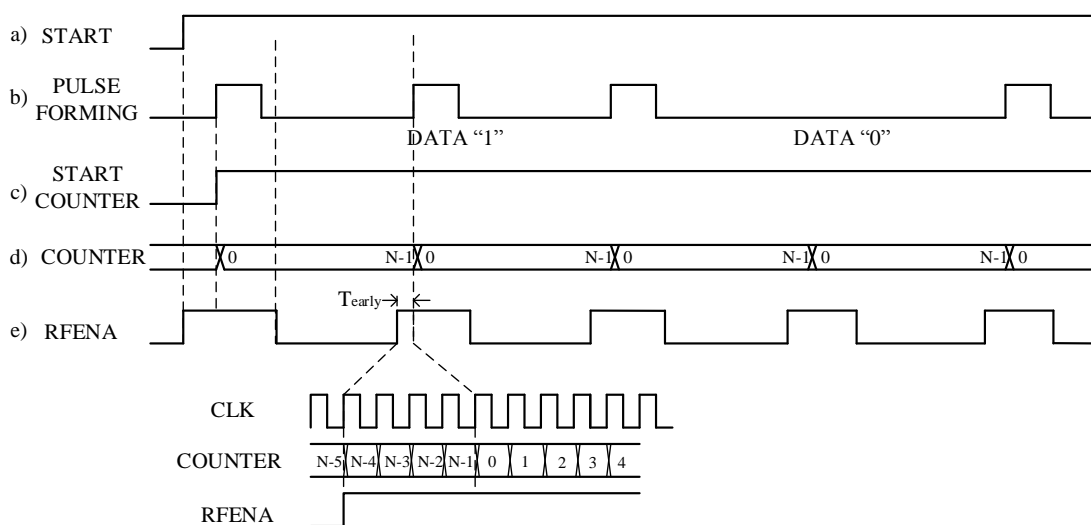


**Fig. 5.16:** Timing chart for RFENA Generator

basing on external clock signal CLK, where  $N = \frac{T_b}{2T_{CLK}}$ . It will be recounted by the rising edge of *PULSE FORMING* signal which can correspond to data pulse or synchronized pulse. The window signal RFENA will be cleared if  $COUNTER \geq n$  and set high level if  $COUNTER \geq (N - m)$ , where  $n$  and  $m$  are chosen to guarantee that RFENA is wide enough to avoid losing signal. This RFENA will power on analog part earlier than the time point when RF signal comes by  $T_{early}$  and power off when the RF signal finishes. Whereby, analog part, which consumes most power of the RX, only operates when RF signal comes and powers off in remain time. This helps the RX cuts down significantly power consumption.

Fig. 5.17 presents layout picture of the CMS-OOK RX on 65nm SOTB CMOS technology. It occupies an area of  $0.54 \mu\text{m}^2$  in total.

### 5.3 Simulation results

In this section, simulation results of a CMS-OOK based on 65nm SOTB CMOS technology are described. In which, the analog part is simulated by HSPICE simulator while the digital part is simulated by MODELSIM.

Because rc-extractor tool is not able to extract inductance parameter of on-chip inductor, the simulation of analog part here is pre-layout simulation. In this simulation, parasitic capacitor of PADs and ESD protection circuits, parasitic inductor of bonding wires are accounted. Parasitic parameters are estimated as followed:  $C_{ESD} = 0.5\text{pF}$ ,  $L_b = 1\text{nH}$  (correspond to 1mm length). The on-chip inductor:  $L_{g1} = L_{g2} = 9\text{nH}$  with internal resistor  $r_g = 25\Omega$ ,  $L_{d1} = L_{d2} = 20\text{nH}$  with  $r_d = 110\Omega$ . LNA, RF amplifiers and envelope detector are biased by DC voltage:  $V_{B1} = 0.7\text{V}$ ,  $V_{B2} = 0.65\text{V}$ ,  $V_{BED} = 0.47\text{V}$ , respectively. Reference voltage of comparator is  $55\text{mV}$ . All analog part is supplied by  $1\text{V}$  DC voltage.

Firstly, the transient simulation result of RF front-end is shown in Fig. 5.18. This figure displays the result in case of minimum input voltage of  $35\mu\text{V}$  on  $50\Omega$  input impedance (corresponding to  $-76\text{dBm}$  power) where analog part can detect the received signal well. As can be seen from the lowest picture, average power of RF frontend during time interval of RFENA pulse is  $194\mu\text{W}$ . If the ratio between data bit  $T_b$  width and synchronized pulse width  $T_P$  is chosen by 10. The average power consumption of RF frontend for receiving a pair of bit '1' and '0' is  $38.8 \mu\text{W}$ . With the data rate here is  $1\text{kbps}$ , that means the energy per bit is  $38.8\text{nJ/bit}$ .

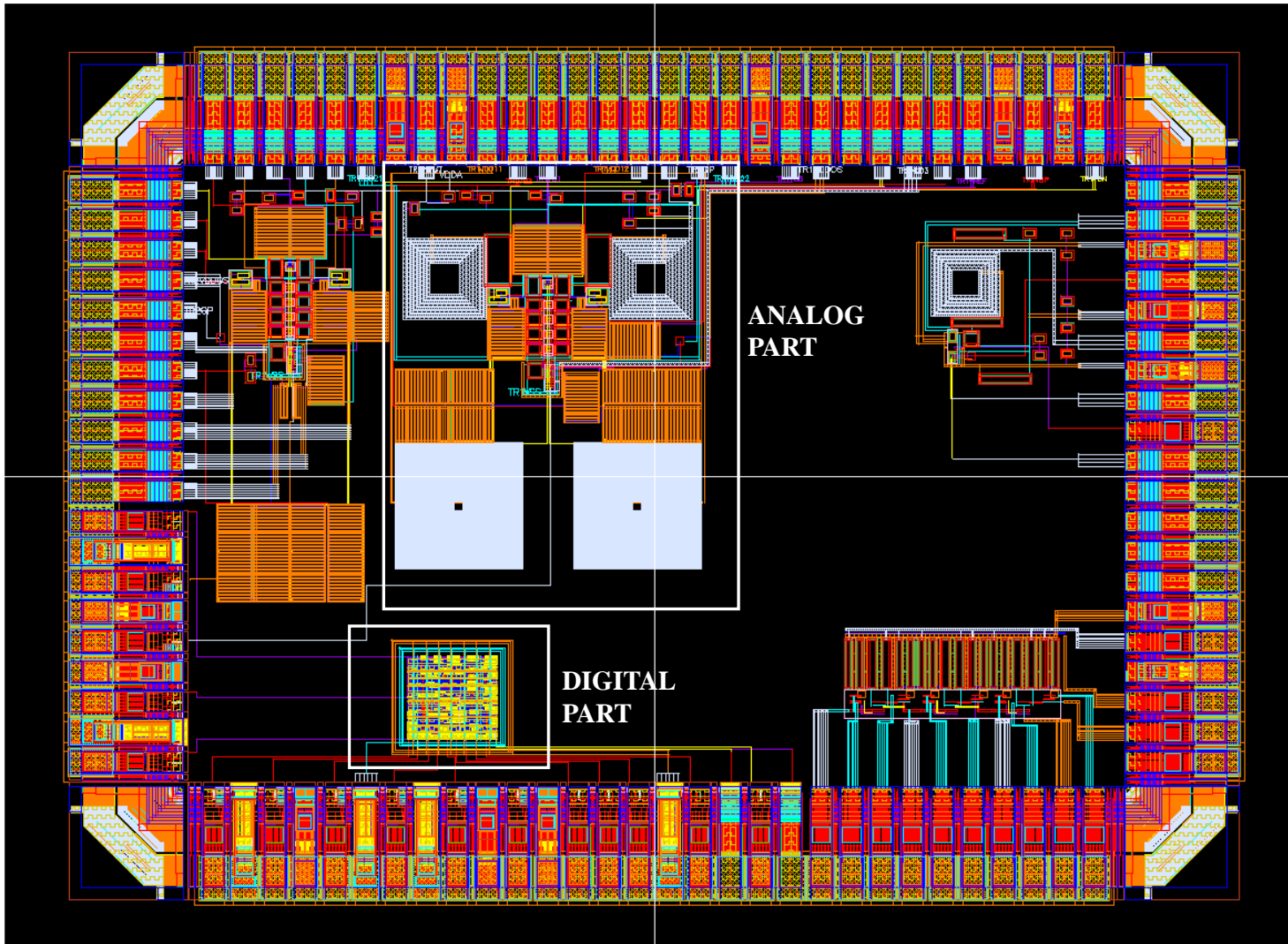


Fig. 5.17: Layout picture of CMS-OOK RX

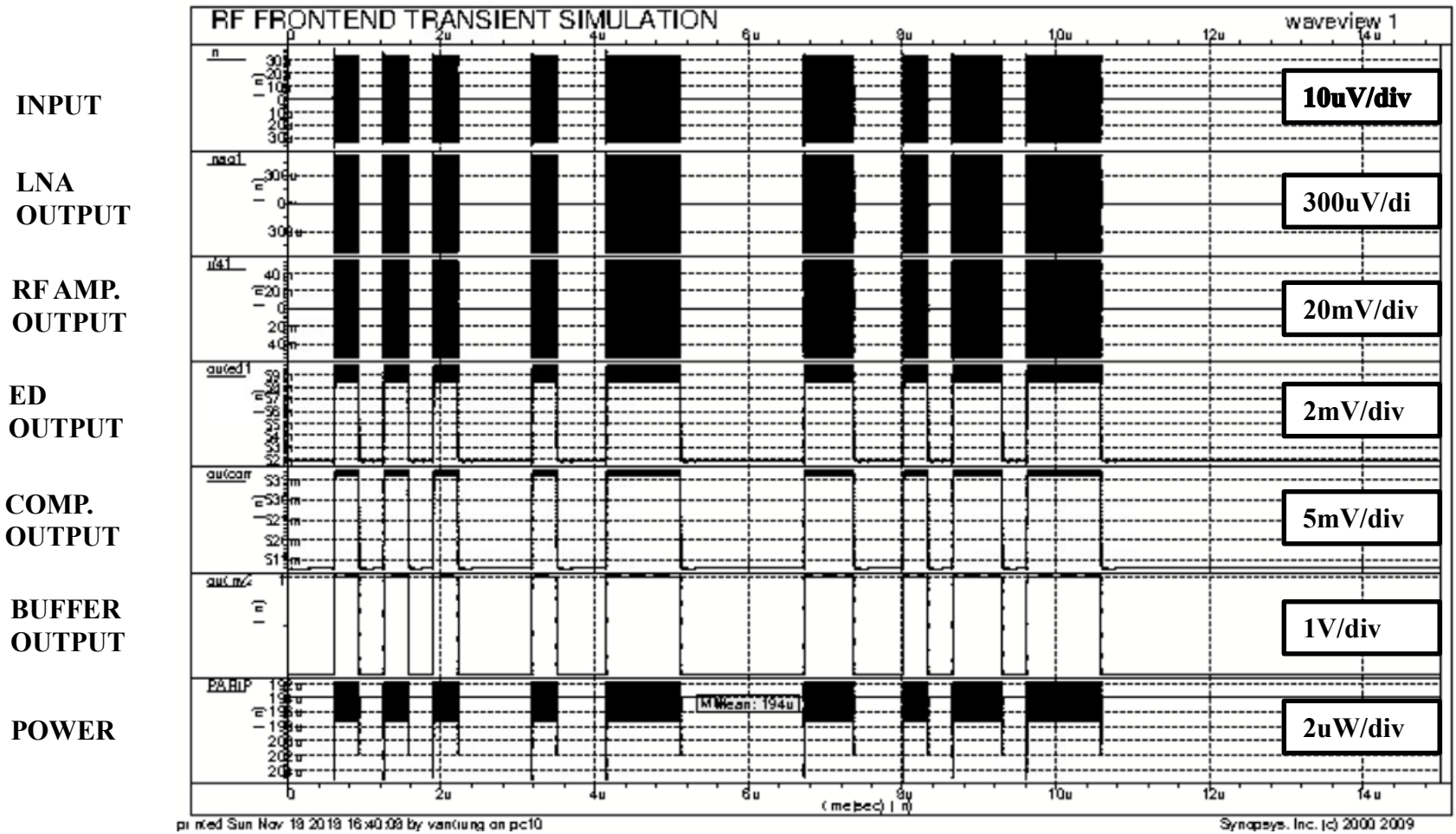


Fig. 5.18: Transient simulation results

Secondly, Fig. 5.19 demonstrates AC simulation results of RF frontend. As can be seen from the highest stack of this figure, NF of the RF front-end is around 8dB which is really close to the minimum NF curve at 2.4GHz. In two lower picture, S-parameters are shown with  $S_{11} = -16.6$  dB and  $S_{21} = 40$ dB at 2.4GHz. The NF value is still quite high because of internal resistor of on-chip inductor  $L_{g1}$  and  $L_{g2}$ .

Digital part is simulated by ModelSim simulator. With give 1kbps data rate, TX clock frequency is 3.1MHz, ratio  $T_b/T_P = 10$ , oversampling clock frequency at RX is 6.2MHz. The

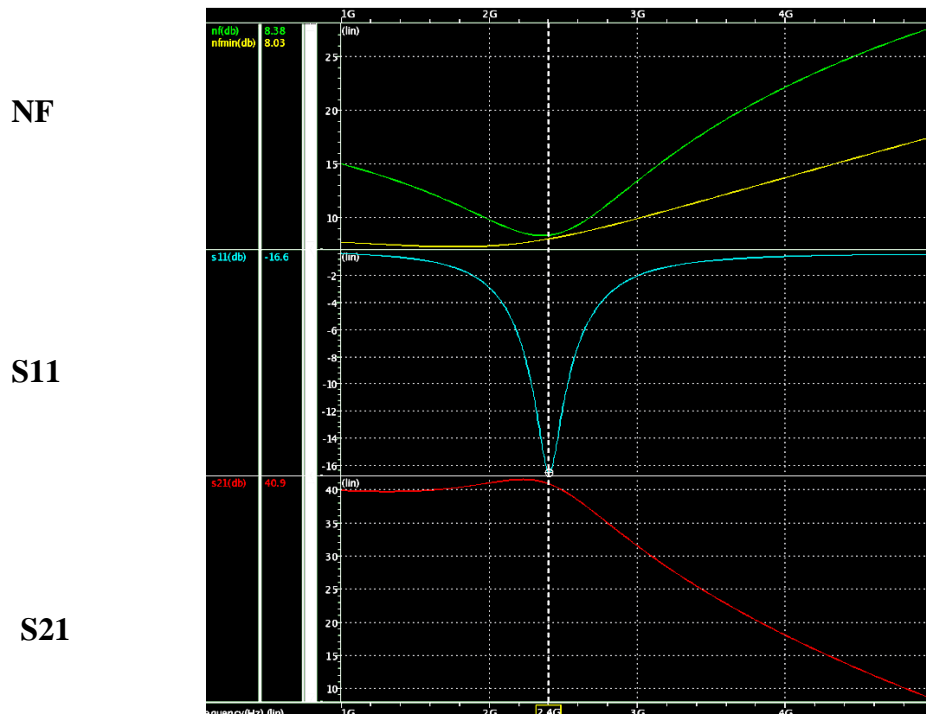


Fig. 5.19: Noise figure, S11 and S21 of RF front-end

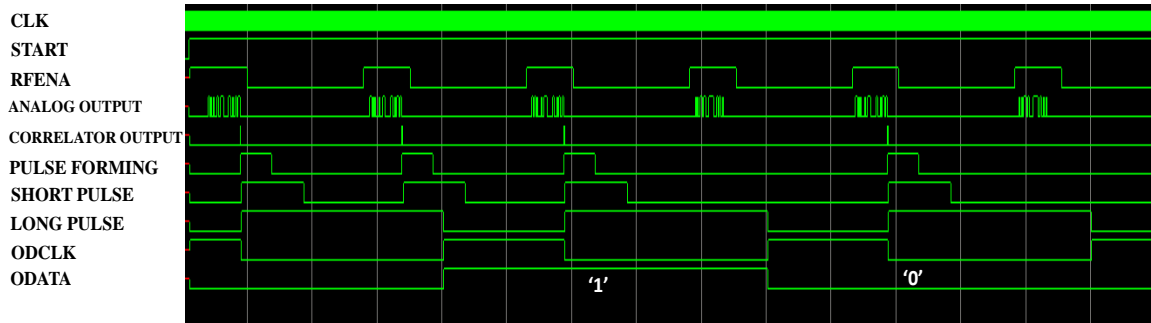


Fig. 5.20: Simulation results of digital part

**Table 5.1:** Comparison with Published State-of Art RX

	[1] ISSCC'11	[2] CICC'13	[3] ISSCC'16	[Thien] Elsevier'16*	[5] TCAS-I'17	[6] JSSCC'18	This work*
<b>Technology</b>	130nm	130nm	65nm	65nm	90nm	180nm	65nm
<b>Carrier Frequency</b>	402 MHz	403 MHz	2.4GHz	312-315 MHz	2.4 GHz	113.5 MHz	2.4GHz
<b>Modulation</b>	FSK	OOK	OOK	S-OOK	OOK, TSSS-OOK	OOK	CMS-OOK
<b>Supply voltage</b>	1V	1.2/0.5 V	1/0.5 V	1/0.6 V	01.2, 1.8, 2.5V V	0.4 V	1/0.75 V
<b>Digital Correlator</b>	No	31-bit	31-bit	No	-	32-bit	31-bit
<b>External Component</b>	XTAL+ LC MN	XTAL+ LC MN	XTAL+ LC MN	RLC MN	Transformer/image filter	Transformer/filter	LC MN
<b>Oscillator</b>	Inj-locked osc.	XTAL Osc.	XTAL Osc.	-	Dual-mode of PLL/FLL	Relaxation Osc.	Relaxation Osc.
<b>Gain Stages</b>	IF	ED	ED/ED+BB	RF Amp.	LNA+ IF + BB	TF/ED/BB	LNA, RF Amp.+ED
<b>Interference Injection</b>	LC MN+IF filter	LC MN + correlator	Digital Processor	LC MN	LC MN + spur suppression technique	Transformer/filter + Correlator	LC MN +correlator
<b>Data Rate</b>	200kbps	12.5 kbps	8.192kbps	100/10 kbps	1Mcps	0.3 kbps	1kbps
<b>Energy/bit</b>	220pJ	9.3 pJ	912.7/28.8pJ	0.083/0.136 nJ	0.614/ 2.2nJ	15pJ	38.8nJ
<b>Sensitivity [dBm]</b>	-70	-45.5	-39/56.5	-58.5	-91 (Non-coherent)/ -93 (Coherent)	-69	-76
<b>Power consumption</b>	44 $\mu$ W	116nW	104/ 236 nW	8.39/1.36 $\mu$ W	0.614mW/2.2mW	4.5nW	38.8 $\mu$ W

simulation results can be seen in Fig. 5.20. It is clear that digital part can recover successfully the data sent from the TX.

The chip on 65nm SOTB CMOS of CMS-OOK RX was fabricated and evaluated. Although there was a quite good DC operation of RF front-end, AC operation was not good. RF front-end did not output desired signal, which led to no data can be achieved at the output of the digital part. The main reasons maybe because of incorrect values of gate on-chip inductor in LNA, which leads to strong attenuating coming RF signal on input of the LNA. Therefore, demodulation of RX was checked by using discrete RF modules and FPGA board, which is exhibited in the next section.

In the Table 5.1 shows a comparison of this design with other works. As can be seen, this design owns a reasonable power consumption of 38.8  $\mu$ W with quite good sensitivity of -76dBm at low data rate of 1kbps. In comparison with other works which utilize digital correlator for interference injection, the power consumption of this design is much higher than that of others but better sensitivity.

### 5.5 CMS-OOK TRX system experiment with discrete RF module and FPGA board.

Aiming to check operation of CMS-OOK TRX system, an experiment using discrete RF TRX and FPGA board is carried out. The configuration of the experiment diagram is shown in Fig. 5.21.

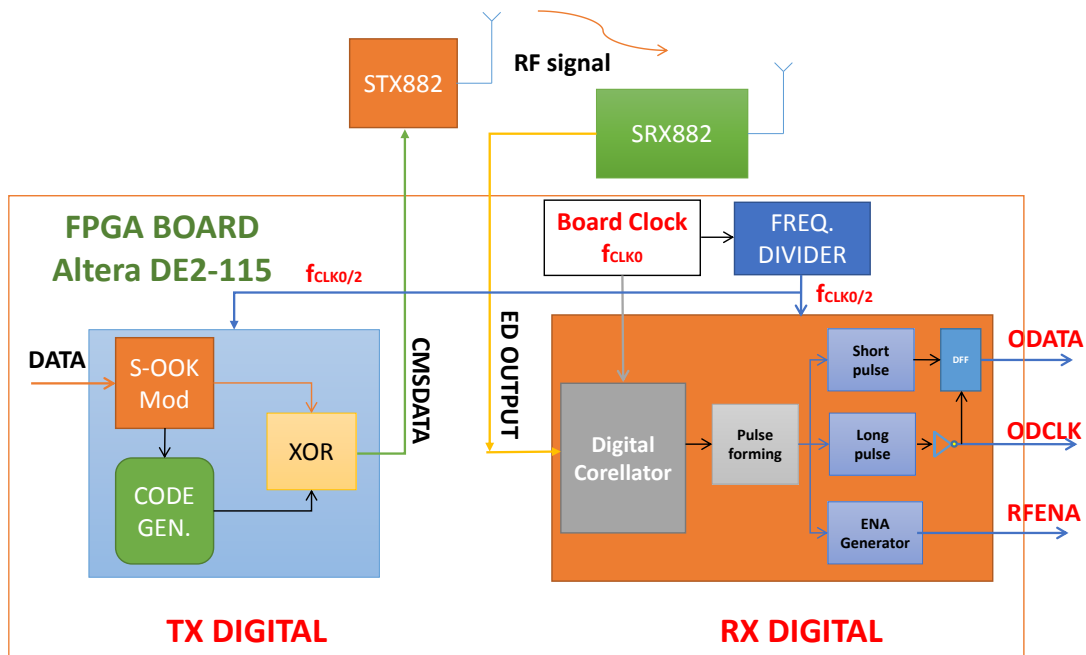


Fig. 5.21: Experiment setting up diagram

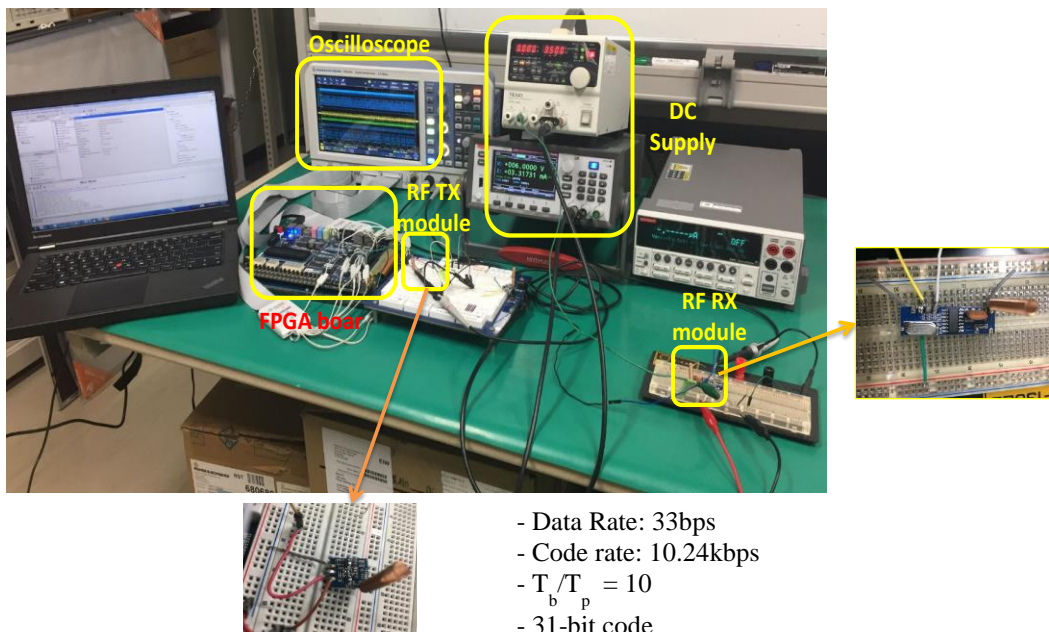


Fig. 5.22: Experiment setting up

Digital part of TX and RX are programmed and implemented on FPGA board Altera DE2-115. Clock signal of both parts is supplied from on-board clock source. Analog part of TX and RX are implemented by ASK transmitter module (STX882) and ASK receiver module (SRX882) – commercial products of NiceRF Wireless Technology Co.,Ltd [5]. These RF modules operate at single frequency of 433 MHz, maximum pulse rate is around 10 kpulse/s. Parameters of TRX are chosen as followed: DATA needs to be sent at rate of 33bps, oversampling clock frequency  $f_{CLK0} = 20.48$  kHz, thus other blocks of TX digital and RX digital operate under 10.24 kHz clock signal, number of code bit is 31.

The experiment was carried out with the configuration as shown in Fig 5.22. Clock signal is generated by on-board PLL oscillator basing on reference crystal oscillator 50MHz and 25MHz of FPGA board. DC voltages are supplied for RF TX module and RF RX module by TEXIO Regulated DC Power Supply and 2280S-32-6 Precision Measurement DC Supply. The operation of system is observed through ROHDE & SCHWARZ RTB2004 Oscilloscope.

Operation waveform of the experiment is demonstrated in Fig. 5.23. As can be seen from the figure, the *ODATA* at the output of RX digital part is completely same to *DATA*

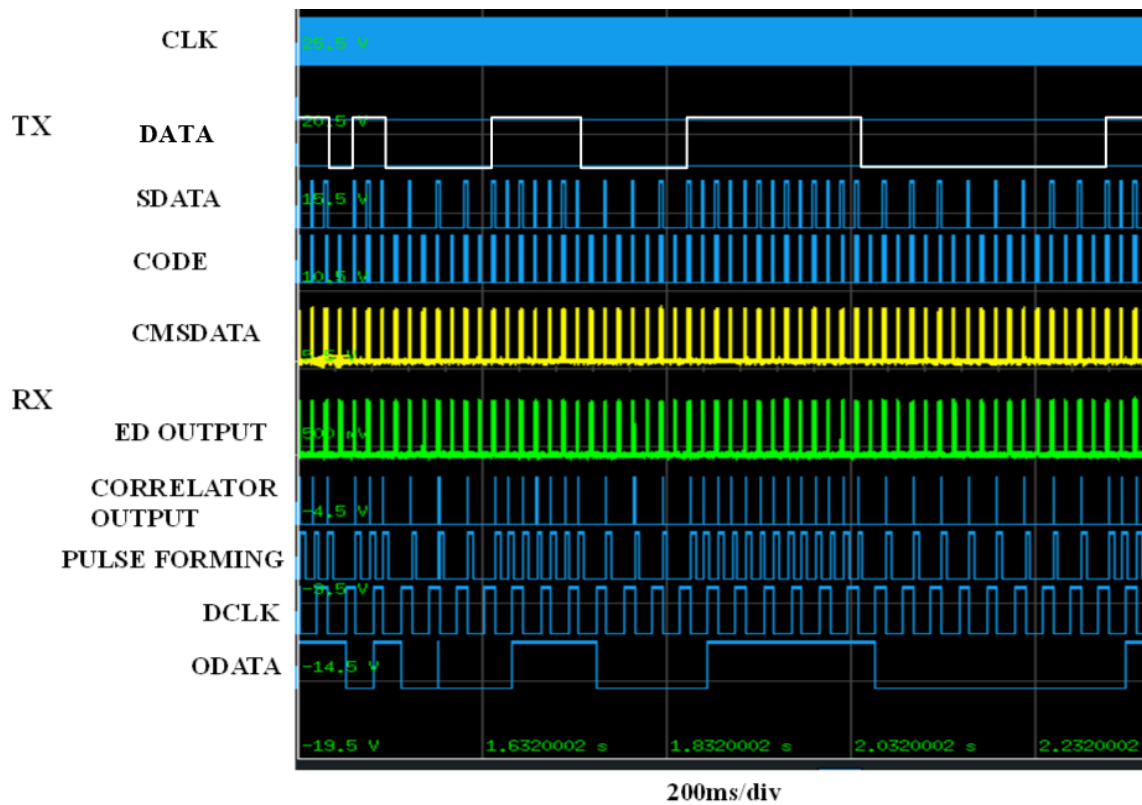


Fig. 5.23: Operation wave form of experiment

sent from the TX with a little bit delay. This proves that CMS-OOK TRX system operates successfully.

## **5.6 Conclusion**

In this chapter, a CMS-OOK RX is proposed and designed based on 65nm SOTB CMOS technology. The design uses LNA and RF amplifier to improve the sensitivity and envelope detector to reduce the power consumption. By using code modulation in combination with adjustable threshold of digital correlator, the immunity of RX is enhanced.

Simulation results of the design show that the RF frontend consumes average  $38.8\mu\text{W}$  for receiving a pair of bit '1' and '0' at 1kbps data rate, corresponding to  $19.4\text{nJ/bit}$ . RX can operate well with signal power higher than the sensitivity of  $-76\text{dBm}$ .

Although the TEG chip of CMS-OOK RX does not operate well when it is evaluated. The experiment of CMS-OOK TRX system shows a good operation, which proves that CMS-OOK TRX can be used for RF communicating of WSNs. Considering of applying CMS-OOK TRX system to low power WSNs will be discussed more in Chapter 6.

## References

- [5-1] M. T. Hoang, N. Suggi, and K. Ishibashi, "A 1.36 $\mu$ W 312-315MHz Synchronized-OOK Receiver for Wireless sensor Networks Using 65nm SOTB CMOS Technology," *Elsevier Solid-State Electronic* 117, 2016, pp. 161-169.
- [5-2] M. T. Hoang, "A Study on Ultra-Low Power and High Sensitivity OOK CMOS RF Receiver for Wireless Sensor Networks," *Doctoral Thesis*, The University of Electro-Communications, Tokyo, 2015.
- [5-3] V. T. Nguyen, R. Ishikawa, and K. Ishibashi, "83nJ/bit Transmitter Using Code-Modulated Synchronized-OOK on 65nm SOTB for Normally-Off Wireless Sensor Networks," *IEICE Trans. On Electronics*, Vo1. E101-C.472 Jul. 2018, pp. 472-472.
- [5-4] M.Crepaldi, C. Li, "An Ultra-Wideband Impulse-Radio Transceiver Chipset Using Synchronized-OOK Modulation," *IEEE Journal Of Solid-State Circuits*, Vol. 46, No. 10, October 2011
- [5-5] J. Chen and J. Liou, "On-chip inductors for RF Applications: An overview," *Journal of Semiconductor Technology and Science*, Vol. 4, No. 3, Sep. 2004, pp. 149-167.
- [5-6] B. Razavi, "RF Microelectronics," *Pearson Education, Inc.*, 2012
- [5-7] Y. Goto and M. Fukishima, "Through-Only De-embedding for On-chip Symmetric Devices," *International Conf. on Solid-State Devices and Materials*, Tsukuba 2007, pp. 49-491.
- [5-8] SRX882 datasheet, NiceRF Wireless Technology Co.,Ltd [Online]. Available: <https://www.nicerf.com/Upload/ueditor/files/2016-08-29/SRX882%20datasheet%20V2.0-54b1c2d6-b433-4af6-ad75-527961adf70b.pdf>. Accessed: 10<sup>th</sup> Oct. 2018
- [5-9] STX882 datasheet, NiceRF Wireless Technology Co.,Ltd [Online]. Available: <https://www.gme.cz/data/attachments/dsh.772-294.1.pdf>. Accessed: 10<sup>th</sup> Oct. 2018.

## **Chapter 6**

### **Consideration of Applying CMS-OOK Transceiver to Low Power Wireless Sensor Networks**

As regarded in Chapter 1, intermittent and normally-off operation modes are good ways to save power consumption of radio communication system for EHWSNs. To accomplish the advantages of this operation modes, it demands RF TX with capability of fast start up to transmit data, turns off or consumes tiny power when no data needs to send. Besides, TX also has to radiate a power which is in margin of FCC radio regulations. Moreover, in circumstances that there are a lot of other wireless devices operating at the same time in the vicinity of RX in WSNs, it is prefer that RX can resist interference as well as possible. In contrast, CMS-OOK also has some issues need to be addressed in order to apply to practical WSNs. In this Chapter, considerations of applying CMS-OOK TRX to low power WSNs are discussed.

#### **6.1 Power consumption of the TX**

As analysis before, in WSNs the active power of TXs regularly is much higher than that of RXs. It is very important to completely shut down the radio or put it in a tiny-power sleep mode when there is no data transmitting or receiving for saving power purpose. Intermittent and normally-off operations are extremely ways to reduce power consumption of EHSNs with limited and not-always-continuous supply energy.

Fig. 6.1 shows a block diagram and power chart of an intermittent TX controlling by MCU of a SN. According this, when there is no data needed to be sent, TX is often in sleep mode with power consumption of reference oscillator (crystal oscillator). Whenever MCU

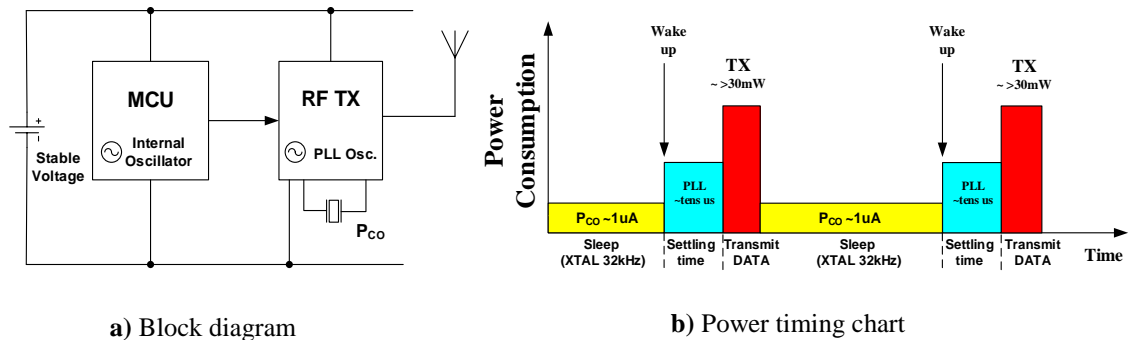


Fig. 6.1: Intermittent operation TX

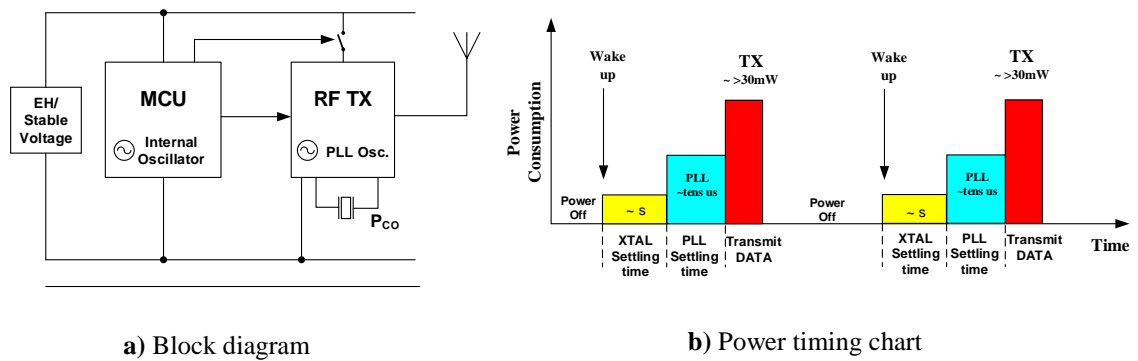


Fig. 6.2: Normally-off operation TX

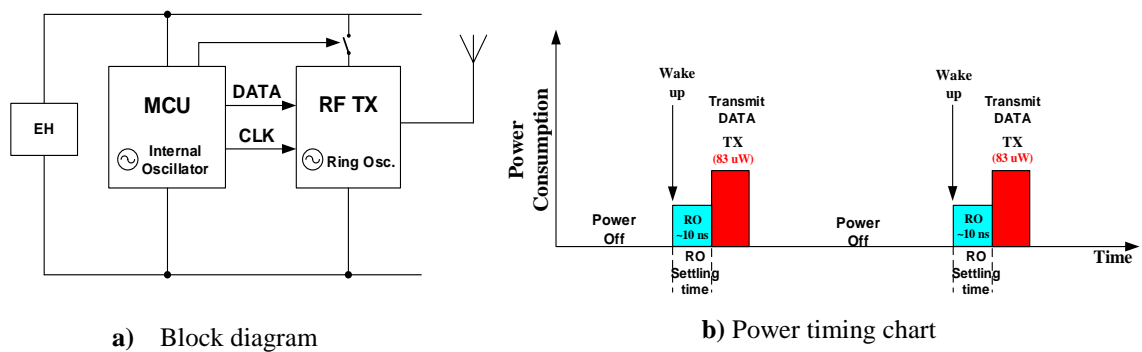


Fig. 6.3: Normally-off operation of CMS-OOK TX

decides that TX wants to send necessary data, a controlled signal will wake up the TX, then it takes time to settle carrier oscillator before transmitting data. If the RF TX utilizes carrier oscillator of crystal or PLL, settling time often is about tens to hundreds microseconds. As a result, it cost significant energy during settling time and sleeping time. In order to maintain crystal oscillator with high accuracy frequency operating continuously, a stable and continuous DC supply is required. Thus, this is not suitable for WSNs which deploy only EH circuits for supplying.

If CMS-OOK TX is used in this case, internal RO with much shorter settling time (Table 2.1) will reduce much power consumption during the settling time (blue area). In addition, commercial TXs [6-1, 6-2, 6-3] often consume about or more than 30mW while CMS-OOK with much smaller power consumption of 83 $\mu$ W also contributes in cutting down power consumption of SN.

With the same SN with above RF TX operating in normally-off mode, the block diagram and power chart are exhibited in Fig. 6.2. In comparison with previous case, the difference here is that the MCU controls to power off or power on the RF TX. According this, whenever SN wants to send data, firstly, MCU will initiate reference crystal oscillator then settle the carrier oscillator (PLL), and finally transmit the data. Normally, the time gap between two events of sending data is quite long, thus normally-off operation can save more power in comparison with above intermittent operation (shorter yellow area).

In case that CMS-OOK TX is applied to above normally-off system, block diagram and power timing chart are illustrated in Fig. 6.3. According to this, MCU will be programmed for normally-off or intermittent operation. Besides, digital part of TX and RX can use external clock which comes from the MCU. It is acceptable to use clock signal from internal oscillator of MCU with relative accuracy of 1-2%. In the RX side, clock signal which is used for decoding should be crystal oscillator with high accuracy. It is noticeable that OOK modulation with transmitted data only depends on amplitude of signal and less sensitive to carrier frequency, jitter, noise as well as distortion of the carrier signals. This allows CMS-OOK, as a special kind of OOK modulation, to deploy relaxed jitter carrier oscillator like internal ring oscillator (RO) without using reference crystal oscillator. This helps TX not only completely turn-off when no data is sent but also wake-up quickly from power-down state to start transmitting data. Also, we can utilize such high efficient and low linearity power amplifier (PA) such as E-class PA stage because OOK RX is normally immune to distortion of the signals. As a result, TX for CMS-OOK likely consumes energy only when transmitting data (red area). Previously, in comparison with the case that TX with crystal or PLL carrier oscillator is used, CMS-OOK TX in normally-off operation can eliminate power during sleeping time (yellow), reduce much power during shorter settling time of RO (blue area) and decrease power for transmitting time (red area) by very low power consumption of the TX. Moreover, it is noticeable that the MCU can wake up the CMS-OOK TX and the

internal RO of this TX with unstable voltage (intermittent energy) from EH circuit as shown in [6-4].

Besides, peak power of the spectrum is reduced by 1) the code modulation and 2) diffusion of the carrier by using body bias control in the RO using 65nm SOTB technology in the proposing CMS-OOK. This helps the CMS-OOK TX to satisfy the radio regulations.

In brief, CMS-OOK TX with intermittent operation or normally-off operation can reduce strongly power consumption.

In addition, general operation of CMS-OOK TX is described in Chapter 3 implies that, in term of power, at a same data rate transmission, CMS-OOK TX consumes much less energy that of OOK and S-OOK TX. Let us observe the Fig. 6.4, in which the baseband data of three types of OOK, S-OOK and CMS-OOK signal at the same data rate are displayed. Assume that three TXs of OOK, S-OOK and CMS-OOK have equal average power consumption  $P_0$ . The baseband data will modulate carrier oscillator, which results in RF radiating of TX during high pulse duration and powering off during low pulse time. In detail, considering in a pair of bit '1' & '0' transmitting, OOK TX will transmit RF signal for bit duration  $T_b$  while S-OOK TX powers on for  $3T_P$ . According to principle of CMS-OOK modulation, the code is PN code with nearly a half number of bit code is bit '1' and the rest is bit '0', thus total time duration of high pulse is  $4 * T_P / 2 = 2T_P$ .

It is easy to calculate the energy to transmit a pair of data '1' & data '0' from 3 TXs as followed:

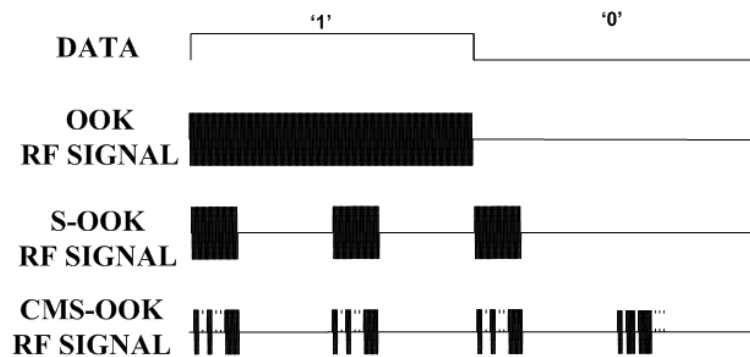


Fig. 6.4: Waveform of original data, synchronized data and CMS data

- OOK TX:  $E_{OOK} = P_0 * T_b;$
- S-OOK TX:  $E_{S-OOK} = P_0 * 3T_p;$
- OOK TX:  $E_{CMS-OOK} = P_0 * 2T_p$

With  $T_b$  is much longer than  $T_p$ , energy of CMS-OOK TX is much reduced in comparison to OOK TX. For instance, if we choose  $T_b = 10T_p$ , the energy of CMS-OOK is 5 times lower than that of OOK TX in condition of same data rate and same average power consumption. The higher ratio of  $T_b$  and  $T_p$ , the much lower energy of CMS-OOK TX in comparison with that of OOK TX. In other way, it also states that with a same energy consumption, CMS-OOK TX has much lower average power consumption.

Other benefit of CMS-OOK TX is that signal spectrum is spread over a very wide range by using code modulation and sweeping carrier frequency. Also, the CMS-OOK RX can demodulate the data even when the carrier frequency changes. Thus, we can drastically reduce the peak power intensity of carrier by modulating the carrier frequency. This provides not only low power peak, power intensity of signal spectrum, which takes part in satisfaction of the radio regulations, but also widen bandwidth of signal which contributes in higher resistance to interference. In other words, CMS-OOK can transmit more power than conventional OOK without increasing peak power intensity, to achieve longer communications distances.

Besides, low power benefit also partly comes from CMS-OOK RX. Thanks to RFENA signal, which is generated by digital part of the CMS-OOK RX, analog part of the RX is turned on when the RF CMS-OOK signal comes and turned off during the time without the RF signal. As a result, the CMS-OOK RX can reduce much power in comparison with full-time operation.

EHSNs can use various energy harvester such as solar harvesters, RF energy harvesters, mechanical harvesters and so on [6-4, 6-5]. It is popular that energy harvesters should supply a power of tens to hundreds  $\mu\text{W}$  for the SNs. The design of CMS-OOK TRX in this study with  $83\mu\text{W}$  analog part of TX and  $38.8\mu$  analog part of RX are suitable to this capacity of energy harvesters.

## 6.2 Interference resistance of CMS-OOK TRX system

RF co-site interference occurs when there are two or more co-located RF systems have bad effects on the other. This is getting worse because the need of new RF communication systems grows up. RF co-site regularly happens when two or more RF systems are operating physically next to the other and they are operating in such a way that TXs negatively impact on one or more RXs [6-6]. In a wide scene, WSNs operating at 2.4GHz band often face to co-located WIFI, Bluetooth and so on. In narrower view, TRX systems of different nodes inside the WSN also become interference sources to each other. Addressing RF co-site interference helps to raise the reliability of WSNs. In this section, this study investigates interference of CMS-OOK TRX system in the scene that there are noise and interference from the TXs of other nodes in the WSN, which makes negative impacts on performance of a pair of CMS-OOK TX and RX (Fig. 6.5).

In principle, OOK modulation is a special case of ASK modulation in which carrier is controlled by baseband data of ‘1’ and ‘0’ bit-stream. Essentially speaking, that is amplitude modulation (AM). Hence, OOK modulation owns all features of AM. Unfortunately, in terms of interference resistance, AM is easily effected by noise and interference because of narrow bandwidth and additive property. The sent information is ‘carried’ on the amplitude of OOK signal which is changed by noise and interference without difficulty. Besides, narrow BW of OOK signal causes it easily be badly impacted by narrow in-band interference. Thus, when there is strong enough interference, OOK TRX communication will be disturbed.

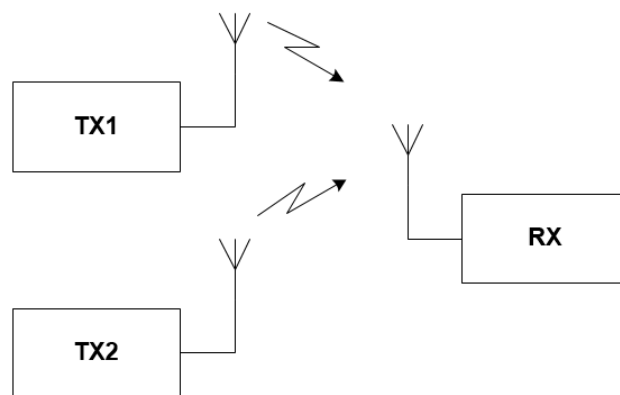


**Fig. 6.5:** Co-located TX inside same WSN as an interference source

Although CMS-OOK modulation has some features similar to those of OOK modulations, it also owns some private properties which help CMS-OOK TRX system enhance the resistance to co-site interference. Firstly, diffusing spectrum by using DS-SS technique and varying carrier frequency by sweeping body bias voltage of SOTB devices helps CMS-OOK signal widen BW broadly. This limits the bad effects of narrow band interference on CMS-OOK signal. Secondly, CMS-OOK TRX deploys code modulation, which allows assigning different codes to different TXs. As a result, only RX with matched code is capable of receiving data from desired TX while the others can not.

In order to investigate immunity to interference of CMS-OOK TRX, a simulation using MATLAB/SIMULINK in combination with ModelSim is carried out. The diagram of simulation configuration is shown in Fig. 6.6. According this, main TX is TX1 sending the DATA1 to the RX through free space loss path while other TX 2 with different code, plays as an interference source, sends DATA2 over free space loss path to the RX. Path loss of both TX corresponding to distance can be adjusted. Parameters of TXs and RX are set up similar to HSPICE simulation results of based 65nm SOTB CMOS technology TRX designed in Chapter 4 and Chapter 5. Output of RF frontend is a bit sequence which is written in a data file. Then, this file is used as input of digital part in ModelSim simulation. Data output of digital part is compared to sent DATA1 to calculate bit error ratio.

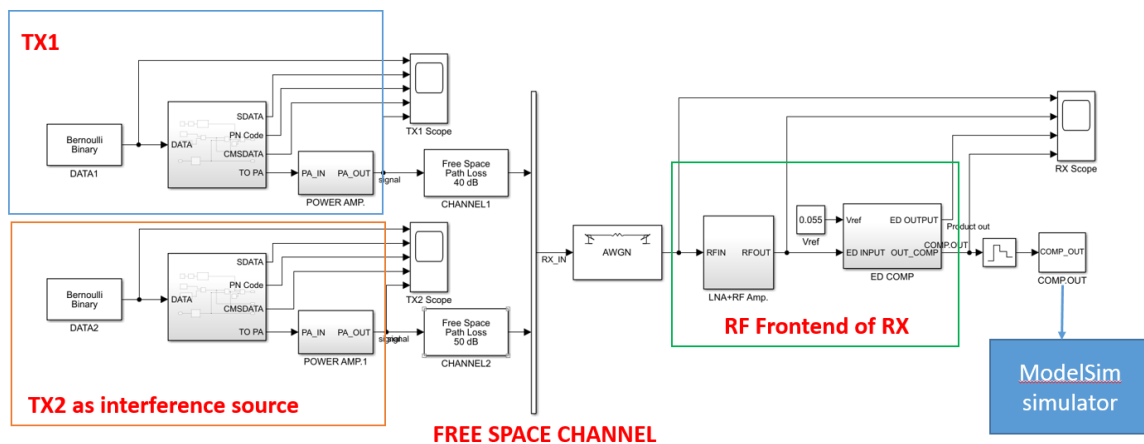


Fig. 6.6: Simulation diagram of system with 2 TXs and 1 RX

As described in Chapter 5, CMS-OOK deploys 2x-oversampling digital correlator which plays role as a matched filter to decode received bit stream from RF front-end. In ideal case, there is no interference, sum of exclusive-OR gate output can reach to maximum value of 62 (according to 31-bit code is used). However, in presence of strong enough interference, there are some bit errors in received bit stream in comparison with sent data from TX1. At that time, if threshold is kept at maximum value of 62, there is no pulse at output of the correlator. Consequently, RX is not able to recover sent data as illustrated in Fig. 6.7a). When the threshold decrease so that the sum is above the threshold, output signal will appear. Depend on strength of interference, there is a range of threshold value in which digital part can recover data with minimum bit error rate. For example, Fig. 6.7b) demonstrates a case when the threshold is reduced but still high (THRESHOLD = 58), clock signal is used to get data DCLK is recovered incorrectly which leads to errors of ODATA. Continue reducing THRESHOLD to suitable value (THRESHOLD = 52 in this example), DCLK and ODATA is recovered correctly (Fig. 6.7c)).

To make comparison between the resistance to interference of OOK TRX and CMS-OOK TRX, above configuration of system using OOK TRX and CMS-OOK TRX is carried

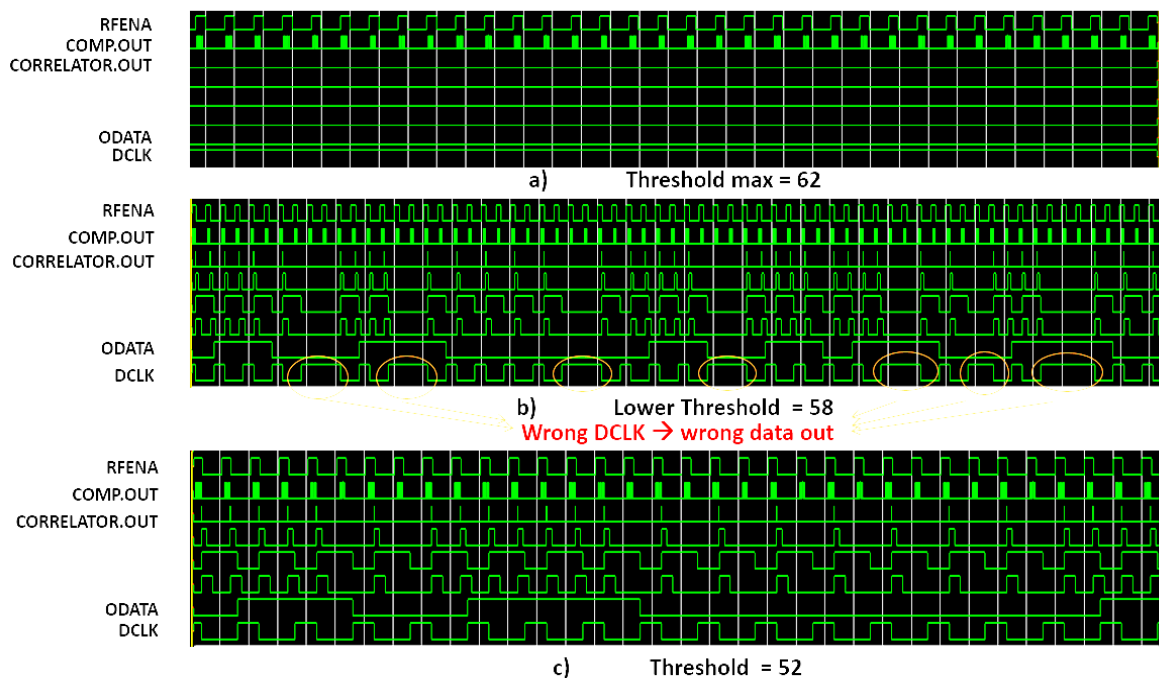
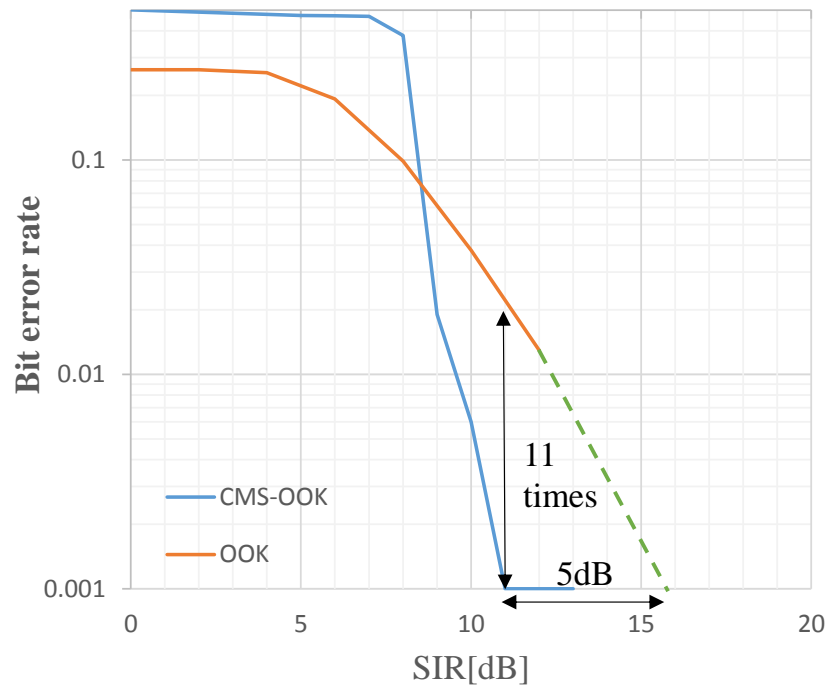
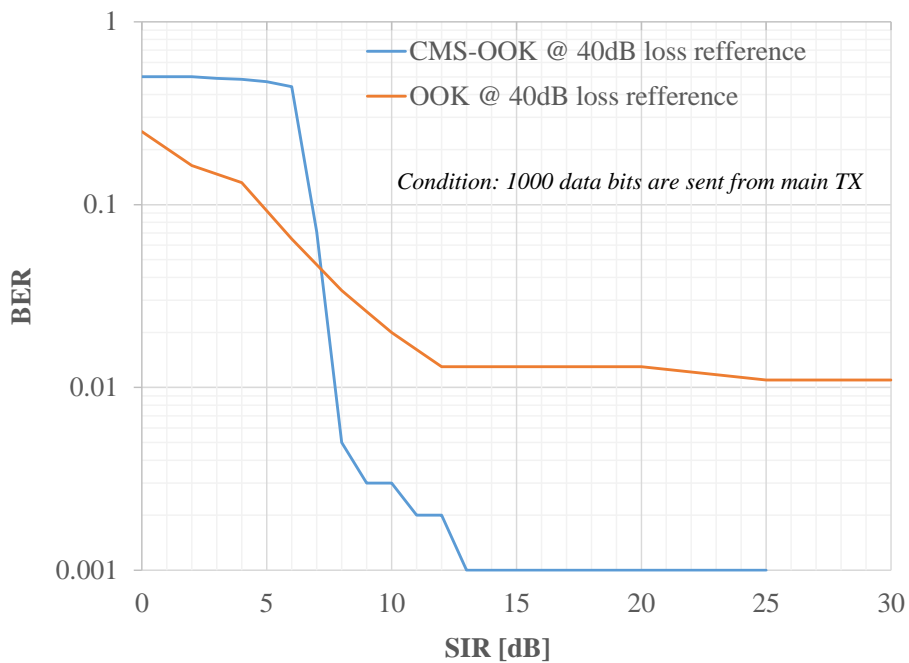


Fig. 6.7: Adjusting threshold of correlator to recover data



**Fig. 6.8:** BER comparison between OOK and CMS-OOK TRX

Under condition: - referred path loss of TX1 is 35dB  
 - 1000 data bits are sent from main TX



**Fig. 6.9:** BER comparison between OOK and CMS-OOK TRX at low SNR

Under condition: - referred path loss of TX1 is 40dB  
 - 1000 data bits are sent from main TX

out in same condition. Here the simulation is executed under followed condition: 1000 data

bit is sent, referred path loss is 35dB. Despite of the small number of data bit in this observe, which can make BER value less accuracy, the difference in co-site interference resistance between OOK TRX and CMS-OOK TRX systems can be seen through Fig. 6.8. At first, it is easy to realize that except case of too strong interference, BER curve of CMS-OOK system is below that of OOK system. At the same value of SIR = 11dB, BER of CMS-OOK TRX is above 10 times smaller than that of OOK TRX.

At lower signal intensity according to smaller SNR, simulation result with 40dB path loss of main TX is shown in Fig. 6.9. At smaller SNR, large noise power can make errors in OOK system even at high SIR. However, in the same condition, with higher 13dB of SIR, even at as low as SNR, CMS-OOK system can operate with 10 times smaller BER than OOK system. It is noticeable in both case that BER curve of CMS-OOK system is only below that of OOK system when SIR is large enough. In situation that SIR is small, corresponding to strong interference, both OOK and CMS-OOK system can not operate correctly.

Above results imply that performance of CMS-OOK TRX is better than that of OOK TRX when interference is not too strong. The reason of this phenomenal is that CMS-OOK is a special type of OOK signal, decoding received signal must base on output of envelope detector and comparator. CMS-OOK RX can only decode if there are not too many error bits in the output of RF front-end. In principle, 2x-sampling digital correlator can correct several bit errors in useful received signal, but when the bit errors in bit stream from RF front-end are over a bound, it makes digital part of CMS-OOK RX meet faults in recovering data. Hence, errors of CMS-OOK TRX are the sum of errors by RF front-end (corresponding to OOK TRX errors) and errors of decoding by digital part. This explains why there is an existing of higher BER of CMS-OOK TRX in comparison with that of OOK TRX. Also, it is noticeable that at different SNR there is a range of SIR in which CMS-OOK TRX operates better than OOK TRX.

### **6.3 Interference experiment of system using discrete RF modules and FPGA**

An experiment of the CMS-OOK system including two TXs and a RX was carried out with the configuration as shown in Fig. 6.10. According this, a CMS-OOK TX1 is the main TX which allocated at a fix distance  $d_l = 40\text{cm}$  from a CMS-OOK RX. A second CMS-OOK

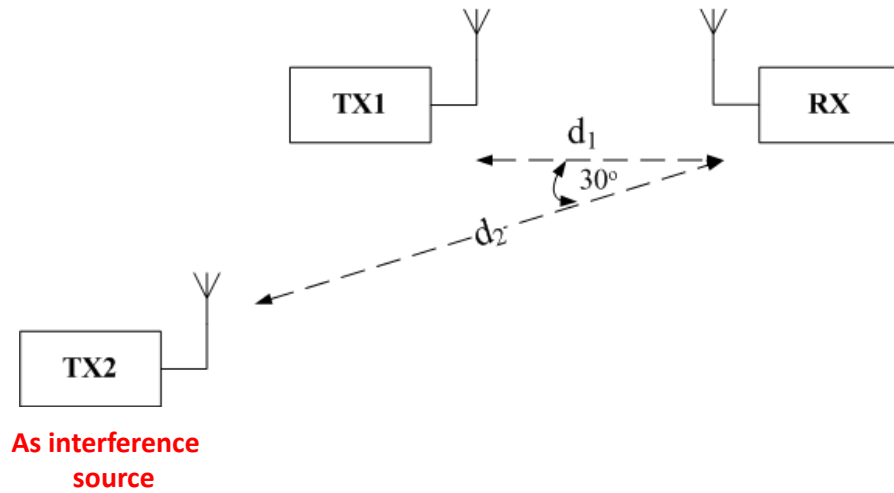


**Fig. 6.10:** Interference experiment of CMS-OOK system with 2 TXs and 1 RX configuration

TX2 using different code plays as co-site interference source at distance  $d_2$  from the RX. The angle between TX1 – RX – TX2 is  $30^\circ$ . Each CMS-OOK TX and RX is established by combining RF module (STX882 and SRX882) and FPGA board (Alter DE2-115). In this experiment, we adjusted the distance  $d_2$  to observe the effect of interference to operation of the TX1 and the RX.

Experiment results are displayed in Fig. 6.11. As can be seen from the figure, with the distance  $d_2$  large enough (further than 140cm), the TX2 nearly has no effect on communications between the TX1 and the RX. However, as soon as the TX2 approaches the RX, corresponding to reduce of  $d_2$ , the bit errors appear and the number of bit errors increases in inverse proportion to  $d_2$ .

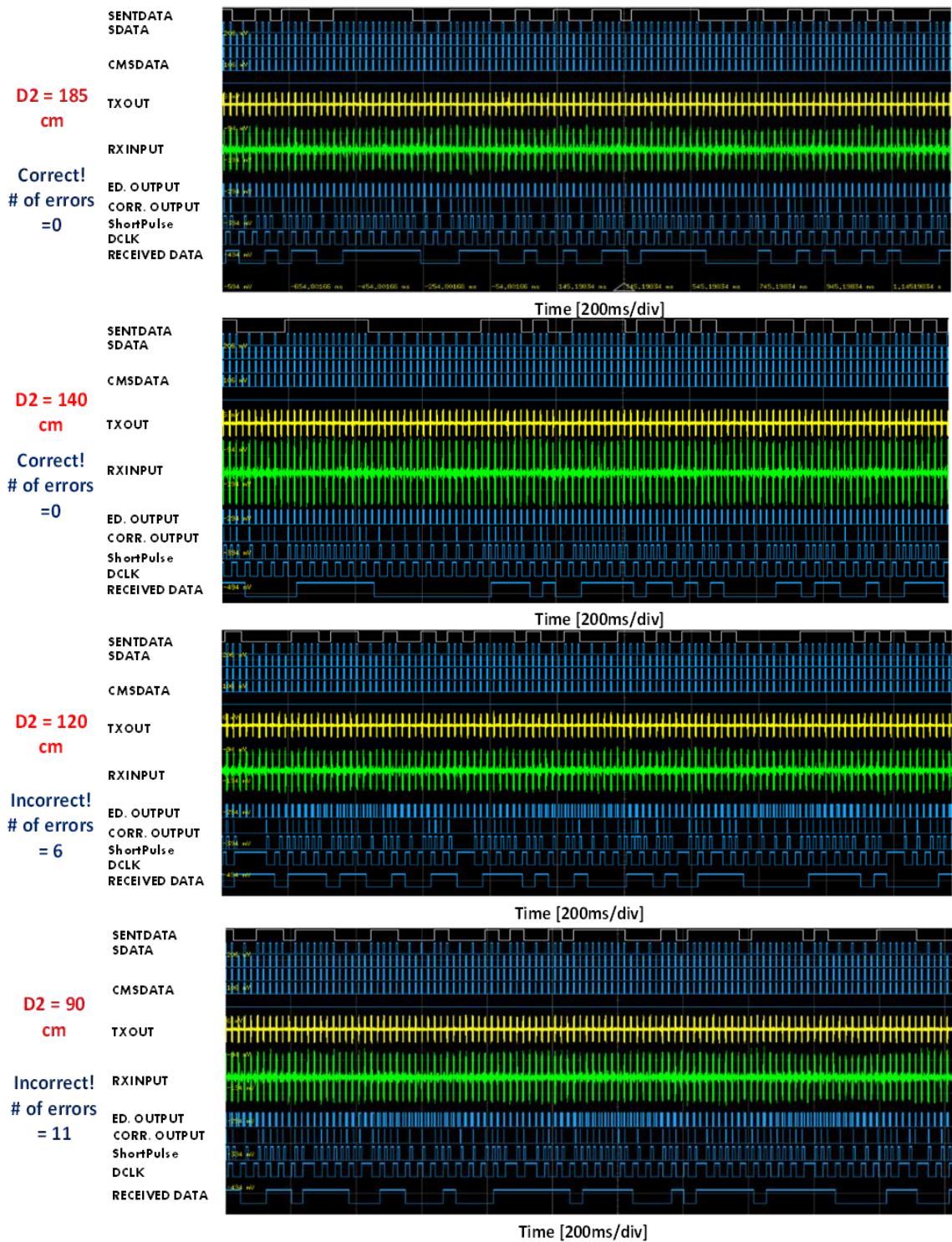


Fig. 6.11: Interference experiment results

## **6.4 Conclusion**

By analyzing CMS-OOK RX in terms of TX's power and immunity to interference, we can realize that CMS-OOK RX is suitable to low power WSNs. Simulation results imply that CMS-OOK TRX can enhance the ability of resistance to co-site interference. However, analyzing of immunity of CMS-OOK TRX here just covers the cases of system with a pair of CMS-OOK TRX and 2TXs – 1RX (inside a WSN). Other situations such as more than two TXs – a RX, external co-site interference sources and so on will be investigated in the future.

## References

- [6-1] NXP Laboratories, "IEEE802.15.4 Wireless Microcontroller," JN5148-001 Datasheet [Online]. Available: <https://fccid.io/TYOJN5148M6/User-Manual/manual-1660523> . Access: Dec. 2018.
- [6-2] ATMEL, "Zigbee IEEE 802.15.4 Radio Transceiver," AT86RF230 Datasheet [Online]. Available: [www.farnell.com/datasheets/9516.pdf?COM=SolarPower](http://www.farnell.com/datasheets/9516.pdf?COM=SolarPower). Access: Dec. 2018.
- [6-3] MEMSIC, "MicaZ Wireless Measurement System," CC2420 Datasheet [Online]. Available: [www.memsic.com/userfiles/files/Datasheets/WSN/micaz\\_datasheet-t.pdf](http://www.memsic.com/userfiles/files/Datasheets/WSN/micaz_datasheet-t.pdf). Access: Dec. 2018.
- [6-4] B. Lucia, V. Balaji, A. Colin, K. Maeng, and E. Ruppel, "Intermittent Computing: Challenges and Opportunities," *2<sup>nd</sup> Summit on Advances in Programming Languages (SNAPL2017)*, 2017.
- [6-5] R. Takitoge and K. Ishibashi et. al., "Temperature Beat: Persistent and Energy Harvesting Wireless Temperature Sensing Scheme," *IEEE SENSORS 2016*, Nov. 2016.
- [6-6] B. A. Culver, "Modern co-site RF interference issues and mitigation techniques," *a General Educational White Paper for Business Professionals and Technical staff*, Southwest Antenna, Inc., 2016.

## Chapter 7

### CONCLUSION

Ultra-low-power radios can open up many applications ranging from IoTs, WSNs to security, healthcare devices and so on. This is always a developing trend of electronics engineering in general and WSNs in particular. It is important to achieve low power consumption while maintaining robust operation includes several tough trade-offs between output power, bandwidth, data rate, sensitivity, reliability etc. This must be coped with a combination of device technology, circuit-level design, novel architectures and system-level considerations. The objective of this study is proposing a radio TRX system using for WSNs with low power operation, longer distance and good immunity to interference. After considering carefully in terms of low power, resistance to interference, technology and architecture to find out solutions, this study proposed a new modulation scheme called Code-Modulation Synchronized-OOK (CMS-OOK). Then, a CMS-OOK TRX was implemented basing on 65nm SOTB CMOS technology to achieve low power and high immunity to disturbances.

For low power operation objective, we mainly focus on reducing power consumption of TX by using CMS-OOK TX with intermittent or normally-off operation. Relaxed jitter ring oscillator is used as carrier source which allows the TX completely turn-off when no data is sent and start up quickly from power off state to transmit data. Regarding to power of RX, in order to get better sensitivity, the CMS-OOK utilizes LNA and RF amplifier which costs more power. Longer communication distance and better immunity to interference can be achieved by combination of code modulation and sweeping carrier frequency technique. Thanks to this combining solution, bandwidth of the CMS-OOK signal becomes wider, the peak of power spectrum is much reduced by 6dB in comparison with that of S-OOK signal, which allows more TX output power without violating radio regulations. The larger TX output power, the longer communication distance is. Besides, broader bandwidth also helps

CMS-OOK signal to avoid negative effects from narrow-band interference. Moreover, code modulation also takes part in enhancing resilient ability to co-site interference.

In addition, the development of the 65nm SOTB CMOS technology produces devices with low threshold voltage, low leakage current and variable body bias, which allows to decrease power consumption of TRX circuit more deeply. In the Chapter 4 and Chapter 5, CMS-OOK TX and RX basing on 65nm SOTB devices were designed and fabricated. Evaluation of analog part of designed CMS-OOK TX chip displays a 15MHz bandwidth at -62dBm/MHz power spectral density peak. It consumes average 83 $\mu$ W DC power at 1kbps. Simulation result indicates that more spectral efficiency can be achieved by increasing sweeping voltage swing on body of CMOS devices in carrier oscillator circuit or raising number of code bit. Regarding to CMS-OOK RX design, pre-layout simulation results show that RF frontend consumes average 38.8 $\mu$ W for receiving a pair of bit '1' and '0' at 1kbps data rate, corresponding to 38.8nJ/bit. RX can operate well with signal power higher than -76dBm sensitivity. Besides, utilizing 2x-oversampling digital correlator with programmable threshold allows to recover data with minimum bit error ratio when interference appears. The system simulation result shows that in presence of not too strong interference, BER of CMS-OOK system is 10 times smaller than that of OOK system. Another speaking, the immunity of RX to interference is improved.

Simulation results of the CMS-OOK TRX system and experiment results of this system using discrete TRX RF modules and FPGA board proved that CMS-OOK TRX system can operate successfully. A comparison of immunity between CMS-OOK and OOK TRX inside narrow scene of a WSN was investigated. It also exhibits that at a specified signal to noise ratio, in a range of SIR the performance of CMS-OOK TRX is better than that of OOK TRX.

Although CMS-OOK TRX owns a lot of advantages, it also exposes several disadvantages. Firstly, CMS-OOK TRX operates at low data rate, which can restrict applications of it. Raising data rate will cause higher frequency of clock frequency in both TX and RX, especially in RX side with 2x or 4x oversampling technique is used. That is exactly challenge to implement high frequency clock oscillator with high stability. Secondly, digital correlator normally takes time to decode received bit stream from analog part of RX, which costs AC power consumption. The longer delay and the higher clock frequency, the

more AC power is consumed. This AC power consumption can be eliminated by timing calculation carefully for TRX. Finally, in a specified margin of SIR, CMS-OOK TRX shows the better performance than OOK TRX in terms of immunity to interference and vice versa at outside of this margin.

In conclusion, despite of the disadvantages, CMS-OOK TRX with intermittent or normally-off operation, low power consumption, broad bandwidth (high spectral efficiency), higher TX output power, longer communicate distance and good immunity to interference is able to apply to low power EHWSNs.

## APPENDIX A

### FULL CHIP LAYOUT MICROGRAPH

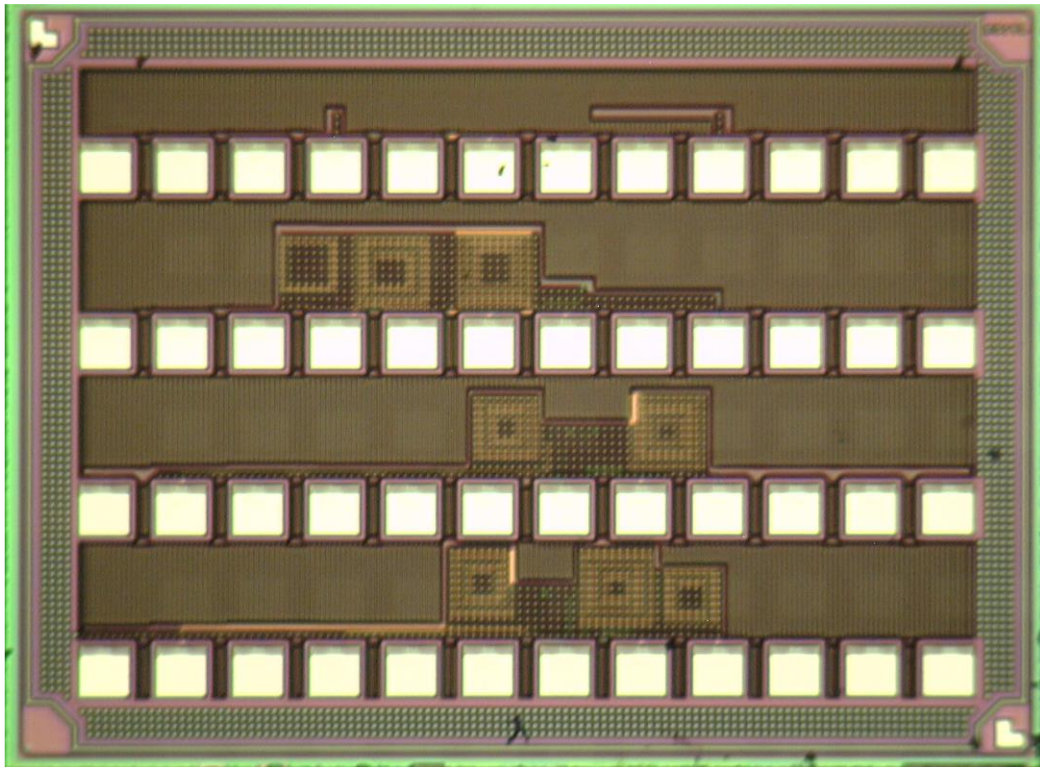


**Fig. A.1:** CMS-OOK Transceiver with On-chip Inductor

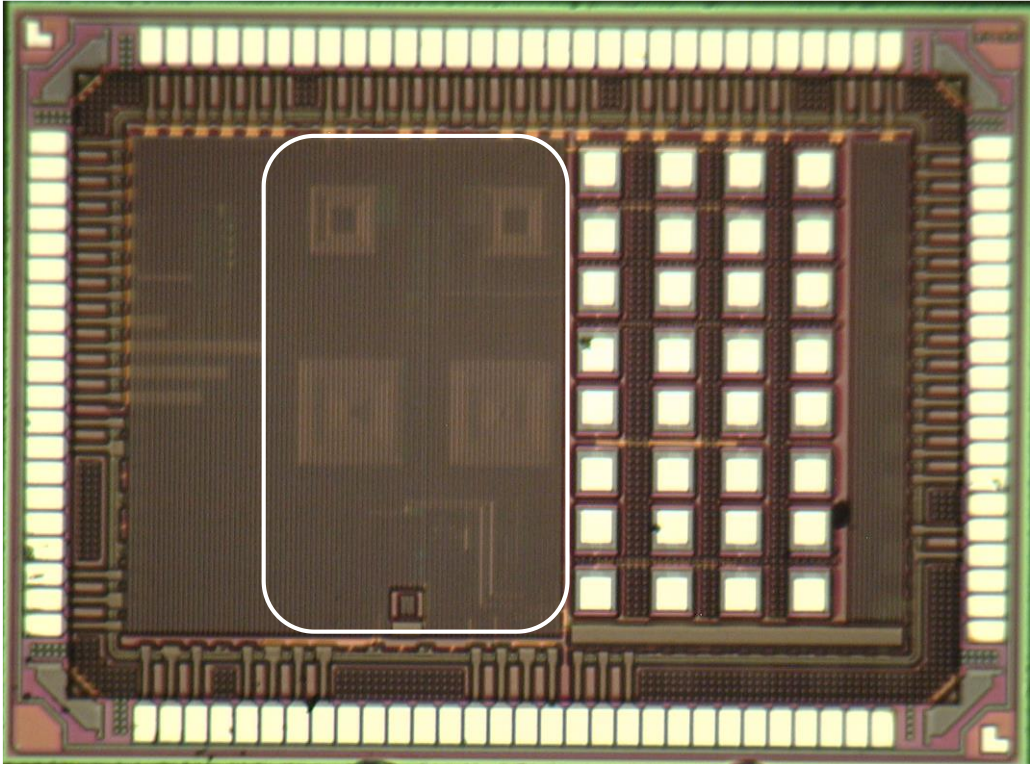


**Fig. A.2:** CMS-OOK Receiver with On-chip Inductor

*This page intentionally left blank*

## APPENDIX B

### List of Publications

#### B.1 JOURNAL PAPER

- [1] V. T. Nguyen, R. Ishikawa, and K. Ishibashi, "83nJ/bit Transmitter Using Code-Modulated Synchronized-OOK on 65nm SOTB for Normally-Off Wireless Sensor Networks," *IEICE Trans. On Electronics*, Vol. E101-C.472 Jul. 2018, pp. 472-472.

#### B.2 CONFERENCE PAPERS

- [1] V. T. Nguyen and K. Ishibashi, "A 65nm based-on Code-Modulated Synchronized-OOK Transmitter for Normally-Off Wireless Sensor Networks," *SDM/ICD/IST*, Sep. 2018.
- [2] V. T. Nguyen and K. Ishibashi, "RF Characteristics of SOTB Devices for GHz Frequency Applications," *Thai-Japan Microwave Conference 2017 (TJMW2017)*, Jun. 2017.
- [3] V. T. Nguyen and K. Ishibashi, "Evaluation of Applying Spectrum Spreading to Synchronized -OOK Modulation Scheme," *The International Workshop on Modern Science and Technology*, Nov. 2016.

*This page intentionally left blank*

## **AUTHOR BIOGRAPHY**

Nguyen Van Trung received the B.Sc. degree in Electricity, Electronics in 2008 and M.Sc. degree in Electronics Engineering in 2012, both from Le Quy Don Technical University (LQDTU), Hanoi, Vietnam. From August 2008 to 2010 and from June 2012 to September 2015, he was with Faculty of Radio-Electronics Engineering from Le Quy Don Technical University, Hanoi as a assistant lecturer and researcher. Since October 2015, he have being pursued the Ph.D. degree at the University of Electro-Communications, Tokyo, Japan. His research interests include low power transceiver designing for wireless sensor networks, RF Energy Harvesting and VLSI designing. He is a member of IEICE.

**THE END**